



University of
Stavanger
Faculty of Science and Technology

MASTER'S THESIS

Study program/ Specialization:

Master Petroleum Engineering
Specialization Drilling

Spring semester, 2014

Open

Writer:

Eirik Aasberg Vandvik

.....
(Writer's signature)

Faculty supervisor: Mesfin Belayneh

External supervisor: Harald Syse, Reelwell

Thesis title:

Experimental investigation at heavy light interface mixture of Reelwell ERD

Credits (ECTS): 30

Key words:

ERD, Heavy over light fluid, Reelwell

Pages: 110

+ enclosure: 47 pages

+ Attachment 1 Experimental CD

Stavanger, 13.06.2014

Acknowledgement

I will thank every one of these persons for their immense help, and for taking time in their busy schedule to help me. Without them this thesis would not have become a reality.

Mesfin Belayneh, Professor of petroleum engineering [UIS].

Harald Syse, Engineering Manager [Reelwell].

Ola M. Vestavik, Chief Technology Officer [Reelwell].

Tom Unsgaard

Vibjørn Dagestad, Senior technical advisor [Wild Well Control].

Laura Belbin Vokey

Sindre Veen Larsen

Abstract

Due to longer offset and large surface area exposure in a reservoir, extended reach drilling (ERD) is a method which is both cost effective and a well potential during the production phase. However, the present ERD method envelope is limited to about 12.3km. In order cross this envelope, the Stavanger based drilling company Reelwell has developed a ultra-long (>20km) ERD method solution. The method is under development and is in field scale testing phase. The results show that the technology is feasible and has several advantages over the conventional methods.

Reelwell uses a range of different features to succeed with increasing the ERD envelope. The heavy over light concept is one of these.

The concept is comprised of utilizing two different drilling fluids at the same time. Because of difference in density between the fluids and an inclined wellbore, an interface is created.

This master thesis deals with an experimental study of this heavy light interface and its behavior when exposed to rotation from the drill string.

In this thesis three test rigs were designed and constructed. Based on the Reelwell operational and fluid properties, a total of 31 experimental studies were carried out.

The studies investigated several parameters that influenced the dynamics of the heavy light interface and the resulting mixing zone.

Table of contents

ACKNOWLEDGEMENT	2
ABSTRACT	3
TABLE OF CONTENTS	4
1 INTRODUCTION	6
1.1 BACKGROUND.....	6
1.2 PROBLEM FORMULATION.....	8
1.3 ASSUMPTIONS.....	9
1.4 OBJECTIVES.....	9
2 REELWELL TECHNOLOGY	10
3 THEORY	14
3.1 FORCE OF GRAVITY.....	14
3.2 THEORY OF ROTATIONAL FORCE.....	15
3.3 INTERFACIAL TENSION.....	15
3.4 RHEOLOGY MODELS.....	16
3.5 FLOW IN ANNULUS WITH PIPE ROTATION.....	20
3.6 THEORY OF FLUID MIXTURE.....	24
4 EXPERIMENTS	28
4.1 DRILLING FLUID PREPARATION AND DESCRIPTION.....	29
4.2 EXPERIMENT EQUIPMENT LAYOUT.....	31
4.3 TEST RIG 1#.....	32
4.3.1 Purpose.....	32
4.3.2 Experimental setup.....	33
4.3.3 Experiments test rig 1.....	34
4.3.3.1 Experiments 1, 2 & 3, effect of inclination.....	34
4.3.3.2 Experiment 4 & 6, Effect of high Yield point.....	36
4.3.3.3 Experiment 5 & 7, Effect of heavy WBM.....	38
4.3.4 Fluid system description.....	40
4.3.5 Results and analysis.....	41
4.4 TEST RIG 2#.....	47
4.4.1 Purpose.....	47
4.4.2 Experimental setup.....	48
4.4.3 Experiments test rig 2.....	49
4.4.3.1 Experiment 8 & 9, Effect of reduced RPM.....	49
4.4.3.2 Experiment 10, 11, 12 & 13, Effect of heavy light ratio.....	51
4.4.3.3 Experiment 14 & 15, Effect of Clockwise (CW) and Anticlockwise (ACW) rotation.....	53
4.4.3.4 Experiment 16 & 18, Effect of low RPM.....	54
4.4.3.5 Experiment 17, 19 & 20, Effect of heavy OBM and negative inclination.....	56
4.4.4 Fluid system description.....	58
4.4.5 Results and analysis.....	59
4.5 TEST RIG 3 #.....	68
4.5.1 Purpose.....	68
4.5.2 Experimental setup.....	69
4.5.3 Experiments test rig 3.....	71
4.5.3.1 Experiment 21, 22, 23 and 24, Effect of RPM and pipe size, Matrix 1.....	71
4.5.3.2 Experiment 25, Effect of low viscous light fluid.....	73
4.5.3.3 Experiment 26, 27, 28 and 29, Effect of RPM and pipe size, Matrix 2.....	74
4.5.3.4 Experiment 30 and 31, Effect of negative inclination.....	75
4.5.4 Fluid system description.....	76
4.5.5 Results and analysis.....	77

4.6	VISCOMETER TEST RIG.....	92
4.6.1	<i>Purpose</i>	92
4.6.2	<i>Experimental setup</i>	92
4.6.1	<i>Viscometer experiment 1 and 2</i>	93
4.6.2	<i>Fluid system description</i>	94
4.6.3	<i>Results and analysis</i>	95
5	DISCUSSION	97
6	CONCLUSION	110
	ABBREVIATIONS	111
	REFERENCES	112
	APPENDIX A – EQUATIONS	114
	APPENDIX B – REELWELL TECHNOLOGY	115
	APPENDIX C – TEST RIG CONSTRUCTION AND GENERAL SPECIFICATIONS	120
	APPENDIX D – EQUIPMENT/TOOLS	138
	APPENDIX E – LIST OF CHARTS	149
	APPENDIX F – LIST OF FIGURES	150
	APPENDIX G – LIST OF GRAPHS	152
	APPENDIX H – LIST OF TABLES	154
	ATTACHMENT – EXPERIMENTAL CD	157

1 Introduction

This thesis discusses the study of heavy light interface mixture phenomenon. The author designed and constructed experimental rigs at smaller and larger scales. The study is new by its very nature. Various fluids to be used for Reelwell methods were considered for the analysis. In order to describe the mixture phenomenon, theories were reviewed to calculate the fluid properties. The study was part of Reelwell technology, which the thesis result gives information for the overall heavy light setup design and the development of the operation procedure.

1.1 Background

The oil industry has always looked for cheaper and more efficient ways of drilling oil wells. One solution has been to drill longer and more complex wells that cover a larger drainage area. This technique is generally called Extended Reach Drilling (ERD) and involves drilling long horizontal directional wells. The main purpose of ERD is to reduce the number of installations needed to reach oil and gas reserves (see figure 2).

Figure 1 is the ERD drilling envelope. The current maximum record is the well drilled in 2011 in Russian. The well is located in Sakhalin-1 - TMD 12345 m & 11475 m horizontal offset [06]. The main challenging with the conventional drilling is torque and drag that limits drilling from reaching to a longer offset.

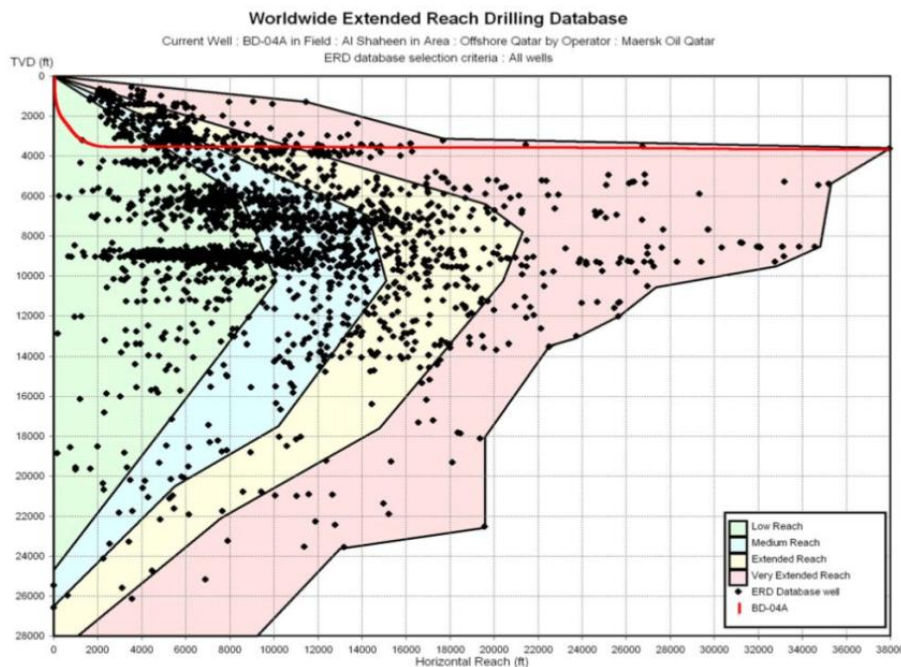


Figure 1: Extended reach drilling envelope. [07]

Throughout the years drilling technology has evolved and allowed ERD wells to grow longer. The main challenges for ERD wells are the mechanical loads on the drill string (especially friction induced torque and drag), hole cleaning and managing downhole pressure. Ever since the invention of steerable mud motors, directional drilling has been pushing its boundaries.

These challenges limit the range of conventional drilling. To solve them different companies have presented unique solutions. Reelwell is one of these companies.

Reelwell™ is a company established with the main goal of drilling and competing over 20 km MD ERD well. To reach this goal they have invented the Reelwell Drilling Method (RDM), which uses a dual conduit drill string. The drill string pumps drilling fluid through outer inner pipe and sucks it in through the inner drill pipe together with cuttings. According to Reelwell, RDM drastically decreases torque and drag, which again allows for longer ERD wells.

The extended reach provided by the RDM decreases the amount of equipment needed to recover hydrocarbon resources from a field. Figure 2 shows a comparison between conventional and Reelwell drainage area [R02]. As shown, the Reelwell technology can replace several platforms and thereby reduce overall cost.



Figure 2: Comparison of Conventional drainage area vs. Reelwell drainage area. [R02]

A main feature of their method is called the “heavy over light” concept (see figure 3) which involves using two separate drilling fluids, one heavy and one light. The heavy fluid is positioned in the annulus and lies stagnant, while the light fluid is circulated in and out of the dual conduit string and provides hole cleaning. Gravity ensures the position of the two liquids. Heavy light technology will be explained in more detail later in the thesis.

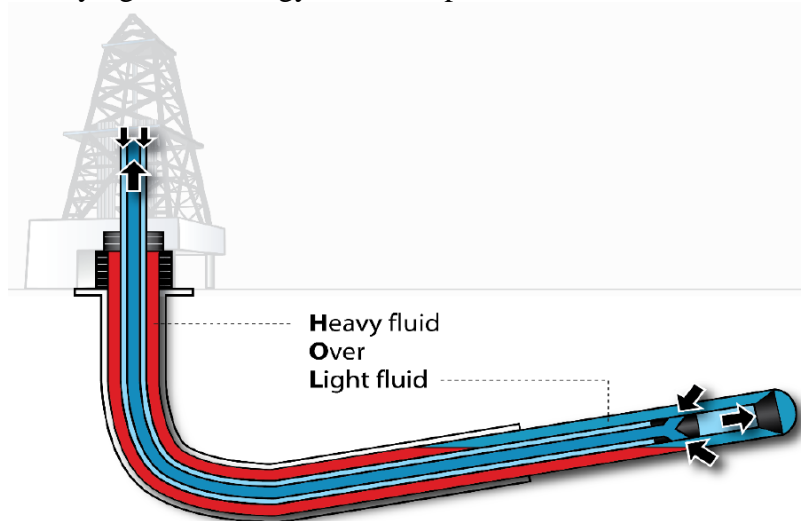


Figure 3: Displays Reelwells heavy over light concept. [R02]

1.2 Problem formulation

The Reelwell heavy light method drills the well with two different density mud systems, a heavy and a light, which forms an interface as shown in the figure 4. These two systems have different properties and purposes, and should remain separate to secure wellbore integrity, hole cleaning and other drilling related purposes. Because of the low inclination the heavy light interface will expose a significant area of the wellbore. This leads to mixing between the two fluids when drilling is engaged

The main question of this thesis is formulated:

What parameters affect the mixing rate and to what degree?

This problem will be dealt with in this thesis.

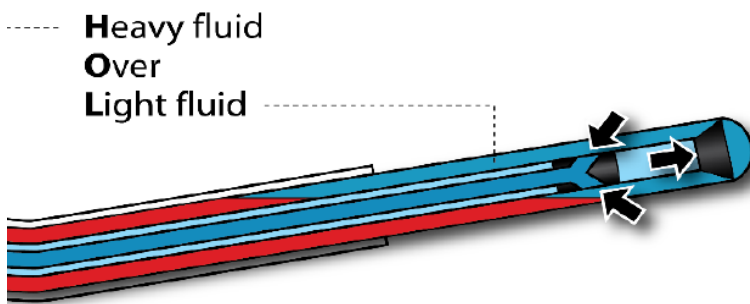


Figure 4: Illustrates Reelwells heavy over light method. [R02]

Other questions to be addressed in this thesis are:

- ✓ What forces keeps the liquids separated or engages mixing?
- ✓ What are the dynamics of the mixing of the mud system?
- ✓ What is the extent of the mix zone?
- ✓ What mixing rate will the interface travel with?
- ✓ Will the current Reelwell fluid properties have a positive or negative effect for the interface movement?

1.3 Assumptions

Under laboratory scale it is difficult to simulate the field conditions. However, the laboratory scale test attempt to investigate the heavy/light interface phenomenon under simplified experimental conditions. Therefore, the following assumptions and conditions are considered:

- Experiments performed at room temperature and pressure
- Figure 5, inclination readings are relative to the horizontal plane.*
- Cutting effects are not considered in the experimental setup
- The effect of pressure at the drilling bit and the pressure delivered by the heavy fluid assumed to cause the interface at static condition. This means that the interface is not moving due to the change in pressure. Therefore, this assumption describes the experimental setup.
- Flow of the light fluid is not taken into account. The fluid is assumed to be stagnant.
- The experimental wellbore is smooth and without cavities or gaps.
- Wellbore instability problems such as, but not limited to unconsolidated formations and shale collapse, are not taken into account, and will not be a part of the experimental systems.
- Pipe eccentricity, buckling and other mechanical malfunctions will not be simulated.

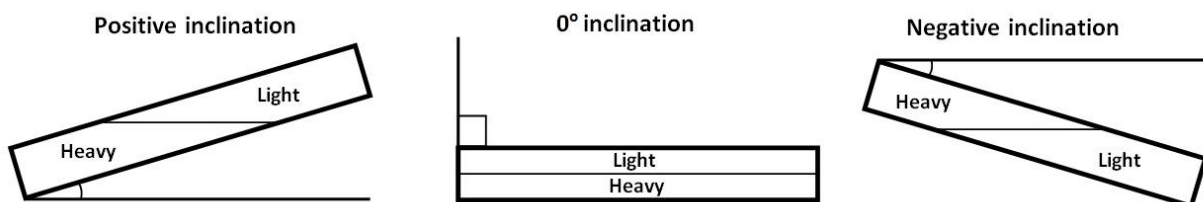


Figure 5: Figures illustrating how inclination is perceived in the thesis. [04]

* = Inclination angle is normally relative to the vertical axis in conventional drilling. For convenience inclination is in this thesis relative to the horizontal plane.

1.4 Objectives

The objective of this thesis is to study/analyze

- the effect of different rheology properties at the interface
- the effect of change in density between the light and the heavy
- the effect of OMB's and WBM's at the interface
- the effect of the change two OBM's of various density and rheology
- the effect of well inclination
- the effect of RPM on mixing interface
- the effect of varying distance between wellbore and pipe
- the effect of different pipe sizes

2 Reelwell technology

[Information about Reelwell and its technology are taken from references [R01, R02, R03]. For more detailed information about Reelwell technology, see [Appendix B](#)]

The drilling technology company Reelwell was founded in 2004 by Dr. Ing. Ola M. Vestavik. They specialize in groundbreaking and innovative drilling solutions for the oil and gas industry. The award winning company's main office is located in Stavanger and is currently employing 17 persons. Reelwell is considered a cutting edge company within ERD and with their Reelwell Drilling Method (RDM) a future force to be reckoned with in development of new ERD procedures.

Reelwells RDM is a new drilling method, developed and refined for use in the oil and gas industry in recent years. It is a multi-purpose drilling method equipped with a unique flow arrangement. RDM is based on using a conventional drill string combined with an inner string to form a dual conduit drill string (see figure 6 on next page). This configuration allows the return fluid, saturated with drill cuttings from the bottom of the well, to be transported back through the inside of the drill string.

Potentially RDM will increase the envelope for EDR, due to several reasons:

- Elimination of the dynamic Equivalent Circulating Density (ECD) gradient, since the ECD is screened from the formation.
- The use of a flotation technique (see Heavy over light) of the drill string will reduce Torque and Drag.
- Optional Hydraulic Weight on Bit (WOB), due to a piston encapsulated drill string.

With these features, RDM can be a dominating factor in ERD in the future.

Heavy over light

The heavy over light concept is one of the main features of Reelwells RDM. A “hook” shaped bore is drilled (see figure 6) to allow the usage of two fluids with different densities in one wellbore. The “hook” shaped well path is made to create a 1 degree inclination in the horizontal section. This is done to maintain the position of the fluids and to prevent *u-tubing*.

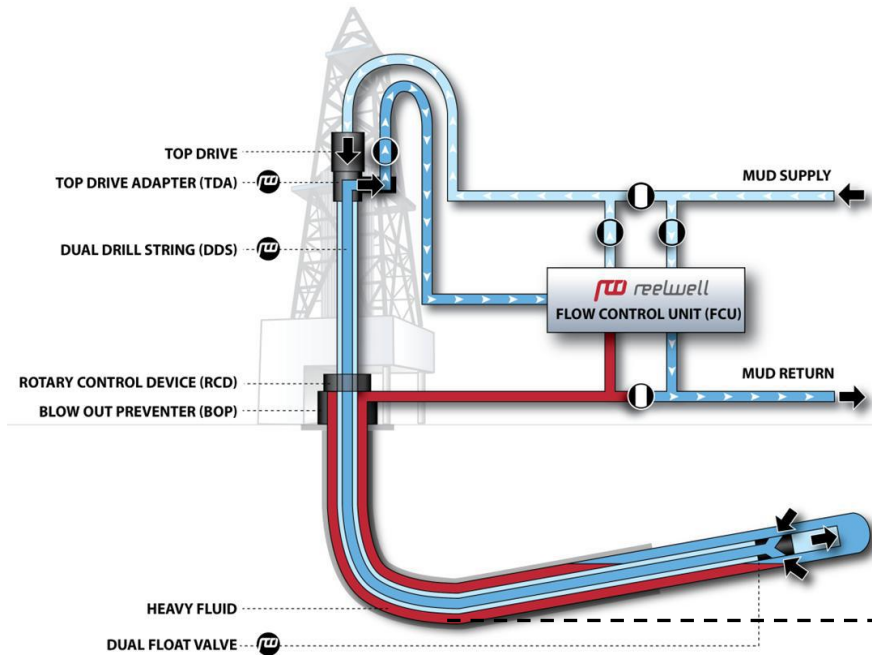


Figure 6: Displays the heavy light setup with all RDM components. [R03]

In the heavy light scenario, a heavy fluid lies stagnant in the annulus, while a light fluid is pumped through the outer drill pipe and out through the drill bits nozzles. The light drilling fluid and the cuttings are sucked into the drill string again through holes approximately 100 meters from the drill bit, and transported to the surface in the inner drill string. When drilling advances, more heavy fluid is pumped into the annulus to secure the correct heavy light interface position and wellbore stability.

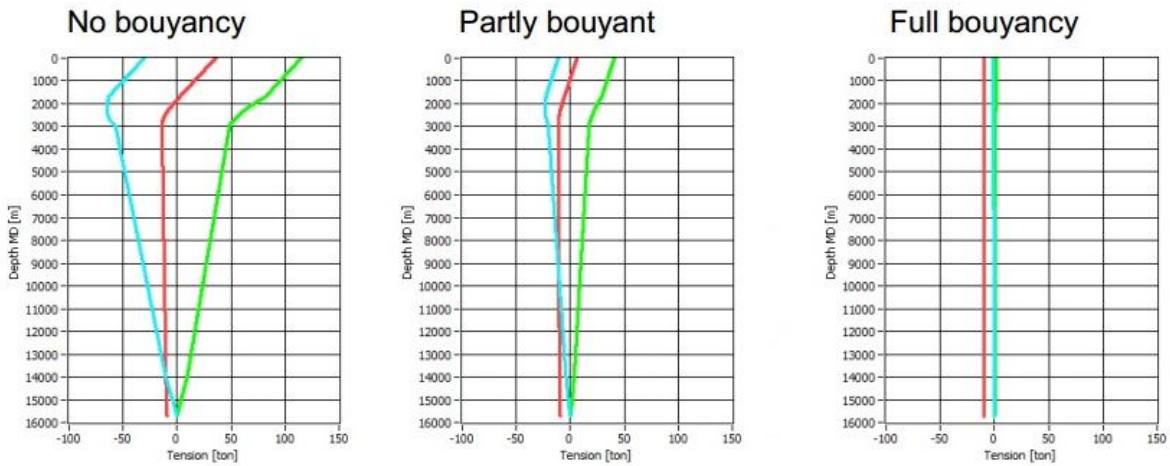
The main purpose of the heavy light concept is to try to keep the drill string buoyant. This will drastically reduce the friction between the wellbore and the drill string, which again will reduce the torque and drag.

The heavy light setup accomplishes buoyancy by utilizing two methods:

- i. Using the density difference between the two liquids to create buoyancy. The higher the difference, the higher the buoyancy.
- ii. Using aluminum as drill pipe material instead of steel (optional). Aluminum has 1/3 of the density of steel, which makes aluminum drill pipes more buoyant than their steel opposites.

The effect of the density difference is displayed in the graphs and tables below. Higher density difference leads to a fully buoyant string that drastically reduces drag.

Buoyancy Effects on Drag

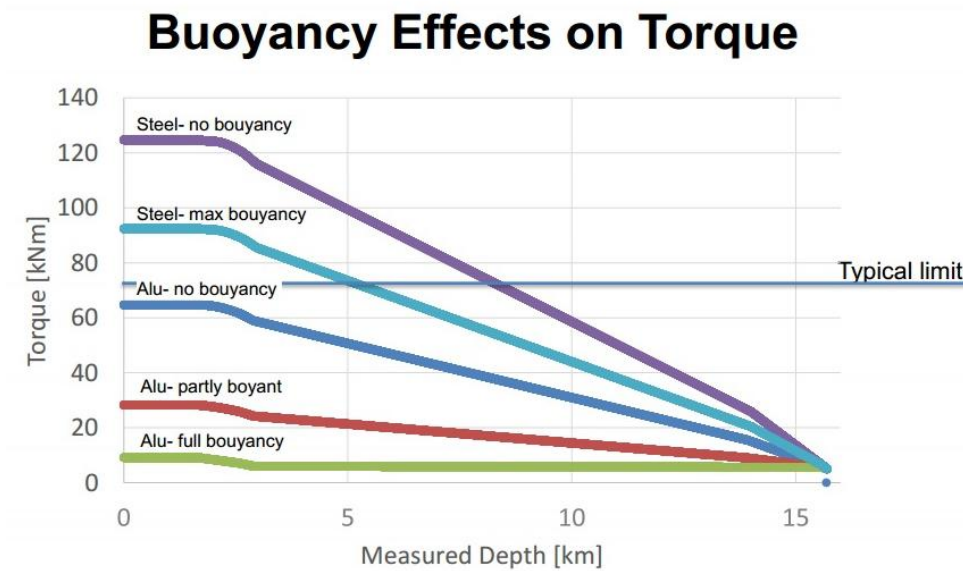


Graph 1: Displays buoyancy effects on drag in a RDM drilling scenario. [R03]

	Well annulus (heavy) fluid density [sg]	Active (light)fluid density [sg]	Density difference Heavy – light [sg]
No buoyancy	1.20	1.20	0
Partly Buoyancy	1.56	1.20	0.36
Full Buoyancy	1.75	1.15	0.50

Table 1: Effect of density difference on drill pipe buoyancy. [R03, 02]

Graph 2 shows a combination of having a difference in density and the usage of aluminum pipe. As seen, the combination results in very low torque numbers. This again allows for an extended horizontal reach, as illustrated in the graph.



Graph 2: Shows the effect of buoyancy and drill pipe material has on torque. [R03]

With a fully buoyant drill string, the heavy over light concept may help Reelwell to accomplish their 20 km goal.

3 Theory

[Information about the theory is obtained from references listed under [Theory](#) in the reference list. All equations used in the theory is displayed in [Appendix A](#)]

The fluids in Reelwells heavy over light principle is subjected to external forces when undergoing a drilling procedure. Together with the fluid rheology, they govern the behavior pattern of the interface. The two major forces are the force of gravity and the force of rotation, while dominating factors of the fluid rheology are assumed to be viscosity and density. In this subsection, these forces and fluid properties will be clarified and explained so that experiment outcome can be predicted.

3.1 Force of gravity

The Reelwell Drilling Method heavy over light is based on Newton's theory of gravity. The theory states that:

“Every point mass attracts every single other point mass by a force pointing along the line intersecting both points. The force is proportional to the product of the two masses and inversely proportional to the square of the distance between them”.

Using the theory of gravity, the gravitational pull on Reelwells heavy over light system can be expressed by this equation:

$$F_{g,heavy} > F_{g,light} \quad (1)$$

The equation shows that the gravitational force between the earth and the heavy liquid is higher than for the light liquid. The heavier fluid will therefore try to position itself beneath the light fluid as fast as possible (depending on the difference in density).

Reelwells heavy over light method depends on these gravitational forces to be sufficient enough to keep the two fluids separated.

3.2 Theory of rotational force

As a drill string rotates with angular velocity ω , the larger deformation is obtained at wall of the drill string and reduces as we go to the outer cylinder as shown in figure 7. The configuration describes the experimental rig presented in chapter 4. Therefore, one can assume that fluid deformation the experimental rigs can be such as this.

The shear rate and the angular velocity for this configuration are given as [T01]:

$$\dot{\gamma} = \frac{\omega r_{DP}}{r_w - r_{DP}} \quad (2)$$

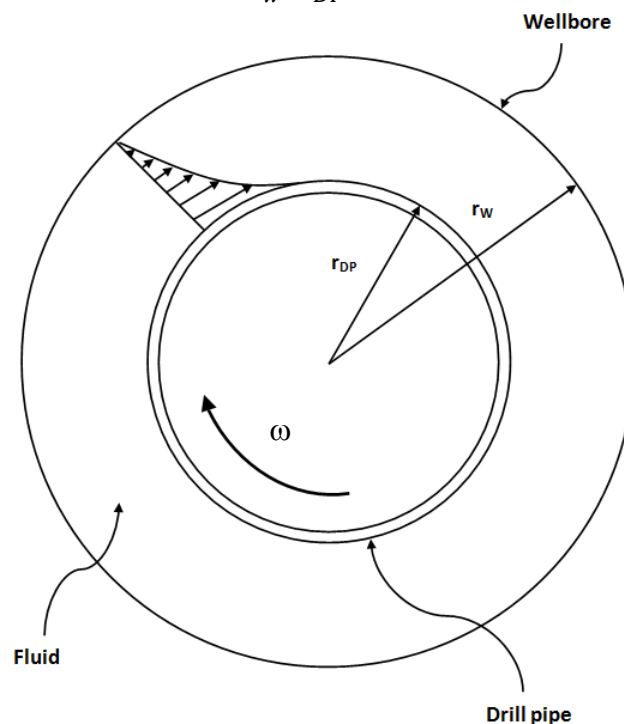


Figure 7: Bottom view of a rotation drill pipe in a wellbore. [04]

3.3 Interfacial tension

Surface tension is a property caused by the different intermolecular forces exerted at the fluid interface. The main forces involved in interfacial tension are adhesive forces (tension) between the liquid phases or liquid phase with either a solid or gas phase. The interaction occurs at the surfaces of the substances involved, i.e. the corresponding interfaces.

Cohesive forces are the intermolecular which cause a tendency in liquids to resist separation. The intermolecular forces include those from hydrogen bonding and Van der Waals forces.

During emulsification process, interfacial tension also plays an important role. Emulsification is a heterogeneous system, consisting of at least one miscible liquid dispersed in another in the form of droplets. In our case, the light drilling fluid mixes with the heavy drilling fluid in the mixture zone. Since two systems are in contact by the action of the rotational force, they will tend to mix.

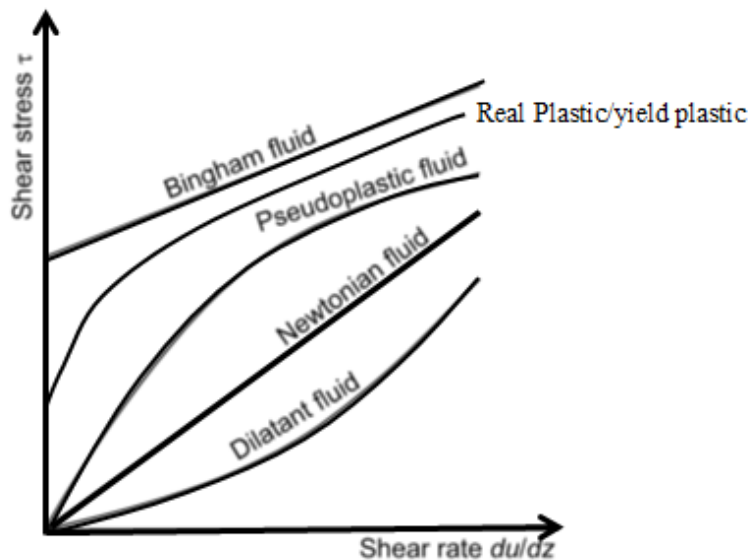
3.4 Rheology models

[Information about the rheology models is taken from reference [T02].]

The rheology is the study of the deformation and flow of fluids. In the literature there are several rheology models to describe the behavior of the fluids. The rotational and axial motions of the drill string have effects on the fluid rheology properties, which are key parameters for the determination of fluid flow patterns. The rheology models categorizes as Newtonian and non-Newtonian. The Non-Newtonian models are Bingham plastic, Power law, API, Herschel-Buckley, Unified, and Robertson-Stiff. These models approximate fluid behavior. Graph 3 illustrates the shear stress-shear rate behavior of the models.

A Fann viscometer is usually used to measure shear stress and shear rate. The apparatus is shown in [Appendix C](#).

The viscometer is also used to measure rheology properties as gel strength and viscosity of various fluids. A range of speed between 300 and 600 rpm is most common but instruments with RPM ranging from 3, 6, 100, 200, 300, 600 are used. The setup of the viscometer is made up out of an inner bob and an outer rotating steel cylinder. When the outer cylinder starts to rotate, the viscous drag of the fluid pulls the bob in the direction of rotation. Torque is created on the bob, which is measured by a spring and a dial which are connected to the bob. The torque which is strained on the bob is called shear stress (τ) and the rotational speed of outer cylinder is called shear rate (γ).



Graph 3: Displays the models shear stress-shear rate behavior. [T03]

When converting laboratory data units to field engineering units, the measured data should be multiplied with the conversion factors shown below

$$\gamma [s^{-1}] = RPM * 1.703$$

$$\tau \left[\frac{lbf}{100sqft} \right] = Fann \text{ Dial Reading} * 1.067$$

Rheology properties

The rheological properties of fluid are determined from Fann measurements. The three parameters are **sometimes** used to better describe fluid behavior. In this thesis, the Newtonian and non-Newtonian (Bingham plastic and Power law) models are considered when describing the rheological properties of fluid systems. From Bingham plastic fluid, PV (plastic viscosity) and YP (Yield point) parameters are measured from the 600 and 300 RPM viscometer readings. Similarly from the viscometer reading, for power-law fluid model, exponent (n) and consistency (k) parameters are also calculated. However, there is also three parameter rheology models used to describe the behavior of fluid system. These are Herschel-Bulkley and Robert and Stiff model.

Newtonian fluid

Newtonian fluid is one parameter rheology mode. According to Newtonian model, the shear stress is directly proportional to shear rate. The model described a fluid system which doesn't contain solid particles and at zero shear rate the fluid is able to flow. The Newtonian fluid has a constant viscosity at any shear rate. Newtonian model describe fluid systems such as water, glycerin, oil, light hydrocarbon. The fluid system can be described by [T04]:

$$\tau = \mu \gamma \quad (3)$$

Where:

μ - viscosity [cP]

γ - shear rate [1/s]

Non-Newtonian fluid

A fluid that can't be described by the Newtonian fluid model is called a non-Newtonian fluid. Examples of non-Newtonian fluids include slurries, pastes, gels, polymer solutions etc. Non-Newtonian fluid can be generally classified as:

- **Thixotropic:** Fluid exhibits decreased viscosity with stress over time
- **Rheopectic:** Fluid exhibits increased viscosity with stress over time
- **Shear thinning:** Fluid exhibits decreased viscosity with increased shear rate
- **Dilatant or shear thickening:** Fluid exhibits viscosity increases with increased shear rate.

Bingham plastic

The Bingham plastic rheology model is commonly used in the industry to describe flow behavior of many types of muds. The Bingham plastic model is a two parameter model. According to the model, the fluid system exhibits constant viscosity at any shear rate. At zero shear rates, the fluid system requires a certain external pressure in order to be set into flow. Mathematically the shear stress-shear rate can be described as:

$$\tau = \mu_p \gamma + YP \quad (4)$$

Where:

μ_p - Plastic viscosity: [cP]

γ - shear rate: [s^{-1}]

YP - Yield point: [lbf/100ft²]

The plastic viscosity part is the measure of fluid-fluid, fluid-particle, or particle-particle friction. For faster drilling operation, the plastic viscosity (PV) needs to be as low as possible. The PV can be obtained by minimizing colloidal solids.

The YP part of the friction is due to an electrostatic force of attraction or repulsion between charges or ions within the drilling fluid system. The drilling fluid needs to have high enough YP in order to carry cutting out of the hole.

Plastic viscosity (PV) is calculated with the following equation:

$$\mu_p(cP) = \theta_{600} - \theta_{300} \quad (5)$$

The yield value can be determined with the following equations:

$$YP = \theta_{300} - PV \quad (6)$$

$$YP = 2\theta_{300} - \theta_{600} \quad (7)$$

YP: lbf/100ft²

Power law

Unlike the Bingham model, the viscosity of fluid decreases as the shear rate increases. This model describes drilling fluid such as water based polymer fluid. Mathematically, the Power-law for fluids is described as [T04]:

$$\tau = k\gamma^n \quad (8)$$

- ***k*** - is the consistency index. It represents the average viscosity of the drilling fluid for the overall shear rate.
- ***n*** - is the flow behavior index. It's a rheological property of matter related to the cohesion of the individual particles of a given material, its ability to deform and its resistance to flow.

$$n = 3.321 \log \left(\frac{R_{600}}{R_{300}} \right) \quad (9)$$

$$k = \frac{R_{300}}{511^n} = \frac{R_{600}}{1022^n} \quad (10)$$

k: lbf/100ft²

3.5 Flow in annulus with pipe rotation

Ramadan and Miska presented theoretical and experimental work on the RPM effect on the drilling fluid rheology [T05]. Figure 8 illustrates the flow behavior under axial and rotational motions.

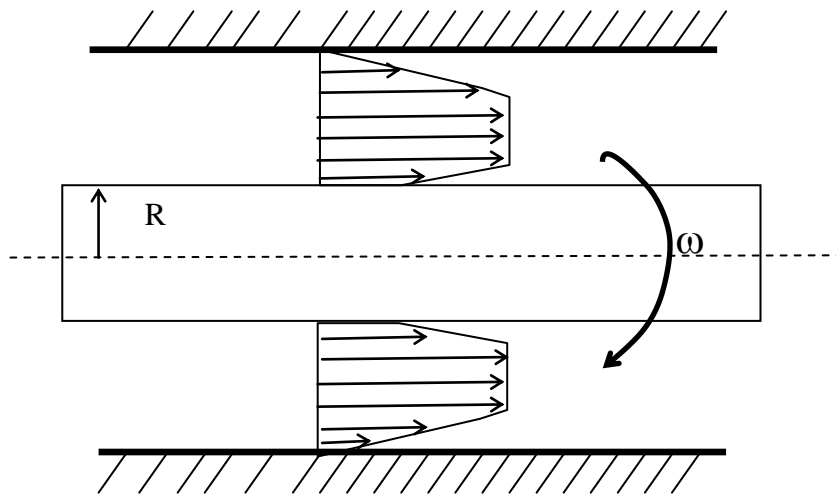


Figure 8: Helical flow of YPL fluid in concentric annulus. [T05]

It is reported that for most drilling fluids, the yield power law rheology model describes the rheology behavior more accurate than the Bingham plastic and power law model. The model is given as (Unified model):

$$\tau_w = \tau_y + k\gamma^m \quad (11)$$

Where k is consistency index and m is fluid flow index. Assume that the axial flow is in the presence of the drill string rotation. The shear velocity will be the resultant of the axial and the rotational speeds, given as (Ramadan and Miska, 2008):

$$\gamma = \sqrt{\gamma_{\theta z}^2 + \gamma_z^2} \quad (12)$$

Where, γ_{θ}^* and γ_z^* are the wall shear rates of axial tangential flows. Applying the narrow slot approximation, the average axial shear rate at the wall can be estimated as:

$$\gamma_z^* = \frac{1+2N}{3N} \frac{12U}{D_o - D_i} \quad (13)$$

The rotational shear rate at the inner pipe wall can be approximated as:

$$\gamma_{\theta}^* = \frac{\omega D_i}{D_o - D_i} \quad (14)$$

The flow behavior index, N is calculated using the following equation:

$$\frac{3N}{2N+1} = \frac{3m}{2m+1} \left[1 - \left(\frac{1}{m+1} \right) x - \left(\frac{m}{m+1} \right) x^2 \right] \quad (15)$$

Where

$$x = \tau_y / \overline{\tau_w}$$

Angular velocity

Suppose we have a yield power law fluid and it flows with an axial and rotational motion. Then we can calculate the angular velocity, ω :

$$\omega = \frac{2\pi}{60} \text{ RPM} \quad (16)$$

Calculate the axial velocity:

$$v = \frac{Q}{A} \quad (17)$$

Calculate mean tangential velocity, V_r :

$$V_r = \omega r_i \quad (18)$$

Reynolds number

When measuring the pressure drop in the string and the annulus, it is crucial to determine which of the three flow regimes which is present. The Reynolds number can be used to figure out the flow regime. The **Reynolds number** “**Re**” is a dimensionless number. It is a function of the ratio of inertial forces to viscous forces. The number quantifies the relative significance these two types of forces for given flow conditions. The Reynolds numbers are used to categorize if the flow regimes are in laminar, transitional or turbulent flow. The Reynolds numbers is for this thesis expressed by equation:

$$\text{Re, slot} = \frac{785D_{eff} \rho v_r}{\eta} \quad (19)$$

Where

$$D_{eff} = D_w - D_p \quad (20)$$

$$\eta = \mu_p + \frac{5YP(D_w - D_p)}{V_r} \quad (21)$$

And

- D_{eff} is the effective diameter (m)
- ρ is the density of the fluid (kg/m³)
- V_r is the rotational velocity of the drill pipe (SI units: m/s)

Other factors used in the equations are described as:

- D_w is the inside diameter of the annulus (m)
- D_p is the outside diameter of the drill pipe (m)
- μ_p is the plastic viscosity of the fluid (Pa·s)
- YP is Yield point (lbf/100sq ft)

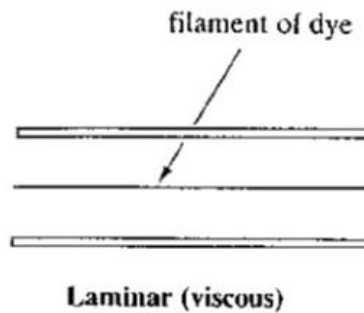
Flow patterns corresponded to Reynolds number:

- Laminar flow: $\text{Re} < 2000$
- Transitional flow: $2000 < \text{Re} < 4000$
- Turbulent flow: $\text{Re} > 4000$

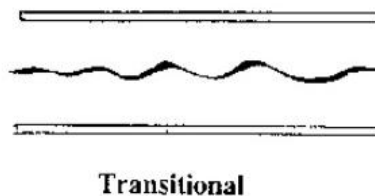
Fluid flow patterns /regimes

Figure 9 illustrates the three flow regimes.

Laminar flow = Characterized by parallel fluid lines that flow relative to each other and velocity that increases towards the center of the stream. Laminar flow typically occurs when the fluid is very viscous and the flow velocity is low. In laminar flow the motion of the particles of fluid is highly organized, with all the particles moving in straight lines parallel to the pipe walls.



Transitional flow = A mixture of laminar and turbulent flow, with laminar flow near the edges of the pipe and turbulence in the middle.



Turbulent flow = Characterized with chaotic motion and high velocity. In turbulent flow, the fluid layers mix together and create a mixture of all liquids in the pipe. Turbulent flow has advantages in cutting removal (conventional drilling method) because the turbulence helps to keep the particles in suspension.

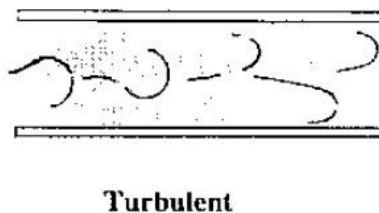


Figure 9: Displays the three flow regimes. [T02]

3.6 Theory of fluid mixture

Since there are only two forces (gravity and rotation) working on the heavy and light fluids, heavy light interface and mixing zone development can be predicted. If we assume that the two fluids are miscible, have the same properties (except density) and are contained within a positive inclined system, one may observe the following:

- With only the force of gravity affecting the system, the heavy light interface should be parallel with the horizontal plane (see figure 11 on next page for illustration).
- With the force of gravity and rotation affecting the system, the mixing interface would be normal to the wellbores inclination (θ) (see figure 12 on next page for illustration).
- The length of the mixing zone will not be longer than the length of the wellbore that is exposed to the mixing zone (see equation 24 below).

These assumed observations are quantified and illustrated below.

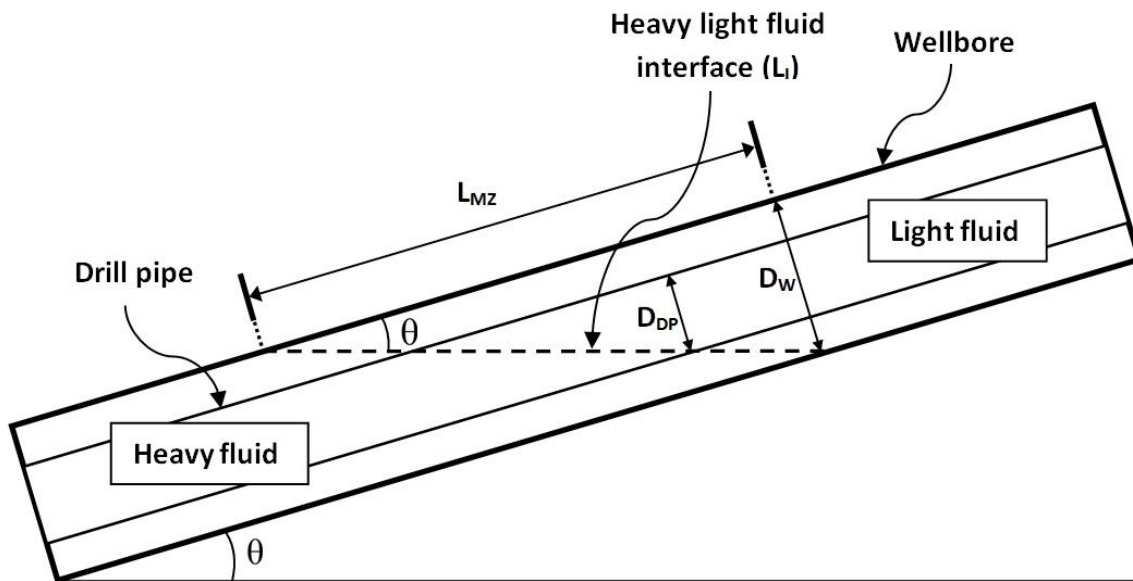


Figure 10: The heavy light fluid scenario displayed with the applicable component names and setup. [04]

The length of the mixing zone was calculated using Pythagoras:

$$L_I = \frac{D_W}{\sin \theta} \quad (22)$$

$$L_{MZ} = \sqrt{L_I^2 - D_W^2} \quad (23)$$

Insert equation 22 into 23 results in:

$$L_{MZ} = D_W \cot \theta \quad (24)^*$$

Where

L_{MZ} = Length of mixing zone

L_I = Length of heavy light interface

D_W = Diameter of wellbore

θ = Wellbore inclination

* = Not applicable for horizontal or negatively inclined wellbores.

Force of gravity

When the only force acting on the liquids is gravity, the two fluids will follow the path of least resistance and create a horizontal interface as displayed in figure 11.

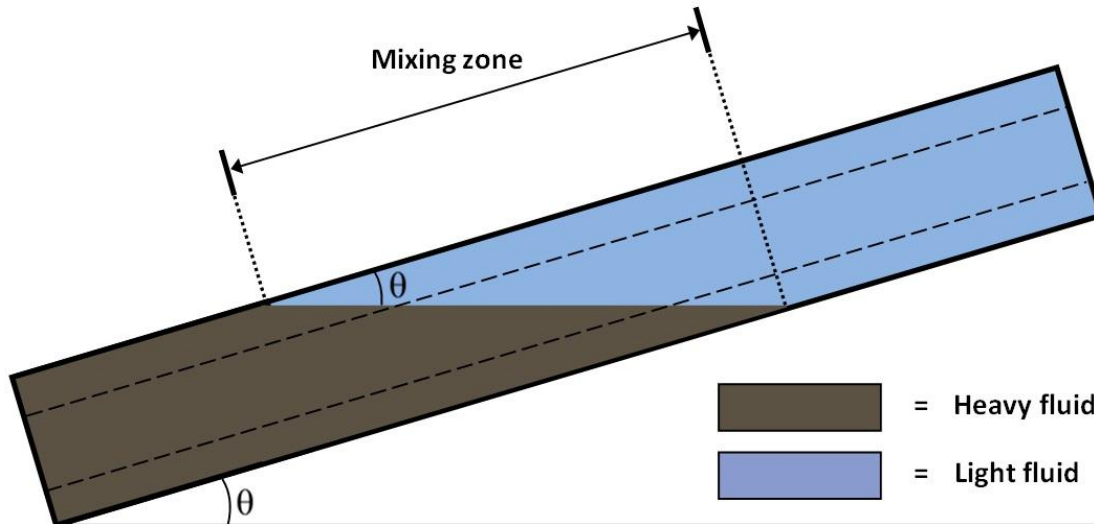


Figure 11: Showing the assumed heavy light interface when only the force of gravity affects the fluids. The dashed lines running throughout the figure represent the drill pipe. [04]

No mixing will occur in this scenario. The fluids and the interface will remain stagnant until an additional force is added.

Force of gravity and rotation

When rotational force is added, the heavy light interface moves and forms a vertical boundary, which is relative to the wellbore wall. Figure 12 illustrates this phenomenon.

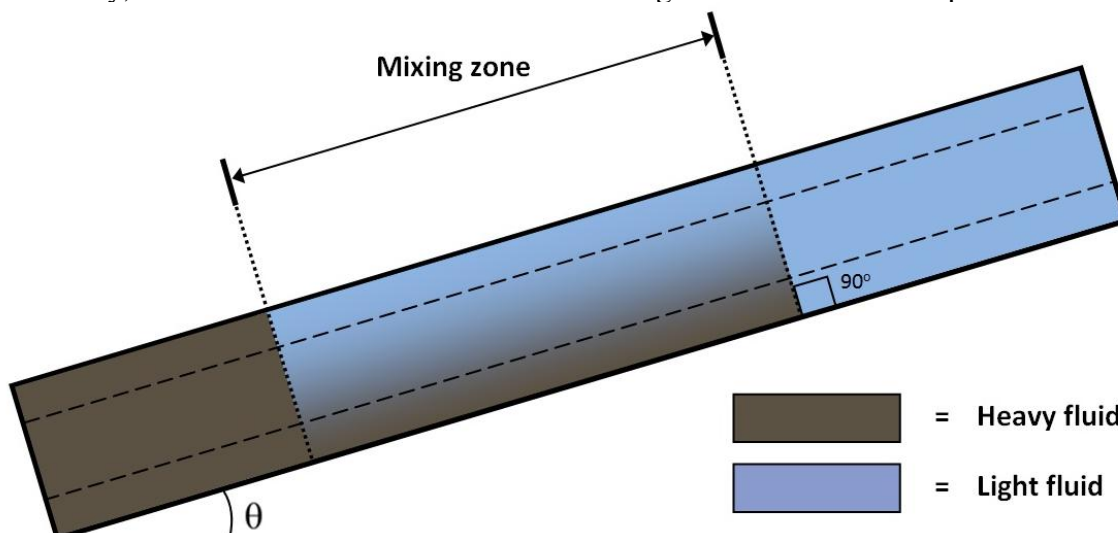


Figure 12: Showing the assumed heavy light interface when the forces of gravity and rotation affect the fluids. The dashed lines running throughout the figure represent the drill pipe. [04]

Since no axial force is provided by the force of rotation from the drill pipe, we can assume that no axial movement of the mixing zone will occur.

Density mixture (light + heavy viscosity mixture)

During kick influx (hydrocarbon or formation fluid), the influx will be mixed with drilling fluid. This modifies the density, the viscosity and the velocity of the fluid. Density is an important parameter that affects both the friction loss and hydrostatic pressures. Assuming that a certain concentration of mud mixed with the gas, the mixture density is given as (Steinar Evje and Kjell Kåre Fjelde, 2002 ^[T06]):

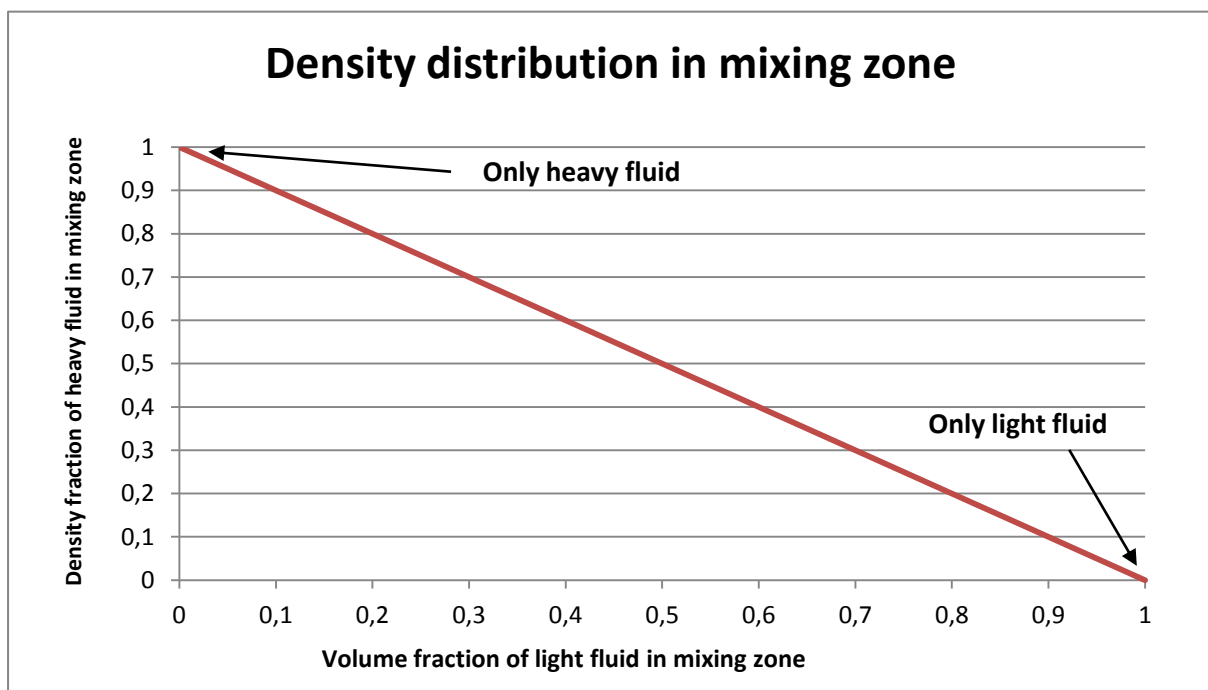
$$\rho_{mix} = \rho_g \alpha_g + (1 - \alpha_g) \rho_m \quad (25)$$

Phase volume fraction of gas and liquid, $\alpha_{g,l}$ is defined as:

$$\alpha_l = 1 - \alpha_g \quad (26)$$

Similarly, the mixture between heavy and light can be determined by equation 25 and the result is illustrated as in graph 4. Remember that the mud density, ρ_m is also a function of temperature and pressure.

The hydrostatic pressure is determined by the average density of mud and cuttings in the annulus. The frictional pressure losses depend on the wellbore geometry, the flow regimes, the pipe rotation and the drill string dynamics.



Graph 4: Displaying the distribution of density in the mixing zone. [02]

Effect of cutting concentration

The effective density of the mud can be determined from the fluid-fluid mix and cutting. This can be derived based on mass balance and given as:

$$\rho_{effective-mud} = \rho_{mix}(1 - C_v) + \rho_{cutting}C_v \quad (27)$$

Where C_v is cutting concentration in the annulus, ρ_{mix} is the density of drilling fluid, and $\rho_{cutting}$ is the density of cutting.

Viscosity mixture

Steinar Evje and Kjell Kåre Fjelde, 2002) also defined the mixture viscosity as [T06]:

$$\mu_{mix} = \mu_l\alpha_l + \mu_h\alpha_h \quad (28)$$

$\mu_{l,h}$ is the heavy and light phase viscosities

$$\alpha_l = 1 - \alpha_h \quad (29)$$

4 Experiments

[All experiments were conducted following the HSE standards of UIS and the Institute of petroleum]

To learn more about the interface mixture phenomenon, a series of experiments was conducted to observe the mixing and spread of the mixing zone between the light and heavy fluids. Every experiment was documented with pictures and videos, which are included in the thesis or in the attached CD as mp4 files.

To be able to conduct a large number of experiments, differently sized test rigs were made. Small scaled experiments allowed for more trial and error, and helped to sort out the importance of the different parameters. The larger scaled experiments would try to simulate the actual conditions and parameters of the RDM heavy over light.

All experiments used the horizontal plane as reference and as baseline for the measured inclination (see [Assumptions](#), section § 1.3)

Reelwell heavy light scenario

Reelwell has given a heavy light scenario, which this thesis will address and use as a benchmark. The following properties are given:

Inclination: 1°
RPM: 20 – 200
ROP: 5 – 10 m/h

Mud type	SG [kg/l]	PV [CPS]	YP [lbs/100ft ²]	LSR YP [lbs/100ft ²]	HTHP Fluid loss [ml/30min]	Drill solids [%]	Activity []	O/W ratio [%]	EI. Stability [Volt]
Heavy OBM	1,40	30	20	-	-	0	0,6	80/20	1000
Light OBM	1,10	20	20	-	-	0	0,6	80/20	1000

Table 2: Reelwell heavy light fluid properties. [R05]

4.1 Drilling fluid preparation and description

For the heavy part of the system, an 80/20 oil water ratio (OWR) drilling fluid was prepared in order to meet the desired Reelwell requirements. The drilling fluid was prepared according to MI-SWACO fluid formation procedure and the ingredients are products of MI-SWACO. The rheology and the physical properties of the fluid are measured.

The measurements were carried out at room temperature and pressure. However the properties are depending on the thermodynamics states.

For the light part of the system, food oil was used, having a density of 0.9sg. The density difference at the interface was designed to be 0.3sg. The main reason we didn't prepare a light mud, is because of barite discoloration. The discoloration made it impossible to obtain a contrast between the heavy and light fluid. It made it difficult to monitor the dynamics of the mixing zone.

To investigate the effect of density contrast, we vary the density of the heavy mud by adding an appropriate Baryte in order to obtain the desired density.

The drilling fluid consists of primarily three phases (oil, water, particles). The additives are Emulsifiers, Viscosifiers and Filter control substances.

The preparation procedure is displayed in Experimental fluids recipe and the viscosity information are shown in the individual test rigs Fluid system description (subsections § 5.3.4, 5.4.4, 5.5.4 and 5.6.4).

Experimental fluids recipe

When conducting experiments with the four test rigs, certain customized liquids were made to fit these experiments purposes. The recipes and preparation procedures of these liquids are displayed below.

Syrup 1 and 2

The two Syrup fluids were mixed with the trial and error method. Commercial syrup was added to water until desired density was reached.

Bentonite 1

Bentonite 1 was made by adding 50 g of bentonite to every 1000 g of water.

Baryte 1

The heavy WBM was made by adding a pre calculated amount of barite (see equation 30) to the Bentonite 1.

OBM 1, 2 and 3

Product name	Use	80/20 OBM	Mixing time
EDC 95/11	Base Fluid	440	
Paramul	Emulsifier	20	
Parawet	Wetting agent	8	5 min
Lime(Hydratkalk)	pH modifier	20	5 min
Water (mix water + salt separately and add the brine mixture)		137	
CaCl ₂ (mix water + salt separately and add the brine mixture)	Osmotic control	37	10 min
Versatrol M	Fluid loss control	10	5 min
Benton 128	Viscosifier	9	5min
Barite (All Grades)	Weighting agent	341	25 min

Table 3: Mud formulation and ingredients. [05]

Amount of needed Barite was calculated using equation

$$m_p = \frac{\rho_p}{\rho_f} * \frac{\rho_{ff} - \rho_f}{\rho_p - \rho_{ff}} * m_f \quad 30)$$

Where

m_p : Mass of particles (barite)

m_f : Mass of fluid

ρ_p : Density of particles (4.2sg)

ρ_f : Density of fluid

ρ_{ff} : Density of finished fluid

Diesel and Rapeseed oil mixture

The light fluid was made using the trial and error method. The goal was to make a light liquid with the same properties as used in Reelwells proposed fluid scenario. A diesel rapeseed oil ratio was first mixed and then tested with a Viscometer to see if the rheology matched. Results of the trial and error are shown in the table below:

Nr.	Diesel Rapeseed ratio	PV (cP)
1	4:1	6
2	2:1	8,5
3	1:1	14,5
4	4:5	17
5	2:3	20

Table 4: Trial and error diesel rapeseed ratio.

A diesel rapeseed ratio of 2:3 gave the correct plastic viscosity (PV) according to Reelwells fluid scenario.

4.2 Experiment equipment layout

Several different equipment, ingredients and tools were used prior, during and after the experiments. They can be divided into four main groups:

- Experiment tools: *Equipment/tools used to conduct the experiments.*
- Fabrication equipment: *Tools and equipment used under the fabrication process of the various test rigs and their components.*
- Measuring equipment: *Devices used to measure, test, inspect or examine parts or components in order to determine compliance with required specifications and/or tolerances.*
- Safety equipment: *Equipment used to protect individuals and personnel from hazardous conditions faced under experiments.*

For more info the four groups is displayed in [Appendix D](#), containing descriptions and pictures of used equipment and tools.

4.3 Test rig 1#

4.3.1 Purpose

The first test rig's purpose was to determine how different fluid parameters would affect the mixing of the heavy and light fluid. A small scale test rig was built with the intention of easily being able to execute a high number of experiments. The rig allowed for easy and uncomplicated testing of parameters such as:

- Inclination
- Viscosity
- Yield point
- Heavy light density differences

More realistic environments would be tested in a later part of the experimental phase.

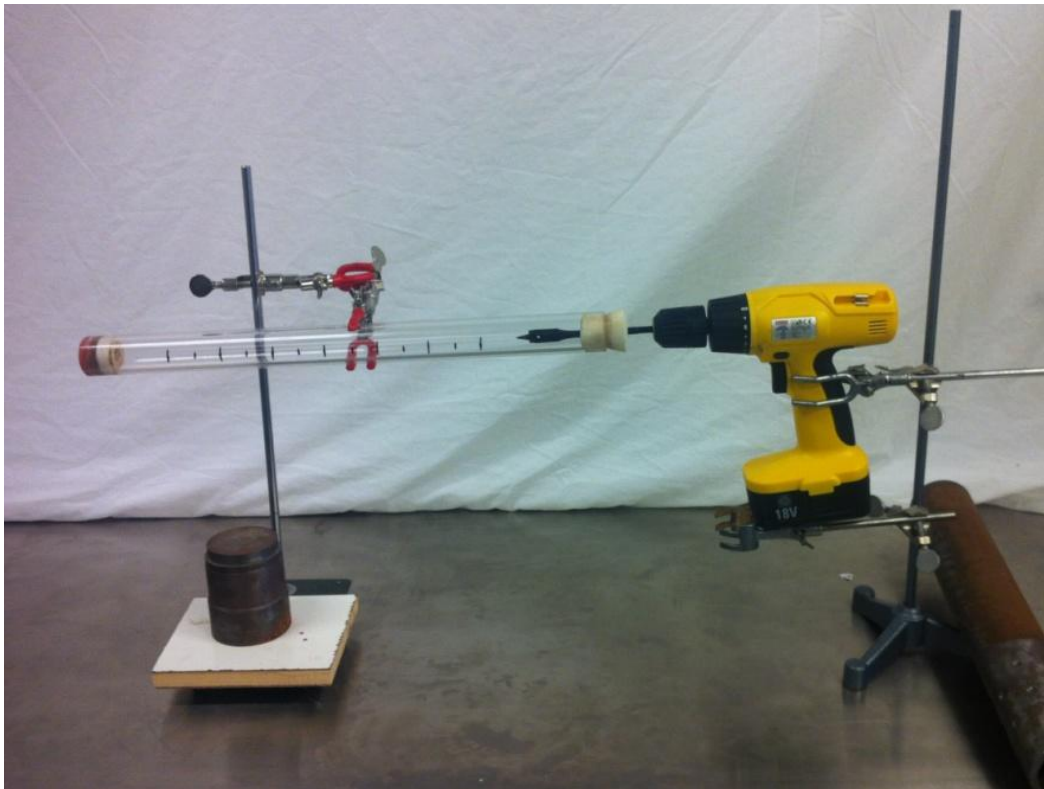
4.3.2 Experimental setup

[See [Appendix C – Test rig construction and experiment execution, test rig 1](#) for detailed information about construction and fabrication of test rig 1]

Rig # 1 is a 0,515 m length by 29,5 mm diameter well. In this rig a wood bit/blade, 14 mm width and 153 mm length, was rotated in the light fluid. It would represent a very simplified drill pipe. The tip of the blade was 28 mm away from the heavy/light interface (in vertical position) before the execution of the experiments. The test rig is shown in picture 1 below.

Wellbore		
Acrylic pipe	Length (mm)	515
	ID (mm)	29,5
	OD (mm)	39,7
Drill pipe		
Wood bit/blade	Length (mm)	153
	Size (mm)	14

Table 5: Test rig 1# setup specifics.



Picture 1: Test rig 1 # layout with used equipment positioned for a test of feasibility of future experiments. The acrylic pipe displayed has an inclination of 3,3° relative to the horizontal plane. The wood bit is as showed mounded trough the sponge plug into the drill. Weights are placed on both stands to ensure stability. [01]

4.3.3 Experiments test rig 1

4.3.3.1 Experiments 1, 2 & 3, effect of inclination

The main purpose of the first experiments was to see how the inclination of the test rig would affect the propagation of the mixing zone. The experiments objective was also to test the durability and rigidity of the rig. Stability and minimization of vibrations were also important factors during the execution of experiments 1, 2 and 3.

Used equipment

[See [Appendix D](#) for detailed information about used equipment and tools]

The equipment/tools used in experiment 1, 2 and 3 are listed in Used equipment test rig 1, [Appendix C](#), except for these modifications:

- Food dye (green)
- iPhone 4 (Ex. 1 & 2)
- GoPro Hero 2

Experiment specifications

All three experiments were conducted using water mixed with green food dye as the light fluid, and syrup 1 as the heavy fluid. Because both liquids are water based, they are miscible and can be mixed. The added food dye helped distinguish the heavy and light liquid, as well as illustrate the distribution of the mixing zone. As shown in the experimental setup, the mixing for test rig 1# was done by using a wooden drill bit. The drill bit was measured to rotate in excess of 1000 RPM.

Detailed parameter information is displayed below:

Experiment nr.	Ex.1	Ex.2	Ex.3
Light fluid	water + green dye	water + green dye	water + green dye
Heavy fluid	syrup 1	syrup 1	syrup 1
Inclination	27,2	12,3	3,3
Heavy light ratio	4:1	4:1	4:1
RPM	>1000	>1000	>1000
Duration	20 min	20 min	20 min
Direction of rotation	Clockwise	Clockwise	Clockwise

Table 6: Shows the technical data for experiments 1, 2 and 3. [02]

Execution

[Experiments 1, 2 and 3 followed the same procedure and execution]

The execution procedure listed in Experiment execution test rig 1, [Appendix C](#).

Specific uncertainties

Under the execution of experiments 1, 2 and 3 certain irregularities may have caused unplanned uncertainties. Listed are the events that were discovered:

- Experiment nr. 1 had the drill bit out of center which caused extensive vibrations. This may have caused the fluids to mix in an unpredictable manner.
- Experiment nr. 2 experienced fluctuating RPM in the end of the experiment, because of the lack of durable restrain of the drills trigger. The varying RPM may have reduced the mixing of the two liquids.

4.3.3.2 Experiment 4 & 6, Effect of high Yield point

Experiment 4 and 6 dealt with how a heavy liquid with high Yield point would affect the mixing zone. The experiments also examined how a heavy fluid with low density but high yield point would react and mix with a marginally lighter fluid.

Used equipment

[See [Appendix D](#) for detailed information about used equipment and tools]

The equipment/tools used in experiment 4 and 6 is listed in Used equipment test rig 1, [Appendix C](#), except for this modification

- Food dye (green and red)

Experiment specifications

Both experiments used the same heavy and light liquids: Bentonite 1 as heavy and dyed water as light. The main difference between the tests was that ex. 4 used a stagnant Bentonite 1 and ex. 6 used a sheared Bentonite 1. The heavy and light fluids in ex. 4 and 6 are water based and therefore miscible.

The inclination of the test rig was kept at 3,3 degrees to maintain a fixed parameter for the following experiments.

Detailed parameter information is displayed in the table below:

Experiment nr.	Ex.4	Ex.6
Light fluid	green dyed water	red dyed water
Heavy fluid	Bentonite 1	Bentonite 1 sheared
Inclination	3,3	3,3
Heavy light ratio	4:1	4:1
RPM	>1000	>1000
Duration	20 min	20 min
Direction of rotation	Clockwise	Clockwise

Table 7: Shows the technical data for ex. 4 and 6. [02]

Execution

[Experiments 4 and 6 followed the same procedure and execution]

The execution procedure listed in Experiment execution test rig 1, [Appendix C](#).

Specific uncertainties

Under the execution of experiments 4 and 6 certain irregularities may have caused unplanned uncertainties. Listed are the events that were discovered:

- Both experiments experienced that the heavy fluid tainted the inner wall of the acrylic tube. This resulted in some of the Bentonite 1 had been mixed with the light fluid before the test started. This may have affected the observation of the mixing zone interface.

4.3.3.3 Experiment 5 & 7, Effect of heavy WBM

The purpose of experiments 5 and 7 was to see how a barite saturated heavy fluid would react in a mixing situation. A second objective was to observe the effect of the density difference and how it would affect the propagation speed of the mixing zone.

Used equipment

[See [Appendix D](#) for detailed information about used equipment and tools]

The equipment/tools used in experiment 5 and 7 are listed in Used equipment test rig 1, [Appendix C](#), except for these modifications:

- Food dye (green and black)

Experiment specifications

Each of the experiments used Baryte 1 as heavy and dyed water as light fluid. The experiments were differentiated by the color of the light liquid. The water in ex. 5 had a green color (same as used in ex. 1, 2, 3 and 4) while the light fluid in ex. 7 were strongly dyed and had a black color. The black dye was added in ex. 7 to simplify the observation of the mixing zone propagation.

The inclination was kept at 3,3 degrees to ensure comparable results.

Detailed parameter information is displayed in the table below:

Experiment nr.	Ex.5	Ex.7
Light fluid	red dyed water	strongly dyed water (Black)
Heavy fluid	Baryte 1	Baryte 1
Inclination	3,3	3,3
Heavy light ratio	4:1	4:1
RPM	>1000	>1000
Duration	20 min	20 min
Direction of rotation	Clockwise	Clockwise

Table 8: Displays the technical data for ex. 5 and 7. [02]

Execution

[Experiments 5 and 7 followed the same procedure and execution]

The execution procedure listed in Experiment execution test rig 1, [Appendix C](#).

Specific uncertainties

Under the execution of experiments 5 and 7 certain irregularities may have caused unplanned uncertainties. Listed are the events that were discovered:

- Experiment 5 and 7 were exposed to similar uncertainties as ex. 4 and 6 because of the characteristics of the heavy fluid. The Barite 1 discolored the inner wall of the acrylic tube, which may have caused the mixing zone to spread faster.
- The uncertainty mentioned above (tainting of the acrylic wall) also reduced visibility into the tube. This made it difficult to place the correct amount of heavy liquid into the system. The circumstances may have had an effect on the expansion of the mixing zone.

4.3.4 Fluid system description

The rheology of the heavy fluids was measured using a (Fann) Viscometer. The liquids density was determined by using a mud scale.

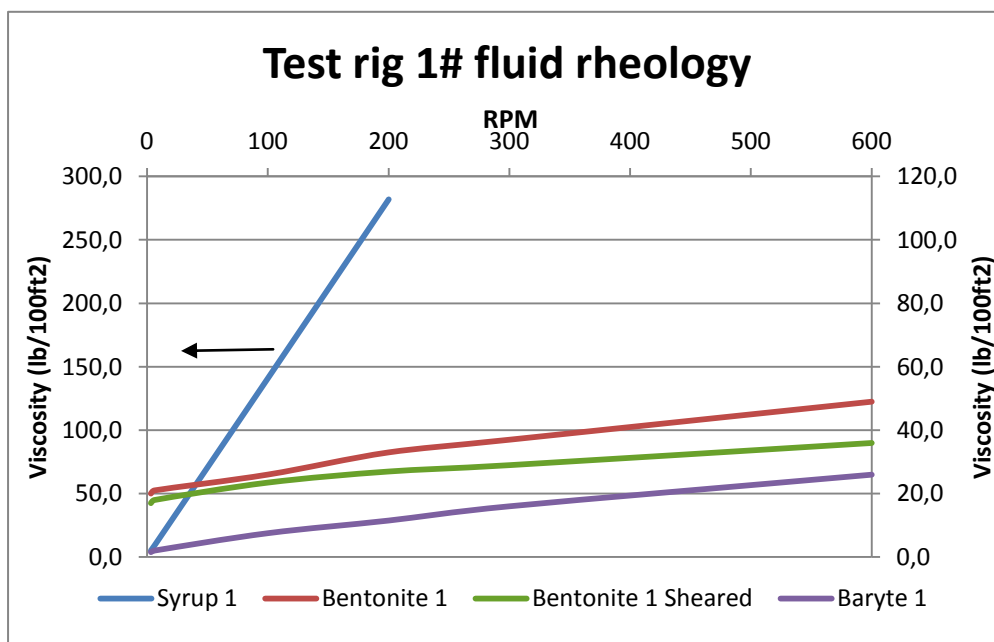
Rpm	Syrup 1	Bentonite 1	Bentonite 1 Sheared	Baryte 1
θ600	>300	49,0	36,0	26,0
θ300	>300	37,0	29,0	16,0
θ200	282,0	33,0	27,0	11,5
θ100	141,0	26,0	23,5	7,5
θ6	9,0	21,0	18,0	2,0
θ3	5,0	20,0	17,0	1,5

PV (cp)		12,0	7,0	10,0
YP (lb/100 ft ²)		25,0	22,0	6,0

ρ (s.g)	1,380	1,050	1,050	1,375
n		0,405	0,312	0,700

Table 9: Showing the fluid properties for the heavy liquids used in test rig 1#. [02]

 = Not able to measure/beyond the scale.

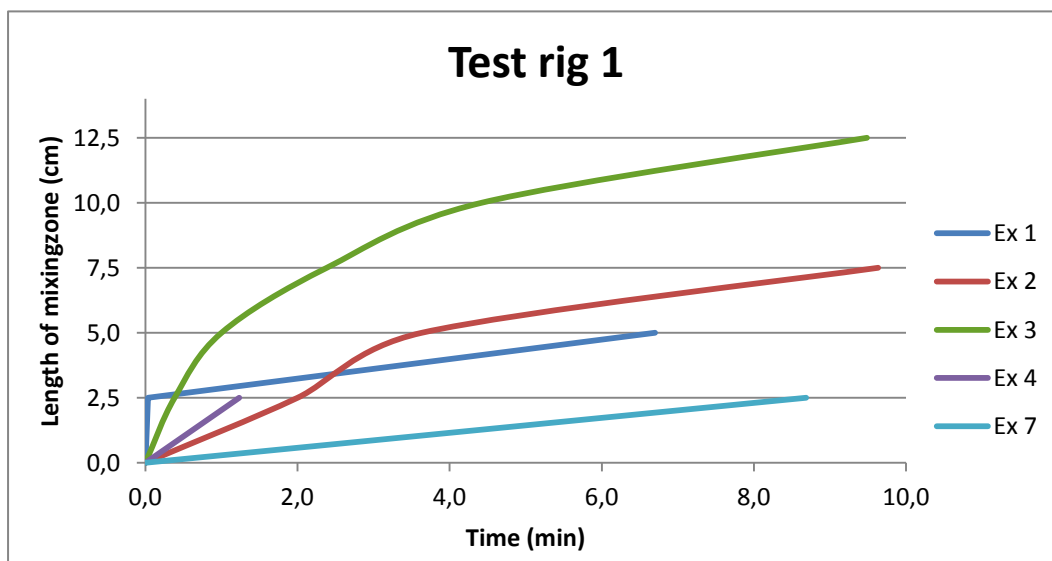


Graph 5: Displays the fluid rheology to the liquids used in test rig 1#. The vertical axis to the left refers only to Syrup 1. [02]

4.3.5 Results and analysis

This subsection presents the results obtained from experiments conducted with test rig 1# and discusses their significance. The discussion part of the subsection will discuss the results from “Experiment sheet”, pictures, as well as edited and unedited footage.

All measurable movement of the mixing zone in test rig 1# experiments were documented. Results of that documentation are shown in the graphs and tables below.

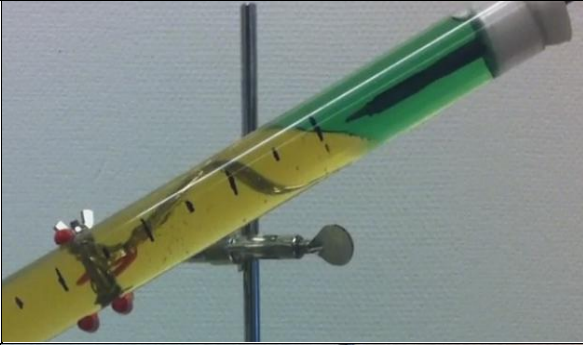
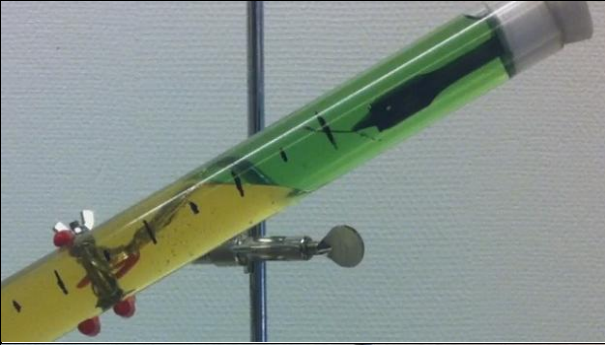
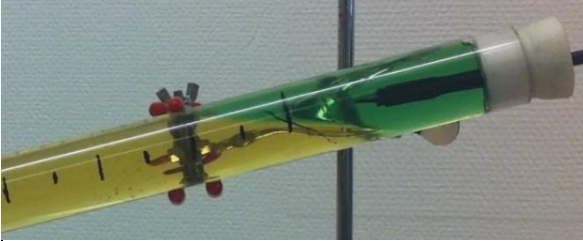





Graph 6: Illustrates the propagation of the mixing interface for all applicable experiments conducted with test rig 1#. [02]

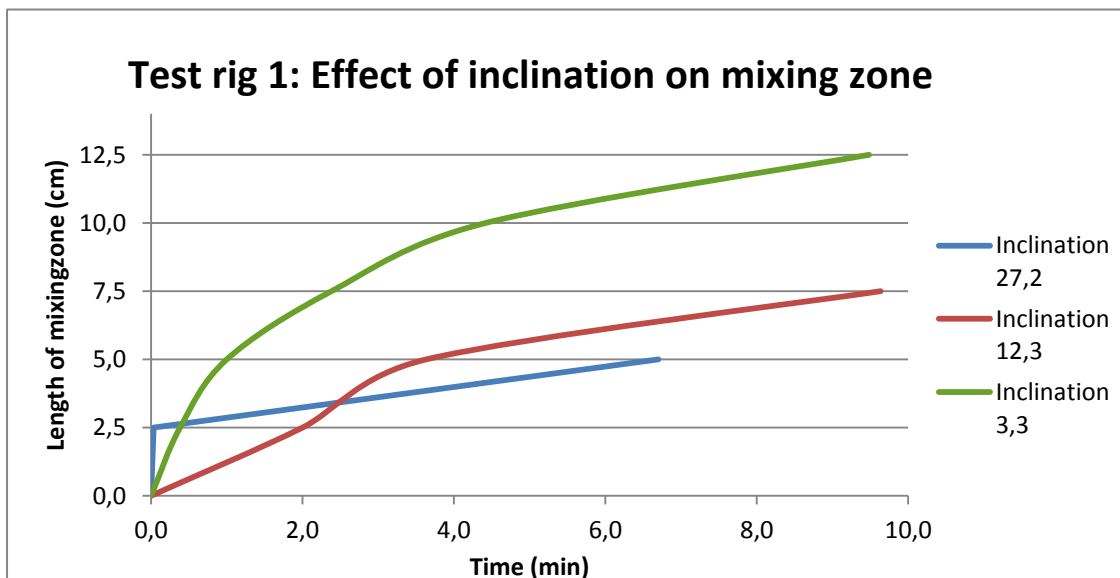
Experiments 5 and 6 are not displayed in the graph above due to inconclusive results. See specific experiments for more information.

Experiment 1, 2 and 3, Effect of inclination

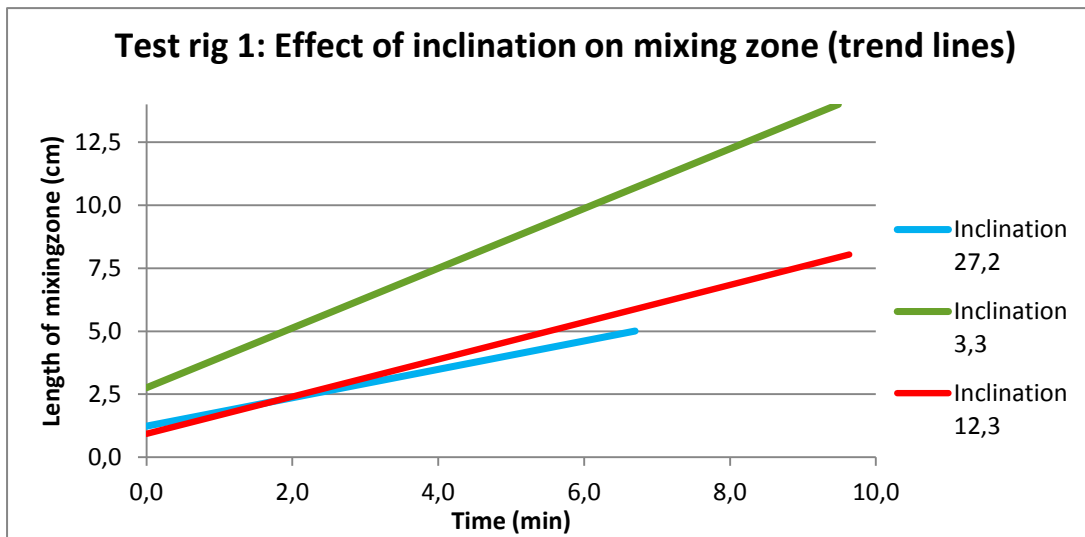
Results from the three experiments are displayed using screenshots from the experimental footage [03] and graphs and tables from the Experiment sheet [02].

Ex. info	Experiment start (time 0.00 min)	Experiment stop (time 20.00 min)
1# 27,2°		
2# 12,3°		
3# 3,3°		

Screenshot tables 1: Screenshots from the experimental footage taken under the execution of experiments 1, 2 and 3. [03]



Graph 7: Displays the effect of inclination gained from experiment 1, 2 and 3. [02]



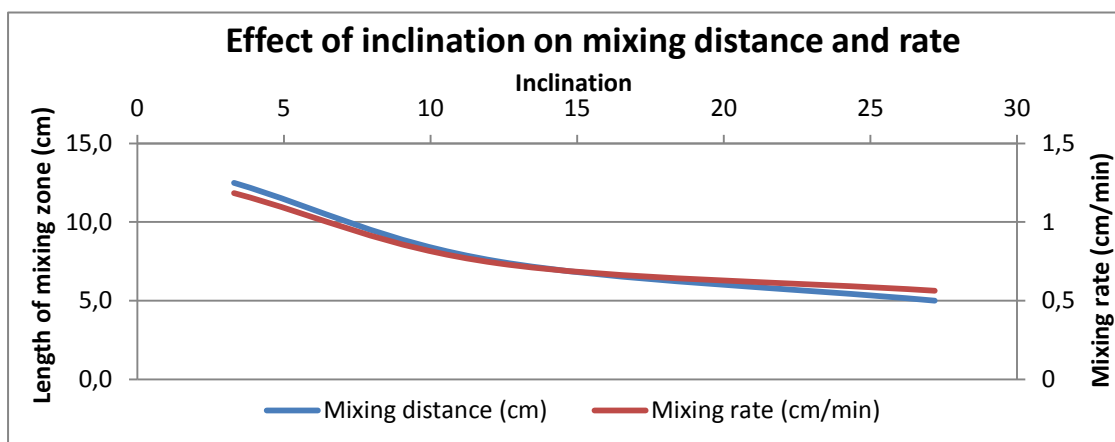
Graph 8: Trend lines of the curves displayed in graph 6. [02]

Graph 7 and 8 indicate that mixing speed correlates with inclination. Findings from experiment 1, 2 and 3 are displayed in the table below:

Inclination (degrees)	Trend line equation	Mixing distance (cm)	Mixing rate (cm/min)	Increased mixing distance (%)	Increased mixing rate (%)
27,2	$Y_{27,2} = 0,5625x + 1,2375$	5,0	0,5625	0	0
12,3	$Y_{12,3} = 0,7377x + 0,9343$	7,5	0,7377	33,33 %	23,75 %
3,3	$Y_{3,3} = 1,1848x + 2,7613$	12,5	1,1848	60,00 %	52,52 %

Table 10: Displaying the numerical data for the three experiments.

■ = Highest mixing distance and mixing rate
■ = Lowest mixing distance and mixing rate



Graph 9: Visual presentation of inclinations effect on mixing distance and mixing rate. [02]





As seen in table 10 and graph 9, inclination has a clear, significant effect on the movement of the mixing zone. As shown in graph 9 the mixing zone distance (cm) and mixing zones rate (cm/min) increases accordingly when the inclination drops.

With lower inclination, the heavy light fluid interface widens out and comes more and more in contact with the blade. This seems to initiate an accelerated mixing between the two liquids.

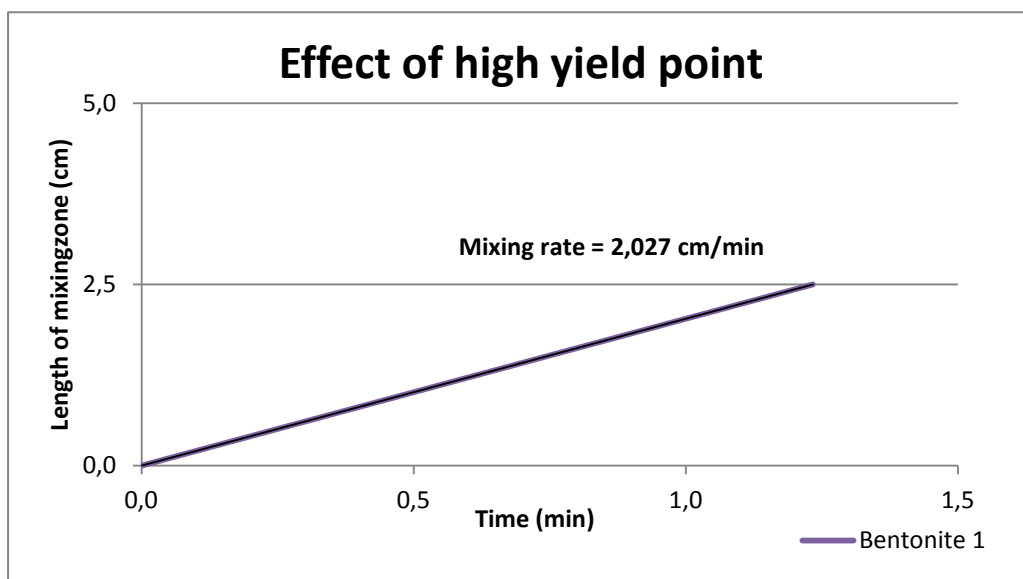
When the interface starts moving down the acrylic tube, it distances itself from the blade and the mixing starts decreasing. This event would not happen in a realistic scenario, where the entire system is affected by the disturbances from the drill pipe.

Experiment 4 and 6, Effect of high yield point

Experiment 4 and 6s results are displayed using screenshots from the experimental footage [03] and graphs and tables from the Experiment sheet [02].

Ex. Info.	Experiment start (time 0.00 min)	Experiment stop (time 20.00 min)
4# Bentonite 1		
6# Bentonite 1 sheared		

Screenshot tables 2: Screenshots of the experimental footage from the execution of experiments 4 and 6. [03]



Graph 10: Displays the data gained from experiment 4. [02]





As seen in screenshot table 2 and graph 9 the mixing zone propagation is marginal for experiment 4 and 6. The screenshots show that in experiment 6, the mixing zone interface does not reach the first measurement line, and the experiment is therefore not displayed in graph 9. Before the execution of the experiments it was expected to observe the highest mixing zone spread between the sheared Bentonite 1 and the dyed water. This was not the case. Bentonite 1 showed a higher reaction to the disturbances than the sheared bentonite 1. A fluid with lower PV and YP would be expected to mix more than a fluid with higher values.

A possible reason for the unexpected result was that the sheared Bentonite 1 had time to settle in the acrylic tube before the experiment started. As seen in the attached experimental CD the experiments mixing is uneven and random, which seem to have affected the end result.

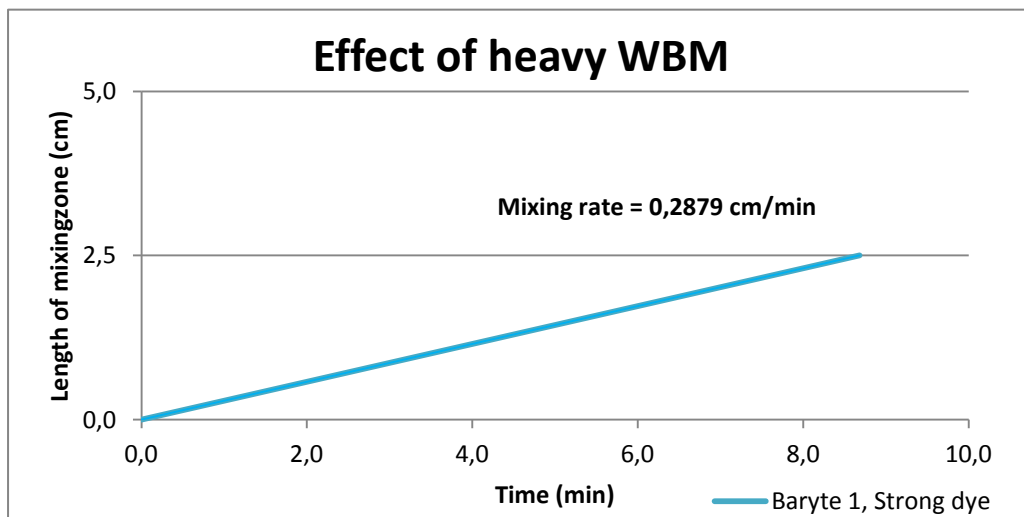
Even with the irregularities, experiment 4 and 6 indicates that a heavy fluid with high yield point will slow down the mixing between the two liquids.

Experiment 5 and 7, Effect of heavy WBM

Experiment 4 and 6s results are displayed using screenshots from the experimental footage [03] and graphs and tables from the Experiment sheet [02].

Ex. Info.	Experiment start (time 0.00 min)	Experiment stop (time 20.00 min)
5# Baryte 1 Weak dye		
7# Baryte 1 Strong dye		

Screenshot tables 3: Screenshots of the experimental footage from execution of experiments 5 and 7. [03]



Graph 11: Displays the data gained from experiment 7. [02]

Experiment 5 and 7s screenshot table and graph show diversities between the two similar tests. Experiment 5s results were inconclusive because of particle filled Baryte 1 overpowered the green dyed light fluid and therefore no mixing zone movement were observed.

Experiment 7 used a more strongly coloured light fluid which revealed that the heavy fluid remained stagnant and resisted most of the disturbances. The WBMs weight and its particles seemed to keep it settled even though the fluid rheology would suggest a more vigorous mixing, such as seen in experiment 5.

The weighting agent seems to have a positive effect on reducing the heavy light interfaces movement.

Conclusion test rig 1#

Out off all factors tested with test rig 1#, low inclination seem to have the highest effect on increasing the mixing zone movement (see table below). High density WBM and high YP Bentonite decreases on the other hand the movement.

Experiment nr.	Test purpose	Mixing distance (cm)	Mixing rate (cm/min)
Ex.1	Inclination 27,2	5,0	0,5625
Ex.2	Inclination 12,3	7,5	0,7377
Ex.3	Inclination 3,3	12,5	1,1848
Ex.4	High YP	2,5	2,0270*
Ex.7	Heavy WBM	2,5	0,2879

Table 11: Summary of viable results from test rig 1#.

* = Experiment 4 experienced a rapid mixing, but only for a short period. The mixing rate is not representable for the total duration of the experiment and can therefore be seen away from.

■ = Highest mixing distance and mixing rate
■ = Lowest mixing distance and mixing rate

Experiments performed with test rig 1# illustrates Reelwells heavy over light concept in a simplified manner. To approach a more realistic system, a drill pipe resembling body should be introduced. This would create genuine disturbances to the system and affect the entire heavy light interface. More genuine fluids similar to Reelwells drilling fluid program should also be tested.

4.4 Test rig 2#

4.4.1 Purpose

The purpose of test rig 2 was to investigate how the fluid interface would change when subjected to a rotating cylindrical body which resembled a drill pipe. Test rig 1 was remodeled to fit the new purpose and to accommodate the testing of other parameters. The new rig allowed for testing of factors like:

- RPM (Reduced capacity, see experiment 9)
- Heavy light fluid ratio
- Mixing of OBM's
- Effect of CW and ACW rotation

These new parameters were able to be tested because of the introduction of the cylindrical object, and the discovery of new measurement methods.

4.4.2 Experimental setup

[See [Appendix C – Test rig construction and experiments general specifications, Test rig 2](#) for detailed information about construction and fabrication of test rig 2]

Rig # 2 is a 0,515 m length by 29,5 mm diameter well. In this rig a plastic rod, 25,4 mm diameter and 560 mm length, was rotated in the entire system. The rod would represent a scaled down drill pipe. The test rig is shown in picture 2 below.

Data of actual wellbore and pipe sizes were gathered from Reelwell to secure correctly scaled experiments [equations 31 and 32 were used to calculate the rod diameter]:

$$\begin{aligned} \text{Wellbore diameter} &= 220 \text{ mm} \\ \text{Pipe OD} &= 190 \text{ mm} \end{aligned}$$

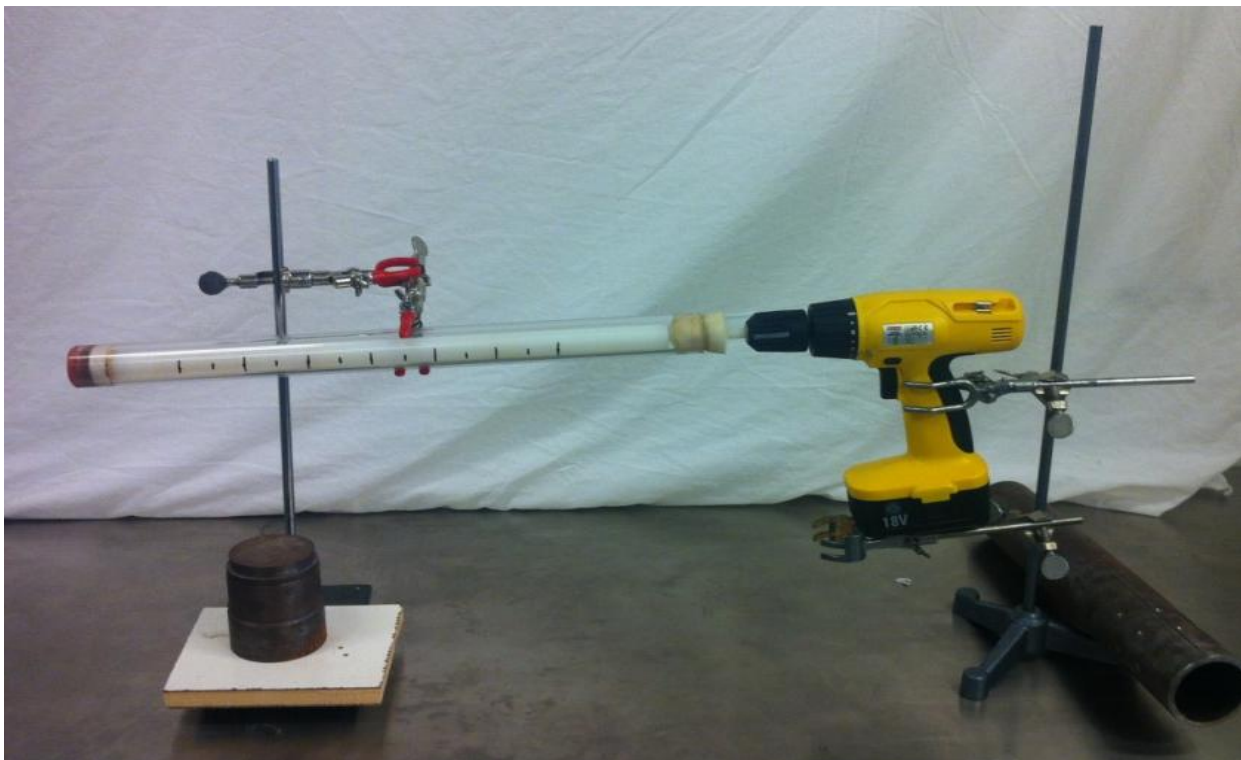
Inserted into equations 30 and 31:

$$\text{Size ratio} = \frac{220 \text{ mm}}{190 \text{ mm}} = 1,16$$

$$\text{Rod diameter} = \frac{29,50 \text{ mm}}{1,16} = \mathbf{25,43 \text{ mm}}$$

Wellbore		
Acrylic pipe	Length (mm)	515
	ID (mm)	29,5
	OD (mm)	39,7
Drill pipe		
Plastic rod	Length (mm)	560
	Diameter (mm)	25,4

Table 12: Test rig 2# setup specifics.



Picture 2: Test rig 2 # setup with used equipment positioned for a test of feasibility of future experiments. The acrylic pipe displayed has an inclination of 3,3° relative to the horizontal plane. The plastic rod is mounded trough the sponge plug into the drill. Weights are placed on both stands to ensure stability. [01]

4.4.3 Experiments test rig 2

4.4.3.1 Experiment 8 & 9, Effect of reduced RPM

The purpose of the eighth and ninth experiments was to explore the difference in mixing zone propagation between test rig 1 and 2. A second objective was to study the effect of reduced RPM on the mixing zone. The two experiments would also test the durability and stability of the new rig.

Used equipment

[See [Appendix D](#) for detailed information about used equipment and tools]

The equipment/tools used in experiment 8 and 9 are listed in Used equipment test rig 2, [Appendix C](#), except this modification

- Food dye (strong/black)

Experiment specifications

Both experiments used syrup 2 as heavy fluid and strongly dyed/black colored water as light fluid. The black dye added to the light liquid was the same as used in [Experiment 7](#). As previously mentioned it helped with differentiate the two fluids.

The difference between the two experiments was the RPM. Ex. 8 subjected the plastic rod to the same RPM used in test rig 1, while ex. 9 rotated the rod at a reduced rate.

The inclination was still kept at 3,3 degrees to maintain a fixed parameter from the first test rig. This allowed for comparable results between test rig 1 and 2.

More specific information is displayed in the table below:

Experiment nr.	Ex.8	Ex.9
Light fluid	water + strong food dye	water + strong food dye
Heavy fluid	syrup 2	syrup 2
Inclination	3,3	3,3
Heavy light ratio	4:1	4:1
RPM	>1000	reduced RPM*
Duration	20 min	20 min
Direction of rotation	Clockwise	Clockwise

Table 13: Displays the technical data for ex. 8 and 9. [02]

* = Not measured, assumed to be over 100 RPM.

Execution

[Experiments 8 and 9 followed the same procedure and execution]

The execution procedure listed in Experiment execution test rig 2 in [Appendix C](#).

Specific uncertainties

Under the execution of experiments 8 and 9 certain irregularities may have caused unplanned uncertainties. Listed are the events that were discovered:

- Experiment 9 was exposed to reduced rotation of the plastic rod, but the RPM was not measured. The extent of the RPM effect on the mixing zone propagation is therefore uncertain.

4.4.3.2 Experiment 10, 11, 12 & 13, Effect of heavy light ratio

The four experiments objective was to test the effect of the heavy light liquid ratio on the mixing zone distribution. The experiments also investigated the heavy fluids impact and its spread through the lighter liquid.

Used equipment

[See [Appendix D](#) for detailed information about used equipment and tools]

The equipment/tools used in the experiments are listed in Used equipment test rig 2, [Appendix C](#), except these modifications

- Food dye (strong/black, red)
- Marker tap

Experiment specifications

All four experiments had reversed heavy light fluid ratio. These experiments had therefore the light fluid in excess. This was done to observe the spread rate of the heavy liquid into the light liquid. Black dye was added to the heavy fluid in ex. 11, 12 and 13 to simplify the observation of the heavy fluids travel through the light fluid. Different heavy light fluid ratios were tested to clarify the effect it had on mixing zone behaviour when using a small test rig.

Inclination was still kept at 3,3 degrees.

More specific information is displayed in the table below:

Experiment nr.	Ex.10	Ex.11	Ex.12	Ex.13
Light fluid	water + strong food dye	water + weak red dye	water + weak red dye	water + weak red dye
Heavy fluid	syrup 2	syrup 2 + black dye	syrup 2 + black dye	syrup 2 + black dye
Inclination	3,3	3,3	3,3	3,3
Heavy light ratio	1:4	1:4	1:5	1:6
RPM	>1000	>1000	>1000	>1000
Duration	20 min	20 min	20 min	20 min
Direction of rotation	Clockwise	Clockwise	Clockwise	Clockwise

Table 14: Displays the technical data for ex. 10, 11, 12 and 13. [02]

Execution

[Experiments 10, 11, 12 and 13 followed the same procedure and execution]

The execution procedure listed in Experiment execution test rig 2, [Appendix C](#).

Specific uncertainties

When performing experiments 10, 11, 12 and 13 certain irregularities may have caused unplanned uncertainties. Listed are the events that were discovered:

- Experiment 10 had an excess of strongly colored light fluid. This made it impossible to observe the movement of the mixing zone.

4.4.3.3 Experiment 14 & 15, Effect of Clockwise (CW) and Anticlockwise (ACW) rotation

Experiment 14 and 15 explored the plastic rods groves effect on the movement of the mixing zone. Both experiments would also explore the light fluids mixing into the heavier liquid at low RPM.

Used equipment

[See [Appendix D](#) for detailed information about used equipment and tools]

The equipment/tools used in the experiments are listed in Used equipment test rig 2, [Appendix C](#), except these modifications:

- Food dye (strong/black)
- Marker tape

Experiment specifications

Experiment 14 and 15 used the same light fluid mix and the same heavy fluid as in previous experiments. The two experiments had measured RPM. A low RPM rate was kept to simplify observation of the mixing zone progression.

Inclination was maintained at 3,3 degrees.

More specific information is displayed in the table below:

Experiment nr.	Ex.14	Ex.15
Light fluid	water + strong food dye	water + strong food dye
Heavy fluid	syrup 2	syrup 2
Inclination	3,3	3,3
Heavy light ratio	4:1	4:1
RPM	63	62
Duration	20 min	20 min
Direction of rotation	Clockwise	Anticlockwise

Table 15: Displays the technical data for ex. 14 and 15. [02]

Execution

[Experiments 14 and 15 followed the same procedure and execution]

The execution procedure listed in Experiment execution test rig 2, [Appendix C](#).

Specific uncertainties

No specific uncertainties were detected under the execution of experiment 14 and 15.

4.4.3.4 Experiment 16 & 18, Effect of low RPM

The purpose of experiments 16 and 18 was to conduct similar experiments as ex. 11, 12 and 13, but with lower RPM. This was done to see the effect the RPM had on the mixing zone in a low heavy light ratio scenario.

Used equipment

[See [Appendix D](#) for detailed information about used equipment and tools]

The equipment/tools used in the experiments are listed in Used equipment test rig 2, [Appendix C](#), except these modifications:

- Food dye (strong/black, blue, red)
- Marker tape

Experiment specifications

The two experiments had the same heavy and light liquid configuration, but with different dye added. The variation in dyes were used as an attempt to clarify the mixing zone interface. A low RPM rate was held to maintain the simplified observation of the propagation of the mixing zone.

Inclination was maintained at 3,3 degrees.

More parameter information is displayed in the table below:

Experiment nr.	Ex.16	Ex.18
Light fluid	water + red dye	Water + red dye
Heavy fluid	syrup 2 + black dye	Syrup 2 + blue dye
Inclination	3,3	3,3
Heavy light ratio	1:6	1:6
RPM	65	63
Duration	20 min	15 min
Direction of rotation	Clockwise	Clockwise

Table 16: Displays the technical data for ex. 16 and 18. [02]

Execution

[Experiments 16 and 18 followed the same procedure and execution]

The execution procedure listed in Experiment execution test rig 2, [Appendix C](#).

Specific uncertainties

When performing experiments 16 and 18 particular irregularities may have caused unplanned uncertainties. Listed are the events that were discovered:

- When wrapping the drills trigger to a constant tension with the duct tape, certain give in the tape have caused slightly different rotational speeds in the two experiments. This may have affected the spread of the mixing zone.
- Both experiments had an unclear mixing distribution. This was due to dye compatibility failure. The mixing zone spread was therefore impossible to observe. See [Results and analysis](#) for more information.
- Experiment 18 was not run for the full 20 minutes because dye from the heavy fluid discoloured the acrylic tube.

4.4.3.5 Experiment 17, 19 & 20, Effect of heavy OBM and negative inclination

The three experiments would explore the mixing propagation of a heavy OBM through light cooking oil. The purpose of the experiments was also to test how the heavy OBM would react at different inclinations.

Used equipment

[See [Appendix D](#) for detailed information about used equipment and tools]

The equipment/tools used in the experiments are listed in Used equipment test rig 2, [Appendix C](#), except this modification:

- Marker tape

Experiment specifications

OBM 1 and olive oil were used as heavy and light fluid in the three experiments. The two fluids would simulate Reelwells authentic OBM program. To create a clear and observable contrast to the OBM 1 olive oil was used.

RPM was still kept low to get a more realistic rotational speed of the plastic rod.

Inclination of the acrylic tube was adjusted from 3,3 to -3,3 degrees after the execution of ex. 17. The negative inclination would represent a downwards slope in a horizontal well.

More parameter information is displayed in the table below:

Experiment nr.	Ex.17	Ex.19	Ex.20
Light fluid	olive oil	olive oil	olive oil
Heavy fluid	OBM 1	OBM 1 (stagnant)	OBM 1
Inclination	3,3	-3,3	-3,3
Heavy light ratio	1:6	1:6	1:6
RPM	67	64	64
Duration	21 min	25 min	21 min
Direction of rotation	Clockwise	Clockwise	Clockwise

Table 17: Displays the technical data for ex. 17, 19 and 20. [02]

Execution

[Experiments 16 and 18 followed the same procedure and execution]

The execution procedure listed in Experiment execution test rig 2, [Appendix C](#).

Specific uncertainties

When performing experiments 17, 19 and 20 certain irregularities may have caused unplanned uncertainties. Listed are the events that were discovered:

- Experiment 19 was performed using a stagnant OBM 1. This may have caused reduced mixing between the heavy and light fluid, and therefore affected the spread of the mixing zone.
- The three experiments experienced that the heavy fluid tainted the inner wall of the acrylic tube. This resulted in that some of the OBM 1 got mixed instantly when the test started. This may have affected the observation of the mixing zone interface.

4.4.4 Fluid system description

The rheology of the heavy fluids was measured using a (Fann) Viscometer. The liquids density was determined by using a mud scale.

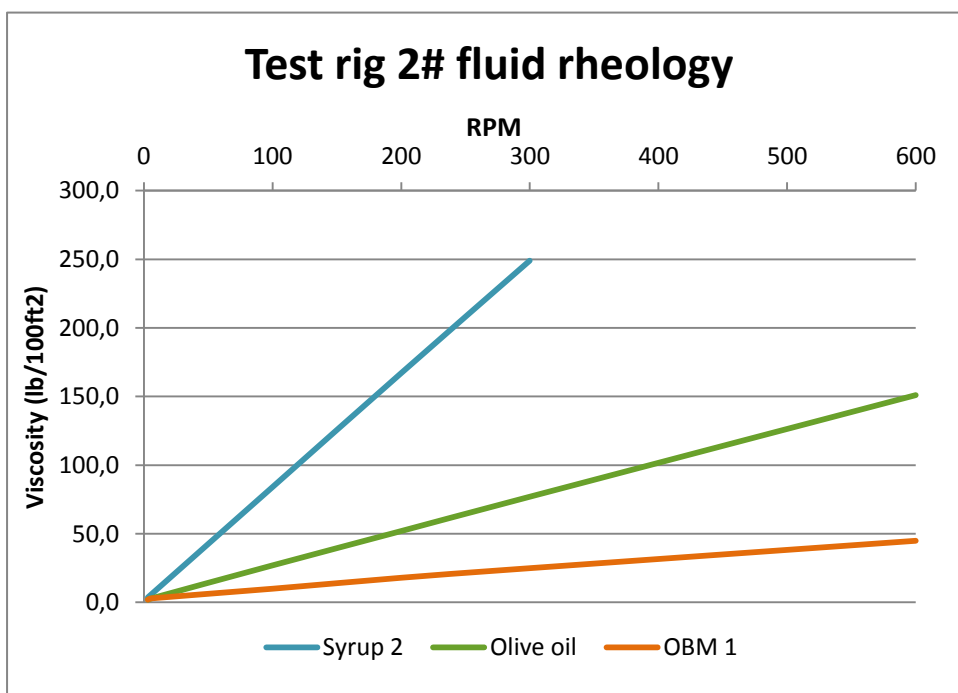
Rpm	Syrup 2	OBM 1	Olive oil
Ø600	>300	45,0	151,0
Ø300	249,0	25,0	77,0
Ø200	167,0	18,0	52,0
Ø100	84,0	10,0	27,0
Ø6	6,0	3,0	3,0
Ø3	3,5	2,0	2,0

PV (cp)	>51	20,0	74,0
YP (lb/100 ft2)	<198	5,0	3,0

ρ (s.g)	1,370	1,210	0,910
n		0,848	0,971

Table 18: Showing the fluid properties for the heavy and light fluids used in test rig 2#. [02]

 = Not able to measure/beyond the scale.

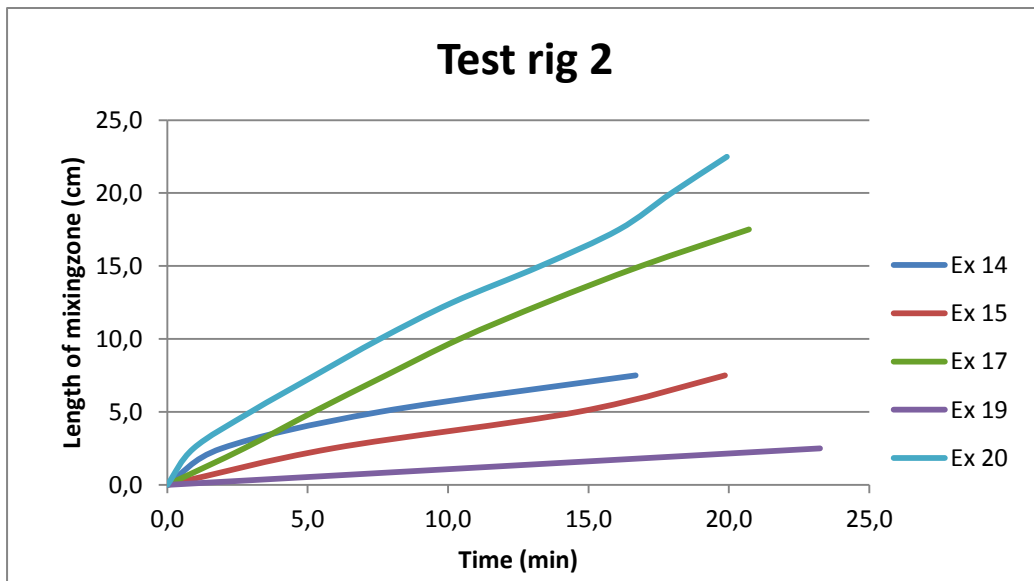


Graph 12: Displays the fluid rheology to the liquids used in test rig 2#. [02]

4.4.5 Results and analysis

This subsection presents the results obtained from experiments conducted with test rig 2# and discusses their significance. The discussion part of the subsection will discuss the results from “Experiment sheet”, pictures, as well as edited and unedited footage.

All measurable movement of the mixing zone in test rig 2# experiments were documented. Results of that documentation are shown in the graphs and tables below.



Graph 13: Illustrates the propagation of the mixing interface for all applicable experiments conducted with test rig 2#. [02]

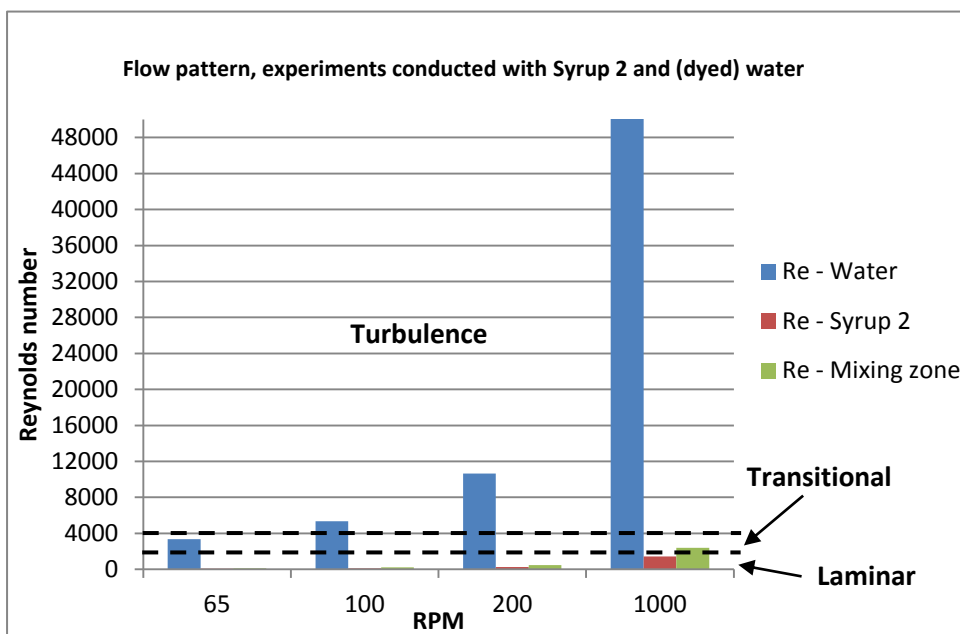






Chart 1: The flow pattern of test rig 2 experiments conducted with Syrup 2 and water. [02]

All experiments conducted with syrup and water can refer to the chart 1. It states that all syrup water experiments with rotational speed higher than 100 RPM has turbulence in the water phase flow. The turbulent flow may have affected the mixing zone propagation.

Experiment 8 & 9, Effect of reduced RPM

Experiment 8 and 9s results are displayed using screenshots from the experimental footage [03].

Ex. 8	High RPM
Experiment start Time 0.00 min	
Experiment stop Time 20.00 min	
Ex. 9	Reduced RPM*
Experiment start Time 0.00 min	
Experiment stop Time 20.00 min	

Screenshot tables 4: Screenshots from the experimental footage taken under the execution of experiments 8 and 9. [03]
* = Assumed to be over 100 RPM

The two experiments results were inconclusive in regard to observation of mixing zone movement. An excess of the blackly dyed water made the heavy light interface stretch through the entire acrylic tube in both experiments (see screenshot table 4). This made it difficult to observe any clear movement of the heavy light interface.









As seen in tables above and in the attached experimental CD, there is a noticeable difference between the experiment conducted with high RPM (ex. 8) and the one with reduced RPM (ex. 9).

The high RPM experiment has a distinct colour difference from the far left to the far right of the acrylic pipe. The distribution of heavy and light liquid seems to have arranged itself after the characteristics of the interface.

In the reduced RPM scenario, mixing zone spread is more uniform which is shown by the similar colour scheme. This development contradicts what is suggested by the Reynolds numbers in chart 1, where a higher rotation speed develops a more turbulent rotational flow.

Experiment 10, 11, 12 & 13, Effect of heavy light ratio

The four experiments results are shown using screenshots from the experimental footage [03].

Ex. 10	1:4 heavy light fluid ratio
Experiment start Time 0.00 min	
Experiment stop Time 20.00 min	
Ex. 11	1:4 heavy light fluid ratio
Experiment start Time 0.00 min	
Experiment stop Time 20.00 min	
Ex. 12	1:5 heavy light fluid ratio
Experiment start Time 0.00 min	
Experiment stop Time 20.00 min	
Ex. 13	1:6 heavy light fluid ratio
Experiment start Time 0.00 min	
Experiment stop Time 20.00 min	

Screenshot tables 5: Screenshots from the footage taken under the execution of experiments 10, 11, 12 and 13. [03]


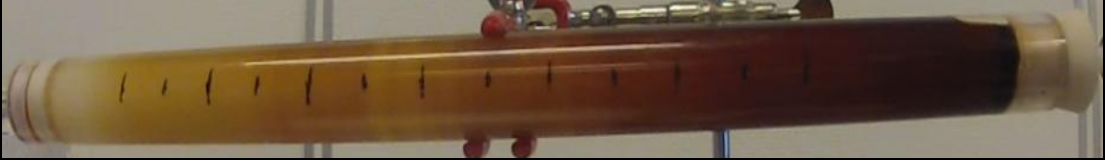


The four experiments resulted in no viable observation of the mixing zone. The dye added to the light fluid (ex. 10) and the heavy fluid (ex. 11, 12 and 13) overpowered the other fluids colour.

Since all experiments were conducted with very high RPM, the fluid movement in the experiments were in turbulence. The turbulence may have accelerated the discoloration of the fluid system.

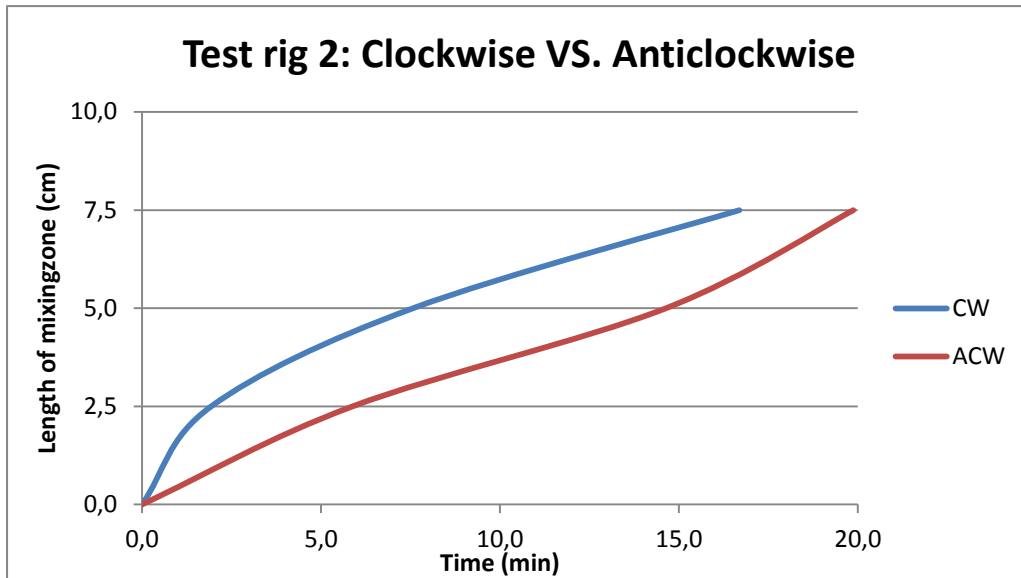
The black dye added to distinguish the heavy and light liquid seems to be too dominant, and clouded any mixing interface observation. Weaker doses of black dye may simplify observation in future experiments.

Experiment 14 & 15, Effect of Clockwise (CW) and Anticlockwise (ACW) rotation

Results from the three experiments are displayed using screenshots from the experimental footage [03] and graphs and tables from the Experiment sheet [02].

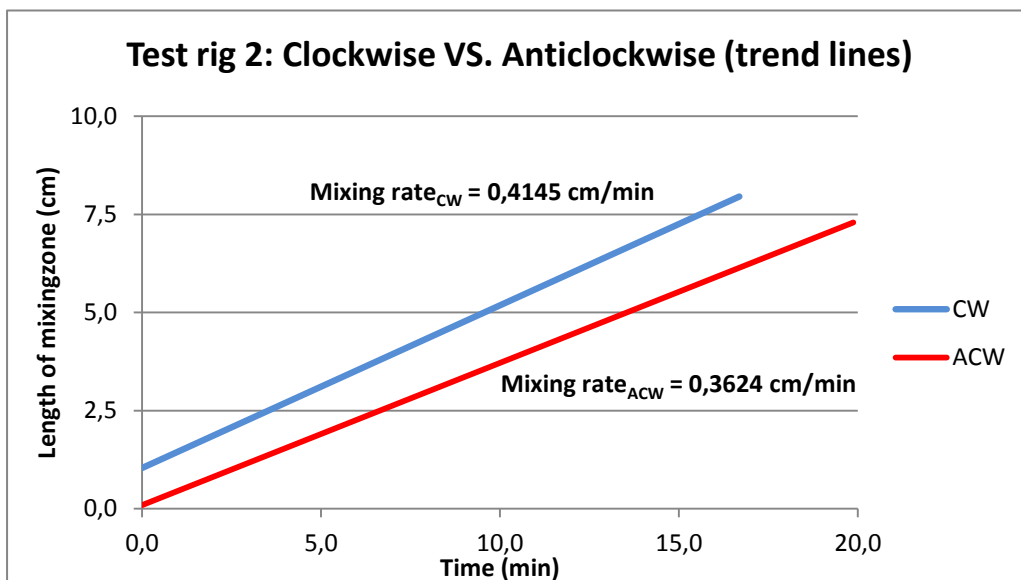
Ex. 14	CW
Experiment start Time 0.00 min	
Experiment stop Time 20.00 min	
Ex. 15	ACW
Experiment start Time 0.00 min	
Experiment stop Time 20.00 min	

Screenshot tables 6: Screenshots from the experimental footage taken under the execution of experiments 14 and 15. [03]



Graph 14: Displays the effect of CW and ACW gained from experiment 14 and 15. [02]

Experiment 14 and 15 showed that the plastic rods grooves have an effect on the mixing interface propagation. The graph 14 and the screenshot table 6 displays a noticeable difference between the experiments performed with CW and ACW rotation. The CW experiment have a more steep mixing rate before it levels out, while the ACW has a more linear trajectory.







Graph 15: Trend lines of the curves displayed in graph 14. [02]

This is supported by the displayed trend lines, that show that the mixing rates of the two experiments are different ($0,4145 \neq 0,3624$).

Experiment 16 & 18, Effect of low RPM

The two experiments results are displayed using screenshots from the experimental footage [03].

Ex. 16	
Experiment start Time 0.00 min	
Experiment stop Time 20.00 min	

Ex. 18	
Experiment start Time 0.00 min	
Experiment stop Time 20.00 min	

Screenshot tables 7: Screenshots from experimental the footage taken under the execution of experiments 16 and 18. [03]







As for experiments 10, 11, 12 and 13, the two tests experienced that the divisive dye scheme failed. Displayed in the table above, the dye malfunction is clear. No observable heavy light mixing interface was seen during experiments 16 and 18.

The low RPM had no noticeable effect on the colour contamination of the test system. The colour distribution spread at a similar rate as in the >1000 RPM scenarios (see attached experimental CD).

Dyed heavy fluids seem to have a negative effect on mixing zone movement observation.

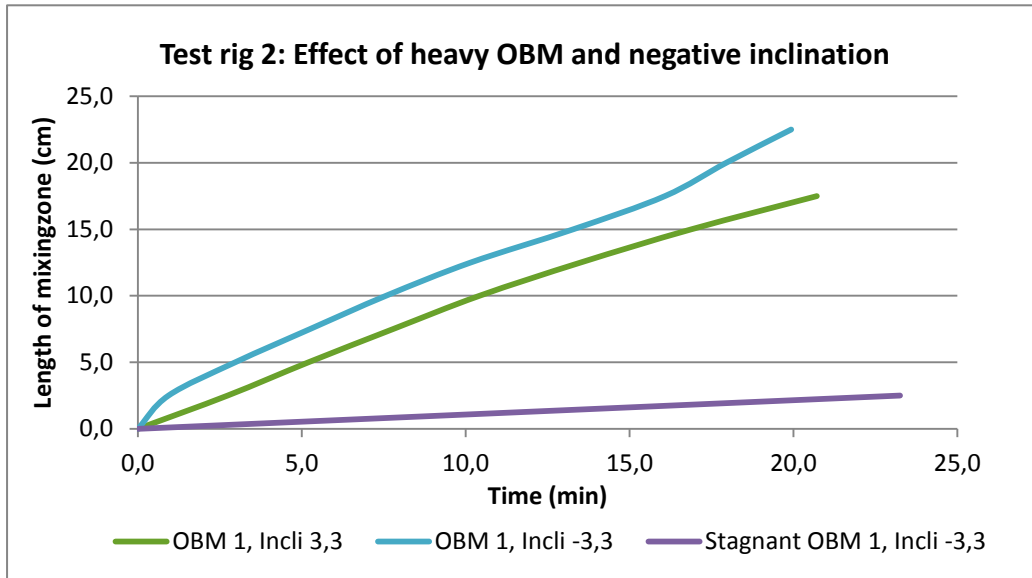
Experiment 17, 19 & 20, Effect of heavy OBM and negative inclination

Results from the three experiments are displayed using screenshots from the experimental footage [03] and graphs and tables from the Experiment sheet [02].

Ex. 17	OBM 1	inclination 3,3
Experiment start Time 0.00 min		
Experiment stop Time 21.00 min		
Ex. 19	Stagnant OBM 1	inclination -3,3
Experiment start Time 0.00 min		
Experiment stop Time 25.00 min		
Ex. 20	OBM 1	inclination -3,3
Experiment start Time 0.00 min		
Experiment stop Time 21.00 min		

Screenshot tables 8: Screenshots from the experimental footage taken under the execution of experiments 17, 19 and 20. [03]

The OBM 1 as heavy and the olive oil as the light fluid created a clear contrast to each other. This simplified the observation process.

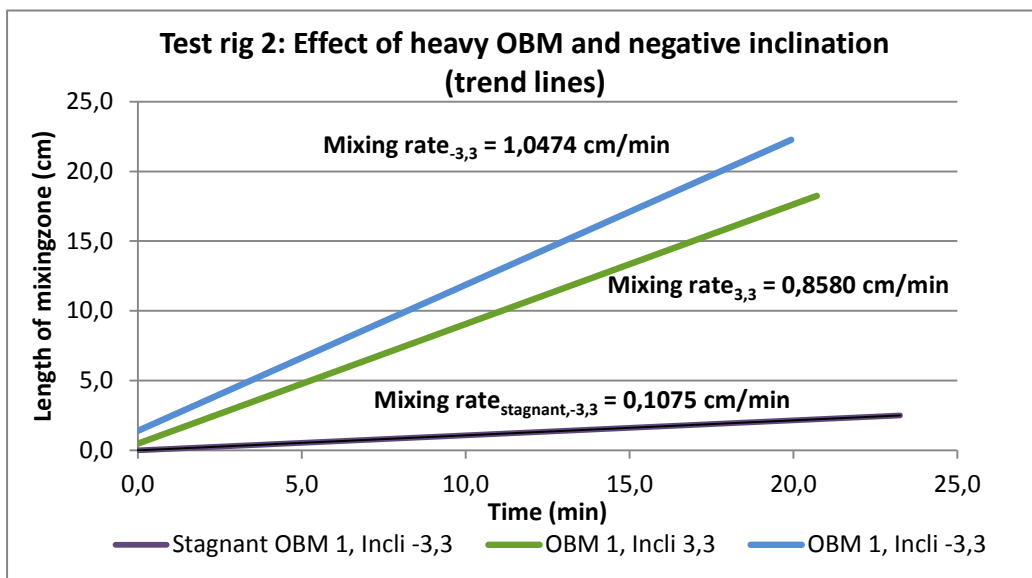


Graph 16: Displays the mixing effect of heavy OBM and negative inclination gained from experiments 17, 19 and 20. [02]

The three experiments showed a clear and observable mixing zone movement which is displayed in the screenshot table 8 and graph 16.

Experiment 19 was performed with OBM 1 which had not been stirred. This resulted in reduced mixing zone propagation.

The two other experiments showed a similar mixing interface movement. The negative inclination seems to have a minor, but noticeable impact on the spread rate of the mixing zone.



Graph 17: Trend lines of the curves displayed in graph 16. [02]

As seen in graph 17, the two comparable experiments have similar trend lines and mixing rates. The trend lines show that the negative inclination has an increasing effect on the heavy light interface movement. To explore further development, larger test parameters are needed.

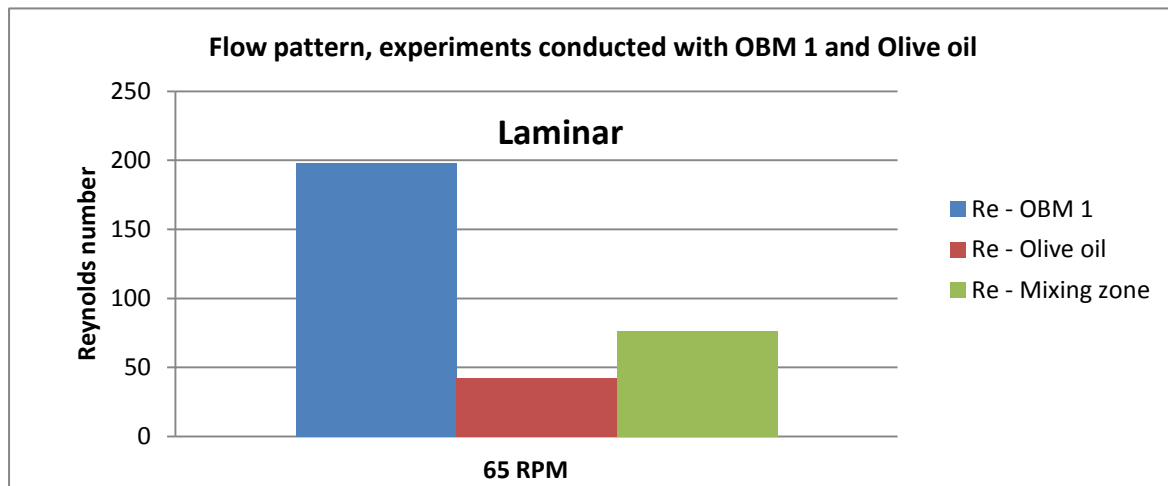


Chart 2: Shown the flow pattern of experiments conducted with OBM 1 and olive oil. [02]

The flow pattern for the three experiments shows that all the liquids are inside the laminar range by a wide margin. This means that the mixing zone is probably not affected by the fluids flow characteristics. Other parameters seem to govern the mixing zone behavior.

Conclusion test rig 2#

Out of all factors tested with test rig 2#, negative inclination seem to have the highest effect on increasing the mixing zone movement (see table below). On the other hand, stagnant OBM almost stopped heavy light interface propagation. This indicates that the rheology of the heavy fluid has a significant effect on the mixing zone distribution.

Experiment nr.	Test purpose	Mixing distance (cm)	Mixing rate (cm/min)
Ex.14	CW	7,5	0,4145
Ex.15	ACW	7,5	0,3624
Ex.17	OBM, inclination 3,3	17,5	0,8580
Ex.19	Stagnant OBM, inclination -3,3	2,5	0,1075
Ex.20	OBM, inclination -3,3	22,5	1,0474

Table 19: Summary of viable results from test rig 2#.

Red = Highest mixing distance and mixing rate
Green = Lowest mixing distance and mixing rate

Test rig 2#s experimental setup approached Reelwells heavy over light scenario, but it lacked size and predictability. RPM, inclination and pipe sizes are parameters that are varied under real conditions. A new test rig should have the capability to test and vary these parameters in experiments with longer duration and at a bigger scale.

4.5 Test rig 3 #

4.5.1 Purpose

The purpose of test rig 3# was to build on the knowledge and experience gained from the previous experiments and rigs. The new test rig would attempt to simulate the propagation of the mixing zone propagation in a more realistic environment. This meant that the run time of the experiments had to be longer, the test parameters had to be bigger and fluids with more realistic properties had to be used. The following parameters could now be tested (as well as previously tested parameters from test rig 1 and 2):

- More accurate RPM variations
- Different pipe ODs
- Prolonged experiment duration
- Extreme inclination variations
- Realistic fluid properties

With these new parameters the third test rig approached Reelwells realistic scenario, and results gained from it would shape the heavy light mixing conclusion.

In test rig #3 the effect of clockwise and anticlockwise rotation is assumed negligible due to the lack of lathe induced grooves and other disturbances created by the aluminum pipe.

4.5.2 Experimental setup

[See [Appendix C – Test rig construction and experiments general specifications, test rig 3](#) for detailed information about construction and fabrication of test rig 3]

Rig # 3 is a 2,0 m length by 32,0 mm diameter well. In this rig two aluminum pipes, OD 20,0 mm and 25,0 mm diameter and 2,014 m length, was rotated in the entire system. The pipes would represent two scaled down drill pipes.

The pipes were scaled after pipe and wellbore size data from Reelwell. Two pipe scenarios were chosen:

- **Scenario 1:** Wellbore size = 12 ¼” Pipe size = 7 ½”
- **Scenario 2:** Wellbore size = 8 ½” Pipe size = 7 ½”

This resulted in scaled down sizes using equation 30) and 31):

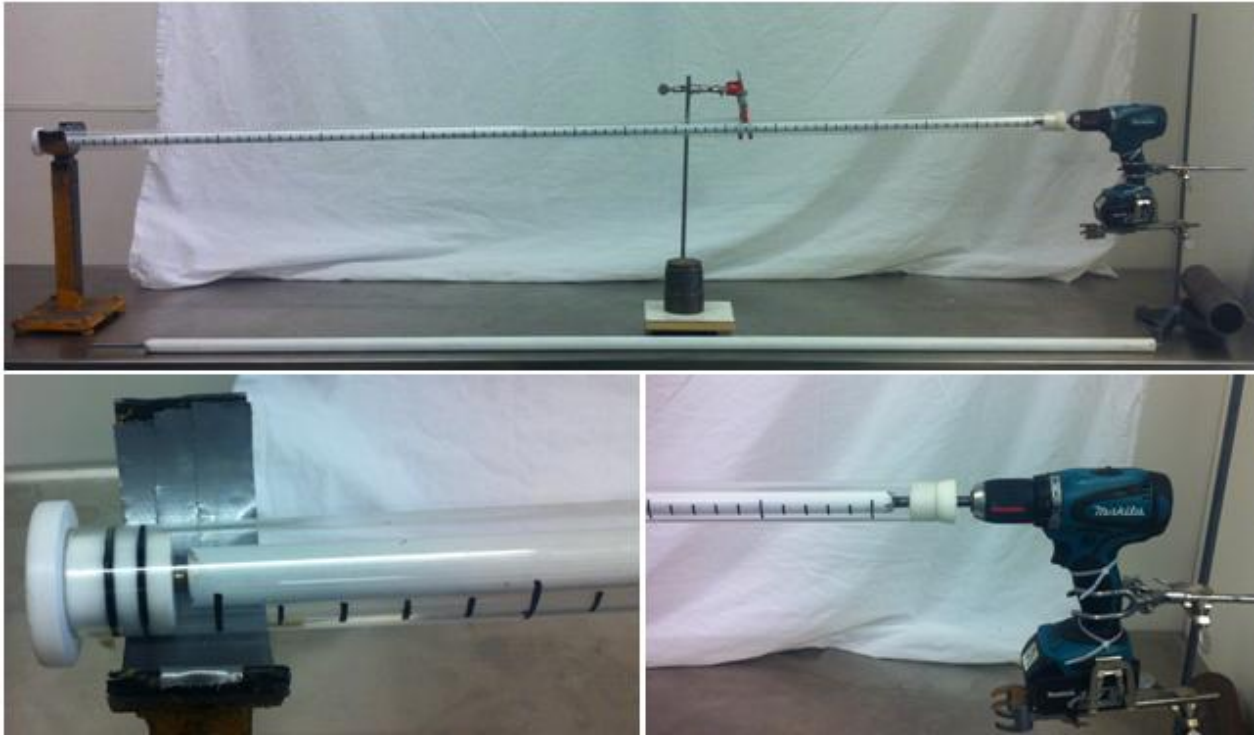
	Actual wellbore ID (mm)	Actual pipe OD (mm)	WB pipe ratio	Acrylic wellbore ID (mm)	Aluminum pipe OD (mm)	Bought pipe OD (mm)
Scenario 1	311,2	190,5	1,63	32,0	19,6	20,0
Scenario 2	215,9	190,5	1,13	32,0	28,2	25,0

Table 20: Aluminum pipe OD calculation. [02]

Because of inadequate supply, the pipe sizes 20 mm and 25 mm were used.

Wellbore		
Acrylic pipe	Length (m)	2,00
	ID (mm)	32
	OD (mm)	38
Drill pipe		
1# pipe	Length (m)	2,014
	Diameter (mm)	20
2# pipe	Length (m)	2,014
	Diameter (mm)	25

Table 21: Test rig 3# specifics.



Picture 3: Test rig 3 # setup with used equipment positioned for a test of feasibility of future experiments. The acrylic pipe displayed has an inclination of $2,0^\circ$ relative to the horizontal plane. The 20 mm diameter aluminum pipe is mounded through the sponge plug into the drill. The drill are fitted with different tensioned plastic strips. Weights are placed on both stands to ensure stability, while the workshop stand holds the heavy end in angle. [01]

4.5.3 Experiments test rig 3

4.5.3.1 Experiment 21, 22, 23 and 24, Effect of RPM and pipe size, Matrix 1

The purpose of the four experiments was to map how different RPM and pipe sizes effect the spread of the mixing zone. A secondary objective was to test the rigs durability and stability. Battery life of the camera and the drill were also tested.

Used equipment

[See [Appendix D](#) for detailed information about used equipment and tools]

The equipment/tools used in the experiments are listed in Used equipment test rig 3, [Appendix C](#).

No modification to that list was used in these experiments.

Experiment specifications

All four experiments used canola oil as the light liquid and OBM 2 as the heavy liquid. Canola oil was chosen because of its transparency. The feature would highlight the travel of the heavy fluid interfaces up through the acrylic pipe.

RPM and pipe size was varied from experiment to experiment to learn how the two parameters influence the mixing zone movement.

Inclination was put at 2,0 degrees to simulate more realistic conditions. The test rig was not positioned at Reelwells 1,0 degrees because of concerns about the spread of the heavy light interface.

More parameter information is displayed in the table below:

Experiment nr.	Ex.21	Ex.22	Ex.23	Ex.24
Light fluid	canola oil	canola oil	canola oil	canola oil
Heavy fluid	OBM 2	OBM 2	OBM 2	OBM 2
Inclination	2,0	2,0	2,0	2,0
Heavy light ratio	1:2	1:2	1:2	1:2
Pipe OD (mm)	20	20	25	25
RPM	60	150	60	150
Duration	60 min	60 min	60 min	60 min
Direction of rotation	Clockwise	Clockwise	Clockwise	Clockwise

Table 22: Displays the technical data for ex. 21, 22, 23 and 24. [02]

Execution

[Experiments 21, 22, 23 and 24 followed the same procedure and execution]

The execution procedure listed in Experiment execution test rig 3, [Appendix C](#).

Specific uncertainties

When performing experiments 21, 22, 23 and 24 certain irregularities may have caused unplanned events. Listed are the events that were discovered:

- Experiment 23 was performed without using the plastic hose to fill the acrylic tube with heavy fluid. The event made it impossible to observe the mixing zone distribution.

4.5.3.2 Experiment 25, Effect of low viscous light fluid

Experiment 25s main objective was to test the effect of a low viscous light fluid had on the expansion of the mixing zone interface. The experiment would also represent worst case scenario when it came mixing between a heavy and light oil-based liquid.

Used equipment

[See [Appendix D](#) for detailed information about used equipment and tools]

The equipment/tools used in the experiments are listed in Used equipment test rig 3, [Appendix C](#).

No modification to that list was used in these experiments.

Experiment specifications

The experiment used gasoline grade diesel as light liquid and the OBM 2 as heavy. Diesel was used for its viscous abilities which would create a strong contrast to the canola oil used in the previous experiments. The diesel is also a clear fluid, which would simplify interface observation.

Inclination was kept at 2,0 degrees.

More parameter information is displayed in the table below:

Experiment nr.	Ex.25
Light fluid	diesel
Heavy fluid	OBM 2
Inclination	2,0
Heavy light ratio	1:4
Pipe OD (mm)	20
RPM	60
Duration	60 min
Direction of rotation	Clockwise

Table 23: Displays the technical data for ex. 25. [02]

Execution

[Experiment 25 followed the same procedure and execution]

The execution procedure listed in Experiment execution test rig 3, [Appendix C](#).

Specific uncertainties

No specific uncertainties were detected.

4.5.3.3 Experiment 26, 27, 28 and 29, Effect of RPM and pipe size, Matrix 2

The four experiments main objective was to build on experience gained from previous test rig 3# experiments. RPM and pipe sizes mixing effect would be tested in these experiments.

Used equipment

[See [Appendix D](#) for detailed information about used equipment and tools]

The equipment/tools used in the experiments are listed in Used equipment test rig 3, [Appendix C](#).

No modification to that list was used in these experiments.

Experiment specifications

Experiments 26, 27, 28 and 29 used diesel + rapeseed oil as light fluid while OBM 2 were used as heavy fluid. The diesel + rapeseed light liquid was used to create a more similar fluid system relative to Reelwells OBM program.

Inclination was kept at 2,0 degrees.

More parameter information is displayed in the table below:

Experiment nr.	Ex.26	Ex.27	Ex.28	Ex.29
Light fluid	diesel + rapeseed oil	diesel + rapeseed oil	diesel + rapeseed oil	diesel + rapeseed oil
Heavy fluid	OBM 2	OBM 2	OBM 2	OBM 2
Inclination	2,0	2,0	2,0	2,0
Heavy light ratio	1:4	1:4	1:4	1:4
Pipe OD (mm)	20	20	25	25
RPM	60	150	60	150
Duration	60 min	60 min	60 min	60 min
Direction of rotation	Clockwise	Clockwise	Clockwise	Clockwise

Table 24: Displays the technical data for ex. 26, 27, 28 and 29. [02]

Execution

[Experiments 26, 27, 28 and 29 followed the same procedure and execution]

The execution procedure listed in Experiment execution test rig 3, [Appendix C](#).

Specific uncertainties

No specific uncertainties were detected.

4.5.3.4 Experiment 30 and 31, Effect of negative inclination

Experiment 30 and 31 would explore the effect of negative inclination and distinguish between mixing in a positive and negative tilt.

Used equipment

[See [Appendix D](#) for detailed information about used equipment and tools]

The equipment/tools used in the experiments are listed in Used equipment test rig 3, [Appendix C](#).

No modification to that list was used in these experiments.

Experiment specifications

Both experiments had the same fluid configuration as experiments 26, 27, 28 and 29 except for the utilization of OBM 3 instead of OBM 2. Test 30 had a negative inclination of -2,0 degrees to simulate a downwards slope in a horizontally planned wellbore.

Experiment 31 was done as a technical exercise, with an unlikely inclination of -90,0 degrees.

More parameter information is displayed in the table below:

Experiment nr.	Ex.30	Ex.31
Light fluid	diesel + rapeseed oil	diesel + rapeseed oil
Heavy fluid	OBM 3	OBM 3
Inclination	-2,0	-90,0
Heavy light ratio	1:4	1:4
Pipe OD (mm)	20	25
RPM	60	150
Duration	60 min	60 min
Direction of rotation	Clockwise	Clockwise

Table 25: Displays the technical data for ex. 30 and 31. [02]

Execution

[Experiments 30 and 31 followed the same procedure and execution]

The execution procedure listed in Experiment execution test rig 3, [Appendix C](#).

Specific uncertainties

No specific uncertainties were detected.

4.5.4 Fluid system description

The rheology of the heavy fluids was measured using a (Fann) Viscometer. The liquids density was determined by using a mud scale.

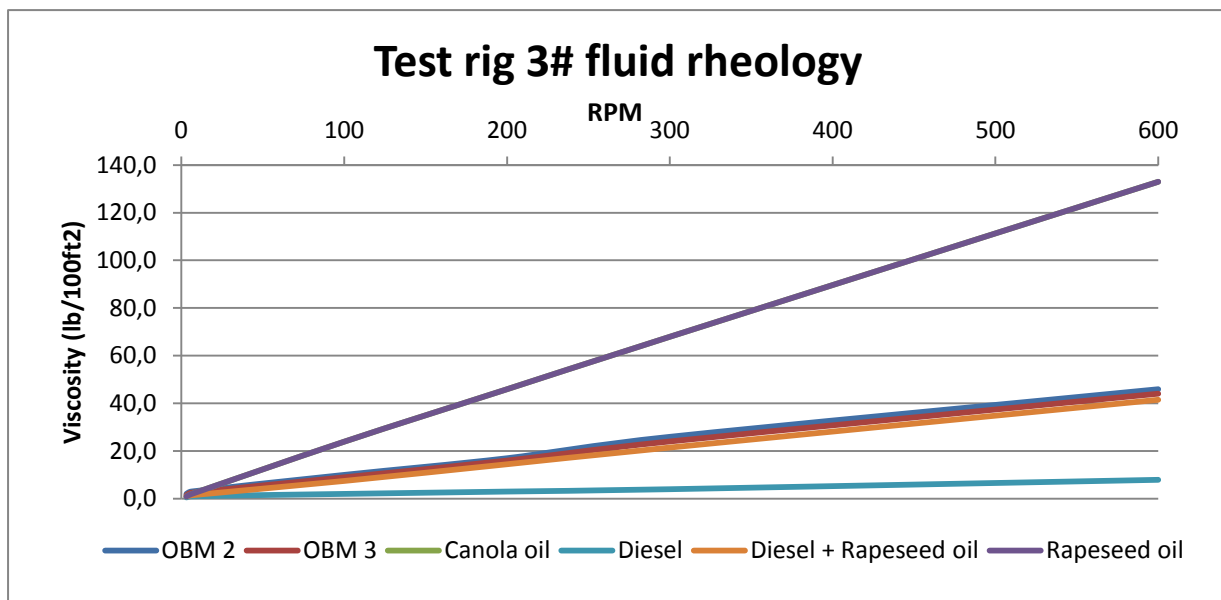
Rpm	OBM 2	OBM 3	Canola oil*	Rapeseed oil*	Diesel	Diesel + Rapeseed oil
θ600	46,0	44,0	133,0	133,0	8,0	41,5
θ300	26,0	24,0	68,0	68,0	4,0	21,5
θ200	17,0	16,0	46,0	46,0	3,0	14,5
θ100	10,0	9,0	24,0	24,0	2,0	7,5
θ6	3,0	2,5	2,0	2,0	1,0	1,5
θ3	2,0	1,5	1,0	1,0	0,5	1,0

PV (cp)	20,0	20,0	65,0	65,0	4,0	20,0
YP (lb/100 ft ²)	6,0	4,0	3,0	3,0	0,0	1,5

ρ (s.g)	1,215	1,200	0,915	0,915	0,845	0,885
n	0,823	0,874	0,967	0,967	0,999	0,948

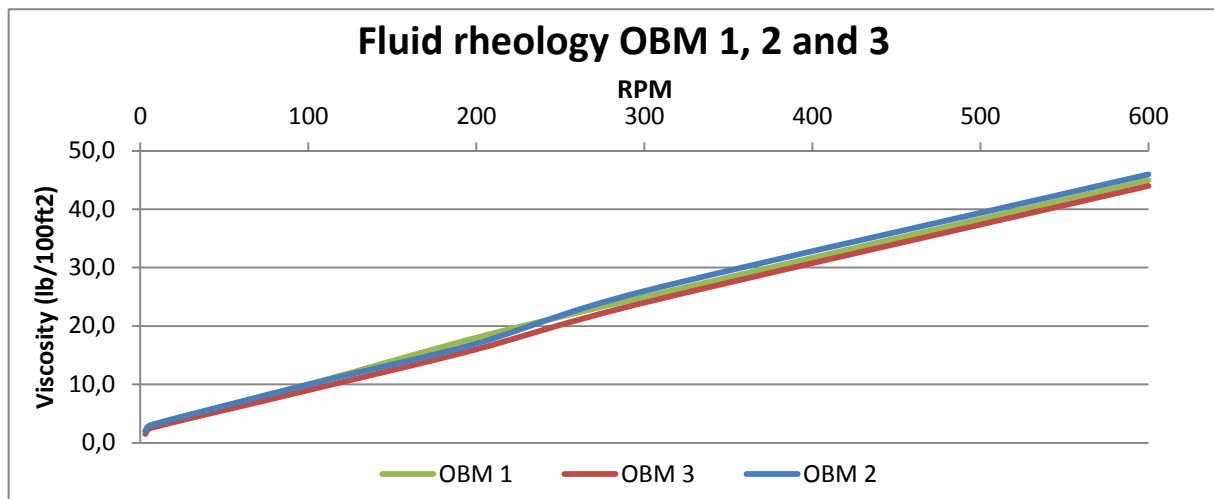
Table 26: Showing the fluid properties for the heavy and light fluids used in test rig 3#. [02]

* = Canola and Rapeseed are the same oil type. Both are displayed because of the use of both terms in thesis.



Graph 18: Displays the fluid rheology to the liquids used in test rig 3#. [02]

As shown in [Drilling fluid preparation and description](#) OBM 1, 2 and 3 have the same recipe. Irregularities in rheology illustrated in graph 19 are due to errors committed when creating the fluids as well as uncertainties in measurement equipment. The irregularities are assumed negligible with regard to comparing experiments performed with the heavy liquid.

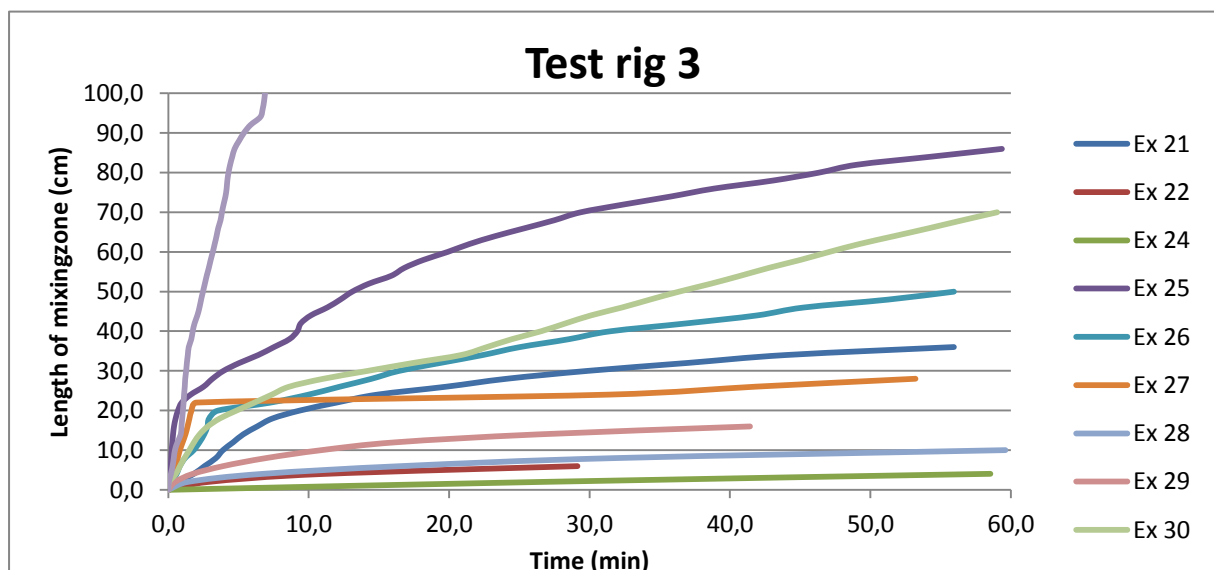


Graph 19: Displays the fluid rheology to OBM 1, 2 and 3. [02]

4.5.5 Results and analysis

This subsection presents the results obtained from experiments conducted with test rig 3# and discusses their significance. The discussion part of the subsection will discuss the results from “Experiment sheet”, pictures, as well as edited and unedited footage.









All measurable movement of the mixing zone in test rig 3# experiments were documented. Results of that documentation are shown in the graphs and tables below.



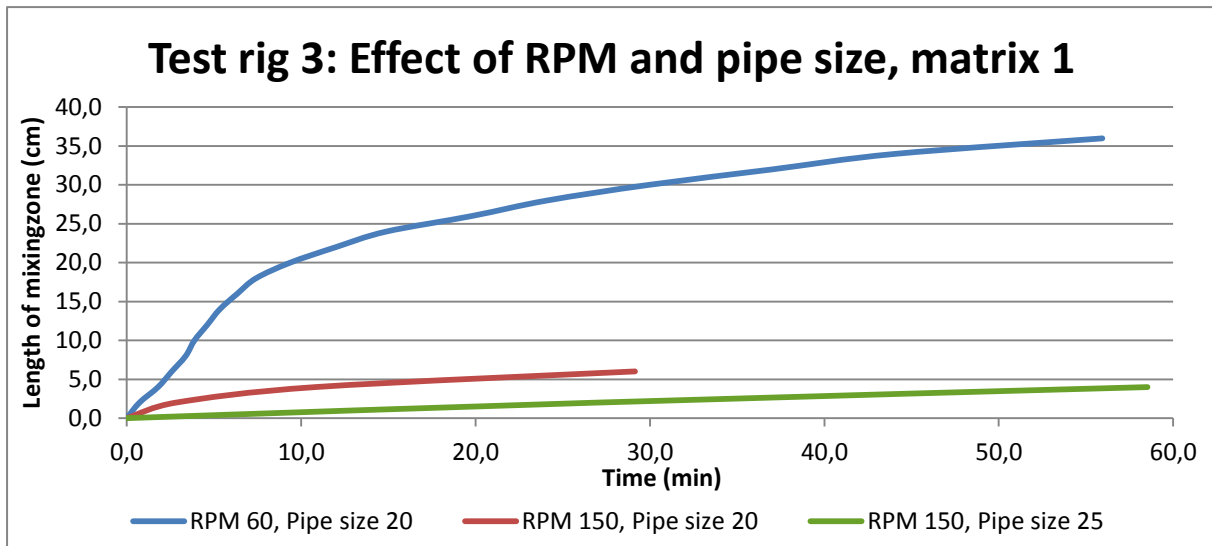
Graph 20: Displays the fluid rheology to the liquids used in test rig 3#. [02]

Experiment 21, 22, 23 and 24, Effect of RPM and pipe size

Results from the three experiments are displayed using screenshots from the experimental footage [03] and graphs and tables from the Experiment sheet [02].

Ex. 21	RPM 60 Pipe size 20 mm
Experiment start Time 0.00 min	
Experiment stop Time 60.00 min	
Ex. 22	RPM 150 Pipe size 20 mm
Experiment start Time 0.00 min	
Experiment stop Time 60.00 min	
Ex. 23*	RPM 60 Pipe size 25 mm
Experiment start Time 0.00 min	
Experiment stop Time 60.00 min	
Ex. 24	RPM 150 Pipe size 25 mm
Experiment start Time 0.00 min	
Experiment stop Time 60.00 min	

Screenshot tables 9: Screenshots from ex. footage taken under the execution of experiments 21, 22, 23 and 24. The bended illustration of some of the experiments is due to a fish eyed lens, not experiment setup. [03]



Graph 21: Displays the mixing effect of RPM and pipe size gained from experiments 21, 22, 23 and 24. [02]

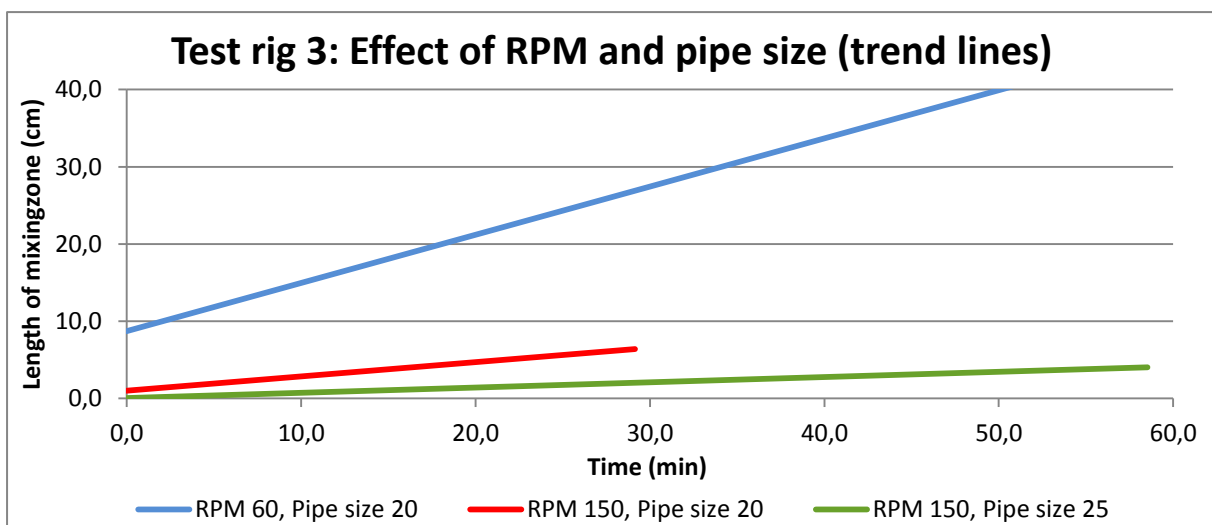
Matrix nr. 1		RPM	
		60	150
Pipe size (mm)	20	Ex 21	Ex 22
	25	Ex 23*	Ex 24

* Experiment 23 was too contaminated to give an observable result. The experiment was not repeated because of OBM shortage and future experiments would repeat the tests major specifics (see ex. 28).

Table 27: Displays matrix nr. 1.

- = Highest interface movement
- = intermediate interface movement
- = Lowest interface movement

As displayed in the tables and graphs above, mixing zone propagation increases with lower RPM and smaller pipe sizes. When subjected to decreasing force of friction from the rotating body, the fluids seem to need longer time to stabilize a constant mixing rate. This event is especially noticeable in experiment 21, where it takes almost 10 minutes before a consistent, decreasing mixing rate is established.



Graph 22: Trend lines of the curves displayed in graph 21. [02]

RPM and pipe size	Trend line equation	Mixing distance (cm)	Mixing rate (cm/min)
60, 20 mm	$y = 0,6248x + 8,6946$	36	0,6248
150, 20 mm	$y = 0,1849x + 1,0191$	6	0,1849
60, 25 mm	VOID	VOID	VOID
150, 25 mm	$y = 0,0682x + 0,0581$	4	0,0682

Table 28: Displays the mixing zone movement results from ex. 21, 22, 23 and 24. [02]

 = Highest mixing distance and mixing rate
 = Lowest mixing distance and mixing rate

Trend lines, mixing distances and mixing rates displayed in graph 22 and table 28 also suggest an increase in heavy light interface movement at small pipe size and low RPM. The table above shows also that the highest mixing rate is relatively low when compared to experiments conducted with OBM and oil in test rig 2. This may be due to the high viscosity of the Canola/Rapeseed oil, which may be reducing the mixing interfaces movement. To see the clear effect of light fluid viscosity, an experiment conducted with a low viscous light fluid should be performed.

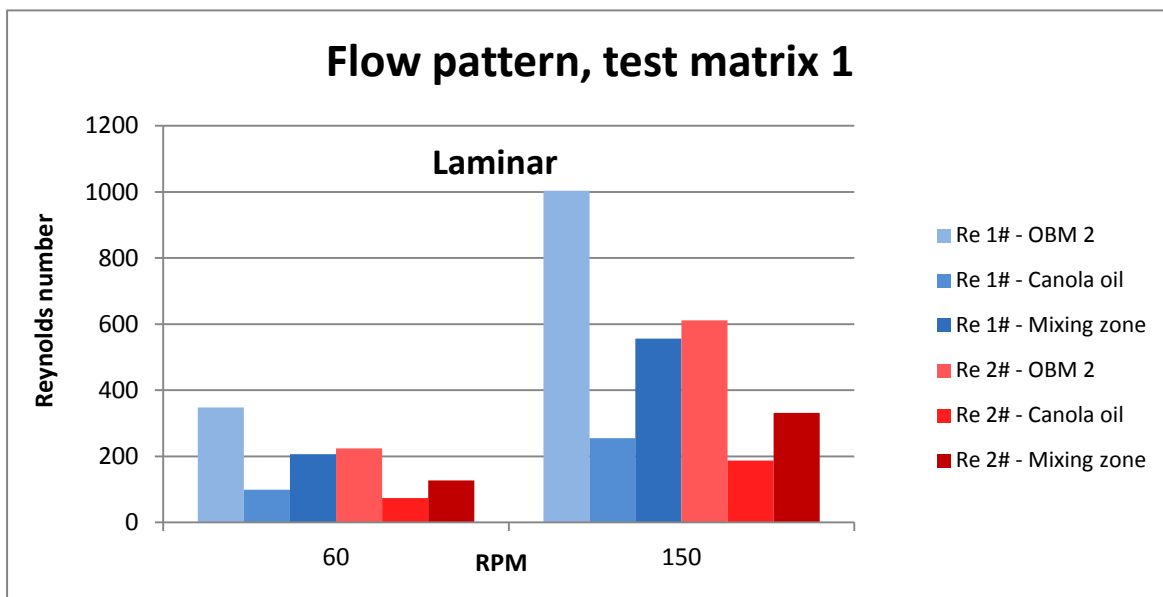




Chart 3: The flow pattern for experiments conducted according to Matrix 1. [02]
1# = Small pipe size (20 mm)
2# = Large pipe size (25 mm)

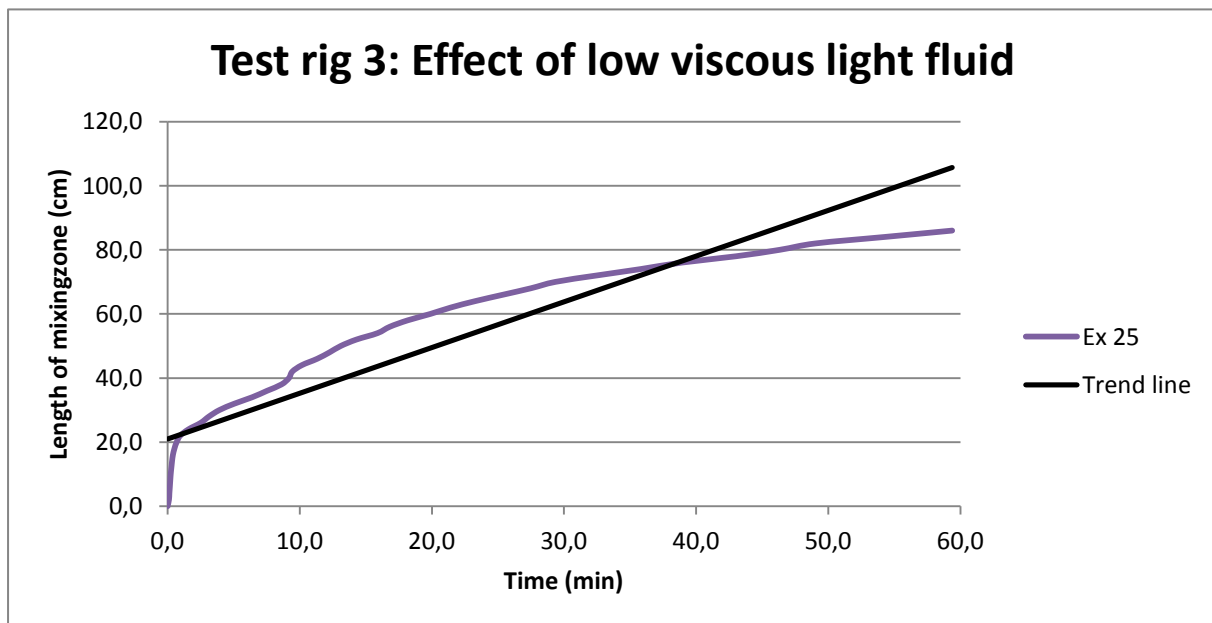
The test matrix 1s flow pattern partly backs up the observed mixing movement in screenshot tables and graphs. Even if all Reynolds numbers are in the laminar range, as seen in the chart, the Re-numbers for pipe size 1# is higher than the ones for pipe size 2#. What doesn't correlate with the flow pattern is that we don't observe an increase in mixing zone movement at higher RPM. Since all the Re-numbers are in the laminar range, the flow characteristics effect may be governed by other parameters.

Experiment 25, Effect of low viscous light fluid

Results from the three experiments are displayed using screenshots from the experimental footage [03] and graphs and tables from the Experiment sheet [02].

Ex. 25	
Experiment start Time 0.00 min	
Before camera angle movement Time 28.00 min	
After camera angle movement Time 28.00 min	
Experiment stop Time 60.00 min	

Screenshot tables 10: Screenshots from ex. footage taken under the execution of experiment 25. The bended illustration of some of the experiments screenshots are due to a fish eyed lens, not experiment setup. [03]



Graph 23: Displays the mixing effect of RPM and pipe size gained from experiments 21, 22, 23 and 24. [02]

RPM and pipe size	Trend line equation	Mixing distance (cm)	Mixing rate (cm/min)
60, 20 mm	$y = 1,4274x + 20,965$	86	1,4274

Table 29: Displays the mixing zone movement result from ex. 25. [02]

As seen in tables 29 and graph 23 the mixing propagation is extensive, and reaches almost a meter an hour. The low viscous diesel shows a low resistance against mixing and allows the OBM 2 to travel through in a slowly decreasing rate. The experiment represents a worst case scenario when it comes to the effect of low viscosity in the light liquid.

As previously seen in ex. 21 the mixing rate needs time to stabilize. Graph 23 shows a mixing *surge* in the beginning of the experiment, before the graph evens out and decreases at a stable rate. The shape of the graph suggests that the mixing interface movement will stop at some point.

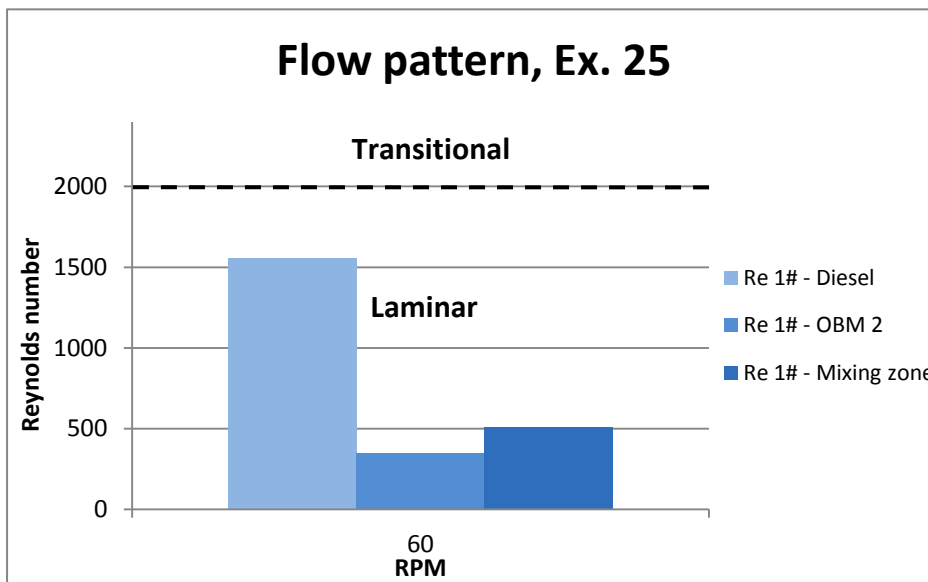






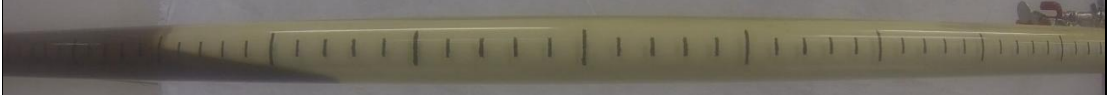
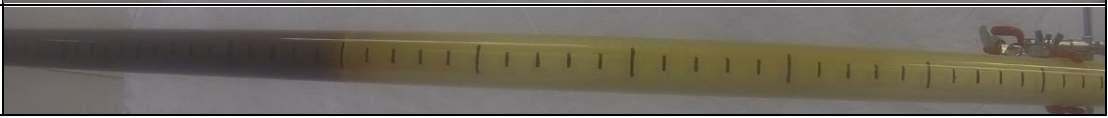


Chart 4: Displays the flow pattern of experiment 25. [02]

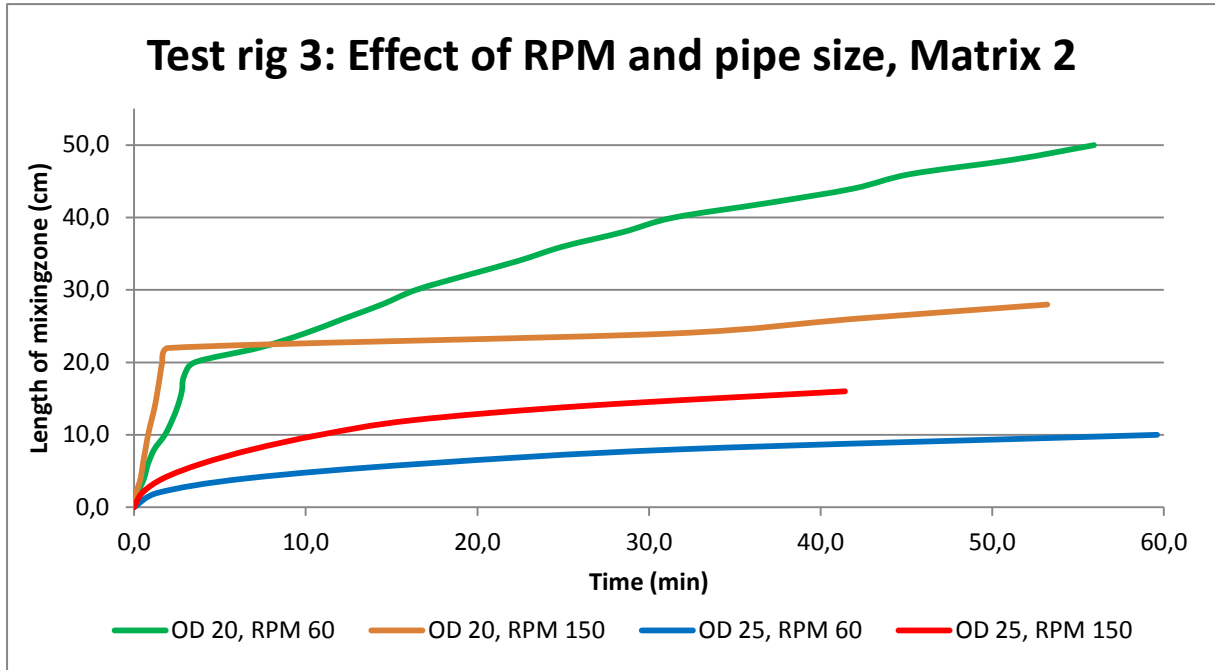
The flow pattern for the experiment is inside the laminar area, but as seen in the chart above, the Reynolds Number of the light fluid (diesel) is approaching transitional flow. The elevated Re-number of the diesel may have been a leading factor in increasing the mixing zone movement.

Experiment 26, 27, 28 and 29, Effect of RPM and pipe size

Results from the three experiments are displayed using screenshots from the experimental footage [03] and graphs and tables from the Experiment sheet [02].

Ex. 26	RPM 60 Pipe size 20 mm
Experiment start Time 0.00 min	
Experiment stop Time 60.00 min	
Ex. 27	RPM 150 Pipe size 20 mm
Experiment start Time 0.00 min	
Experiment stop Time 60.00 min	
Ex. 28	RPM 60 Pipe size 25 mm
Experiment start Time 0.00 min	
Experiment stop Time 60.00 min	
Ex. 29	RPM 150 Pipe size 25 mm
Experiment start Time 0.00 min	
Experiment stop Time 60.00 min	

Screenshot tables 11: Screenshots from ex. footage taken under the execution of experiments 26, 27, 28 and 29. The bended illustrations of some of the experiments are due to a fish eyed lens, not experiment setup. [03]

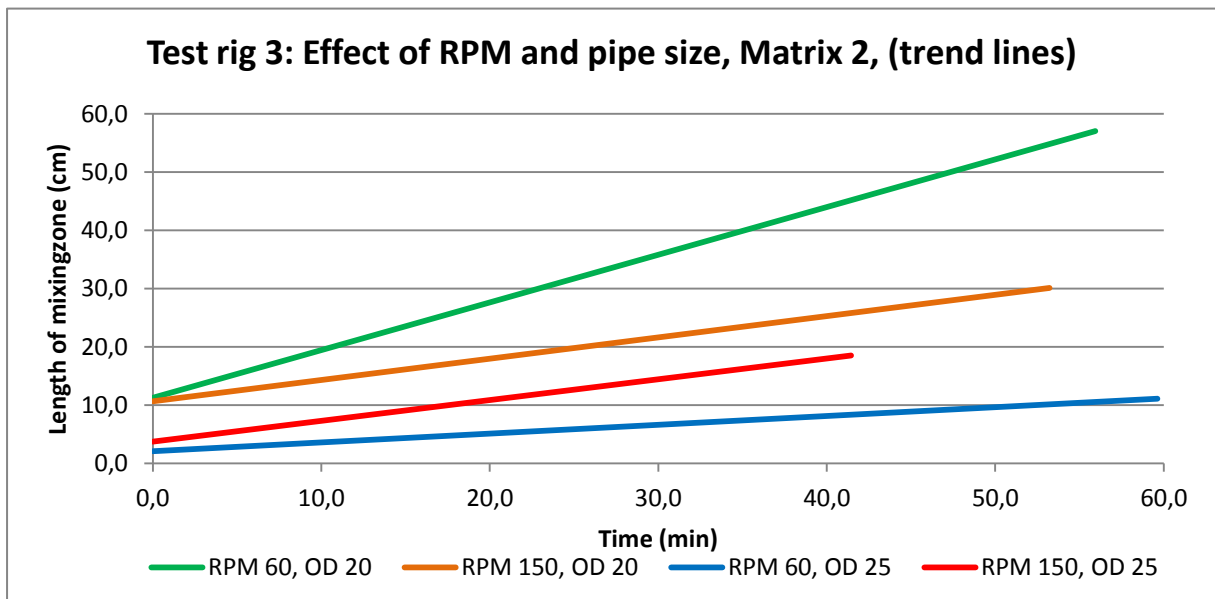


Graph 24: Displays the mixing effect of RPM and pipe size gained from experiments 26, 27, 28 and 29. [02]

Matrix nr. 2		RPM	
		60	150
Pipe size (mm)	20	Ex 26	Ex 27
	25	Ex 28	Ex 29

Table 30: Displays matrix nr. 2.

- = Highest interface movement
- = intermediate interface movement
- = Lowest interface movement



Graph 25: Trend lines of the curves displayed in graph 24. [02]

RPM and pipe size	Trend line equation	Mixing distance (cm)	Mixing rate (cm/min)
60, 20 mm	$y = 0,8187x + 11,248$	50	0,8187
150, 20 mm	$y = 0,3652x + 10,648$	28	0,3652
60, 25 mm	$y = 0,1512x + 2,0725$	10	0,1512
150, 25 mm	$y = 0,357x + 3,7203$	16	0,3570

Table 31: Displays the mixing zone movement results from ex. 26, 27, 28 and 29. [02]

■ = Highest mixing distance and mixing rate
■ = Lowest mixing distance and mixing rate

As shown in the tables and graphs above, mixing zone propagation and mixing rate increases with lower RPM and smaller pipe sizes. As seen in previous experiments 21, 22 and 25 decreasing force of friction from the rotating body fail to keep the fluid in suspense from the start. It takes longer time to stabilize the fluids to flow at a constant mixing rate. Experiment 27 seen in graph 24 show an extreme case of the phenomenon. The high RPM fails in rotating the heavy fluid and it travels up the tube at a rapid rate, before it stabilizes together with the light liquid and continues at a severely reduced mixing rate.

The experiments conducted with large pipe size show a different graph movement. A clear heavy light interface gets created almost instantly after start (see attached experimental CD) and moves at a predictable and stable rate. The two experiments performed with the large pipe size has both these traits, but unexpectedly the high RPM experiment has a higher mixing rate and mixing distance than the experiment with a low RPM.

One explanation for the high mixing zone movement in the “RPM 150, 25 mm” experiment could be that the high RPM and large pipe size creates turbulent flow, which then again accelerates mixing. As seen in chart 5 below, this is not the case, but there seems to be a “sweet spot” where a fixed RPM and pipe size results in minimal heavy light interface propagation. As seen in table 14, the “sweet spot” seems to lie in the proximity of 60 RPM and 25 mm pipe size for this test setup.

The four experiments results indicate that high RPM and the large pipe size seems to stabilize the liquid faster and initiates a more horizontal slope than seen in experiments conducted with low RPM and small pipe size.

The results are again partly supported by the experiments flow pattern (see chart below). The small pipe size (20 mm) experiments give higher Reynolds numbers than the tests conducted with the large pipe size (25 mm). This indicates that high Reynolds numbers may have an effect on the mixing zone propagation, even if the flow is inside the laminar area.

The RPM induced flow patterns shown in the chart indicate that the mentioned “sweet spot” seen in the “RPM 150, 25 mm” experiment may be due to its low Reynolds number. The Re-number of the low RPM experiment is almost 1/3 of the experiment conducted with high RPM.

These characteristics are not seen in the experiments conducted with small pipe sizes. As mentioned, other mixing parameter seems to have a more significant effect on the interface movement.

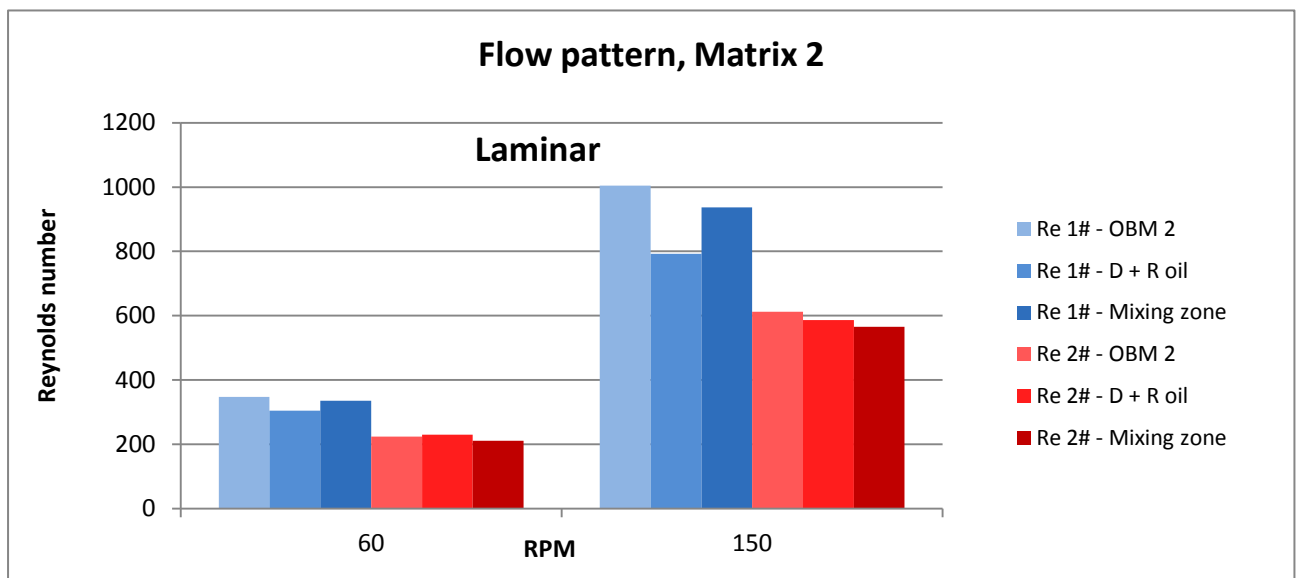


Chart 5: The flow pattern of the experiments conducted in matrix 2. [02]

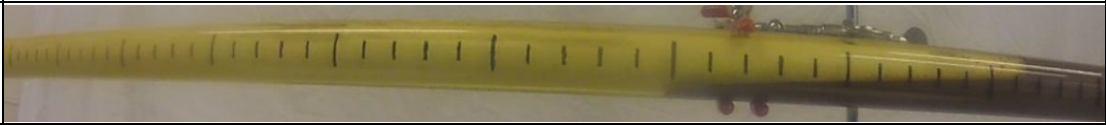



1# = Small pipe size (20 mm)





2# = Large pipe size (25 mm)

D + R = Diesel + Rapeseed oil

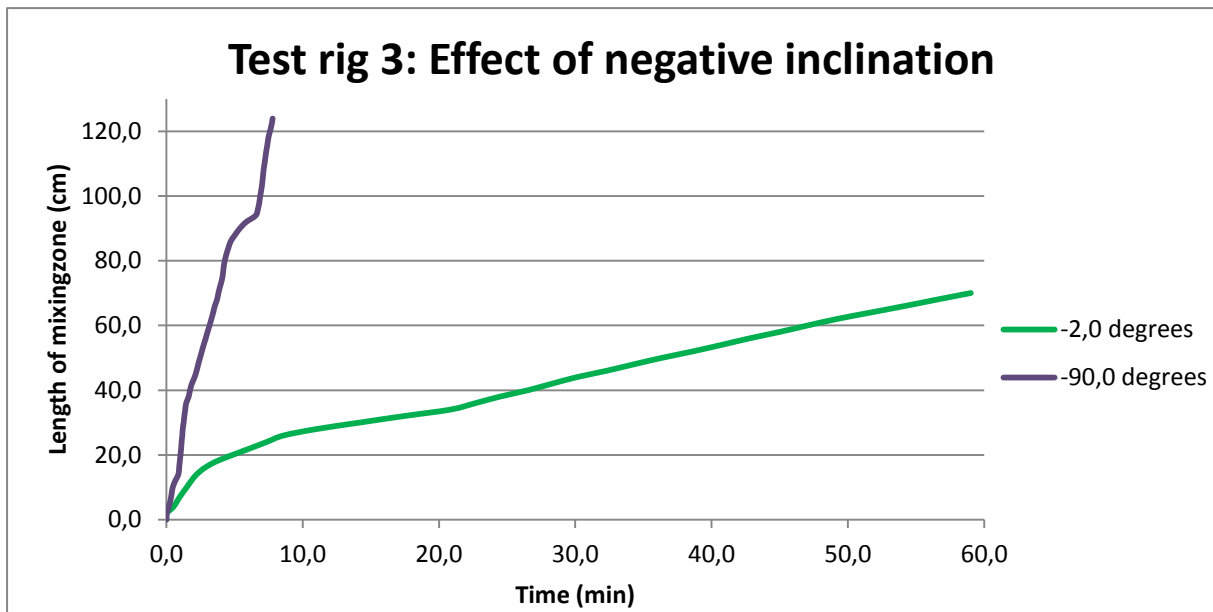
Experiment 30 and 31, Effect of negative inclination

Results from the three experiments are displayed using screenshots from the experimental footage [03] and graphs and tables from the Experiment sheet [02].

Ex. 30	Inclination -2,0
Experiment start Time 0.00 min	
Before camera angle movement Time 14.00 min	
After camera angle movement Time 14.00 min	
Experiment stop Time 60.00 min	

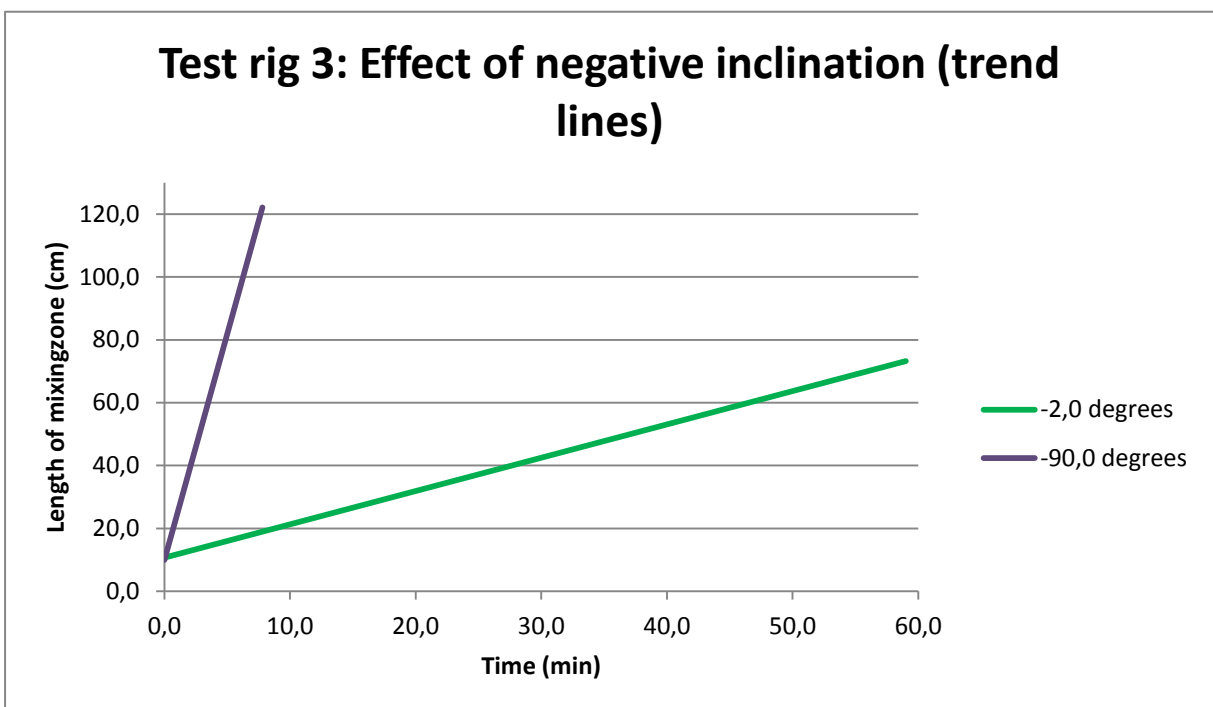
Ex. info	Experiment start Time 0.00 min	Before camera change Time 5.00 min	Before camera change Time 5.00 min	Experiment stop time 20.00 min
31# -90,0°				

Screenshot tables 12: Screenshots from ex. footage taken under the execution of experiments 30 and 31. Screenshots from experiment 31 is taken two different cameras. The second camera took over when the mixing zone had moved past the range of the lens. As seen in the top of the third screenshot from the left, the mixing zone is moving downwards. The bended illustration of some of the experiments is due to a fish eyed lens, not experiment setup. [03]



Graph 26: Displays the mixing effect of negative inclination gained from experiments 30 and 31. [02]

The screenshot tables and the graphs above show that negative inclination has a profound effect on the mixing zone propagation. As partly shown in experiment 20 from test rig 2#, the negative inclination seem to form a linear mixing rate after stabilizing the fluid rotation. This can especially be seen in experiment 30 (inclination -2,0), where the graph seems to follow a linear trend after a stabilizing process lasting 20 minutes.



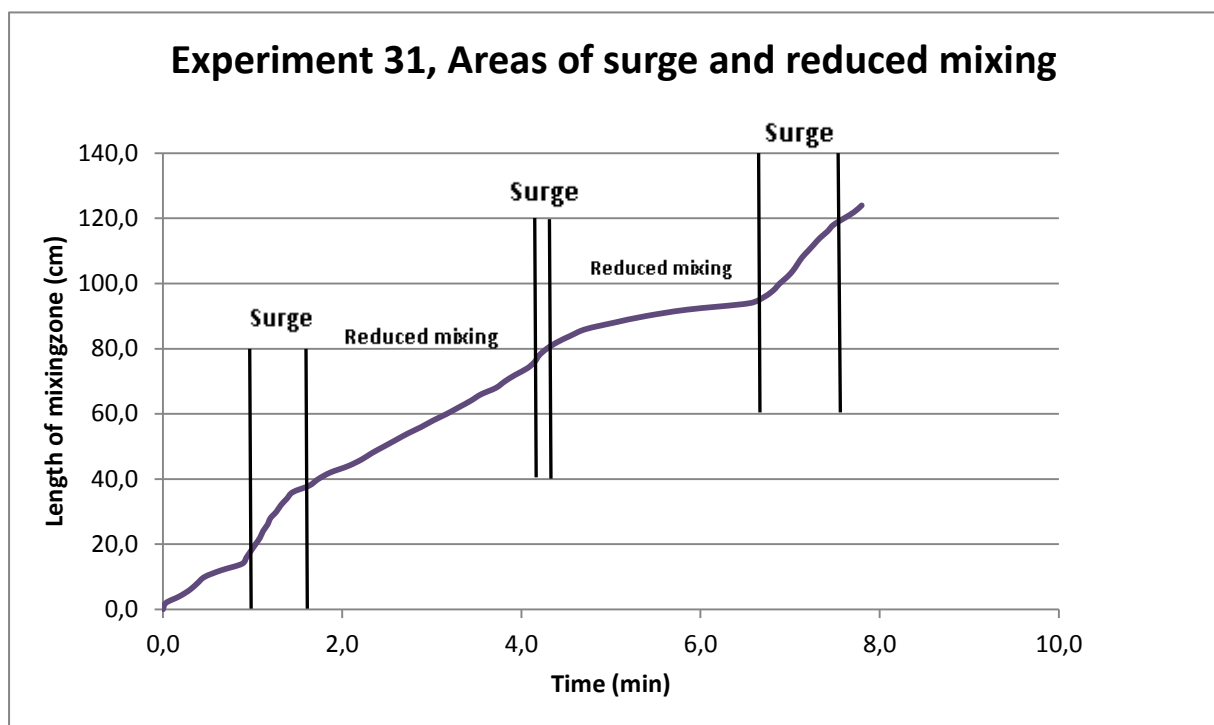
Graph 27: Trend lines of the curves displayed in graph 26. [02]

Inclination	Trend line equation	Mixing distance (cm)	Mixing rate (cm/min)	Increased mixing distance (%)	Increased mixing rate (%)
-2,0	$y = 1,0595x + 10,716$	70	1,0595	VOID	0
-90,0	$y = 14,382x + 9,9664$	124*	14,382	VOID	1357,4

Table 32: Displays the mixing zone movement results from ex. 30 and 31. [02]

* = Experiment 31 was only run 20 minutes. Mixing distance would have been larger if test parameters would have allowed. Increased mixing distance (%) could not be calculated because of lack of test parameters.

The mixing distance and rate of the two experiments seem to confirm the negative inclinations effect. As displayed in table 32 the mixing rate increases with 1357,4 % from negative inclination of -2,0 to -90,0. The high RPM and large pipe size did not seem to slow down the mixing interface movement in any usable manner. As seen in the attached experimental CD, the heavy fluid manages to stick into the wall and escape the movement of the rotating pipe. When the heavy fluid gets picked up by the force of rotation, the heavy light interface has moved considerably farther down the tube. These *surges* can easily be seen in graph 28. The graph also show the periods of less mixing that comes after these *surges*.



Graph 28: Displays the areas of surge and reduced mixing in experiment 31. [02]

The linear shape of the two negative inclination graphs suggest that if the experiments had continued, the mixing zone movement would have kept its present mixing rate until the space had run out. It seems like the constant force of gravity governs the mixing rate for experiments conducted with negative inclination, and sets a constant mixing rate. If that is so, prediction of the mixing rate may be possible.

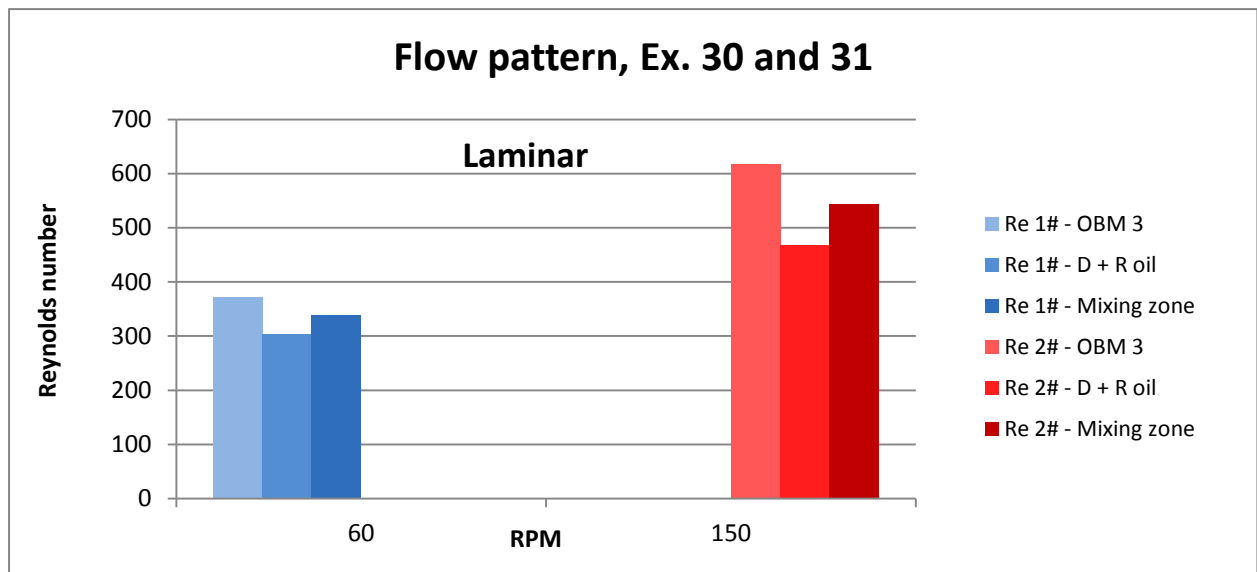


Chart 6: The flow pattern of experiments 30 and 31. [02]

1# = Small pipe size (20 mm)
2# = Large pipe size (25 mm)
D + R = Diesel + Rapeseed oil

The two experiments are conducted with virtually the same fluid configuration as used in Matrix 2 (ex. 26, 27, 28 and 29), with the only difference being the usage of OBM 3 instead of OBM 2. The flow pattern has therefore a similar flow characteristic as Matrix 2 experiments, and is in the laminar area. Because of the extreme difference in inclination between the experiments, the effect of Reynolds number difference is obscured.

Conclusion test rig 3#

The factors that enhanced mixing zone movement in test rig 3# were low viscous light fluid and negative inclination (see table below). Highly viscous light fluid used together with high RPM and large pipe size proved to stagger the heavy light interface propagation most effectively. This indicates that the rheology of the light fluid has a significant effect on the mixing zone distribution.

Experiment nr.	Test purpose	Mixing distance (cm)	Mixing rate (cm/min)
Ex.21	RPM 60, Pipe size 20 mm	36	0,6248
Ex.22	RPM 150, Pipe size 20 mm	6	0,1849
Ex.24	RPM 150, Pipe size 25 mm	4	0,0682
Ex.25	Low viscous light fluid	86	1,4274
Ex.26	RPM 60, Pipe size 20 mm	50	0,8187
Ex.27	RPM 150, Pipe size 20 mm	28	0,3652
Ex.28	RPM 60, Pipe size 25 mm	10	0,1512
Ex.29	RPM 150, Pipe size 25 mm	16	0,3570
Ex.30	Negative inclination -2,0	70	1,0595
Ex.31	Negative inclination -90,0	124*	14,382

Table 33: Summary of viable results from test rig 3#.

■ = Highest mixing distance and mixing rate

■ = Lowest mixing distance and mixing rate

* = See table 32.

Test rig 3#s experimental setup approached Reelwells heavy over light scenario in a realistic manner. RPM, pipe size, inclination and light fluid viscosity were varied according to possible Reelwell drilling scenarios. In this thesis, test rig 3# will be the simulation closest to Reelwells original heavy over light setup.

4.6 Viscometer test rig

4.6.1 Purpose

The Viscometer test rig's purpose was to explore the effect of varying RPM on mixing zone movement in a vertical scenario. This would give a clear representation in how turbulence from rotating objects affects heavy light interface propagation.

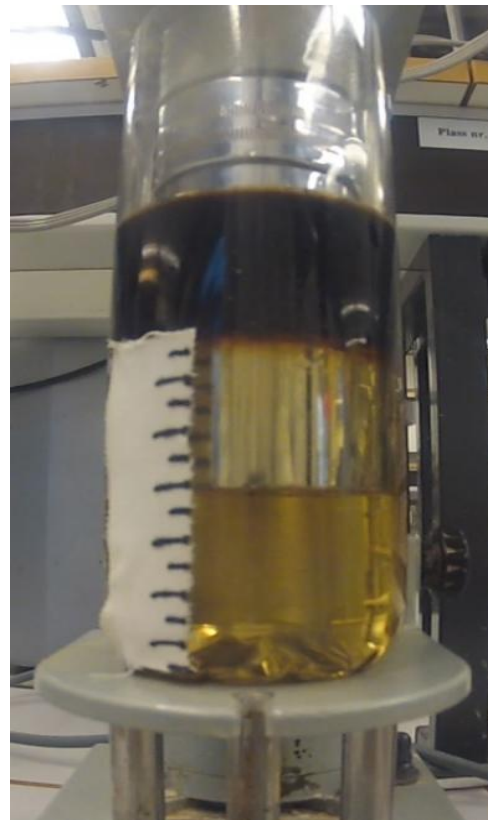
4.6.2 Experimental setup

[See [Appendix C – Test rig construction and experiments general specifications, viscometer test rig](#) for detailed information about construction and fabrication of viscometer test rig]

Viscometer rig is a 100 mm length by 56,3 mm diameter well (measured in accordance to fluid level). In this rig a viscometer steel cylinder, 40,7 mm diameter and 60 mm length, was rotated in the middle of the system 40 mm above the plastic cup bottom. It would represent the drill pipe in a drilling scenario.

Wellbore		
Plastic cup	Length (mm)	100
	ID (mm)	56,3
Drill pipe		
Viscometer steel cylinder	Length (mm)	60
	Diameter (mm)	40,7

Table 34: Viscometer test rig specifics.



Picture 4: Viscometer test rig setup. The plastic cup is displayed positioned onto the Viscometers steel cylinder, filled with fluids from the first experiment. The scale to the left is placed to simplify the observation of the mixing zone movement. [01]

4.6.1 Viscometer experiment 1 and 2

The purpose of the two experiments was to see how the heavy light interface would behave when subjected to quantified RPM. The first experiment would explore the light fluids travel through the heavy, while the second would investigate the heavy liquids mixing with the light.

Used equipment

[See [Appendix D](#) for detailed information about used equipment and tools]

The equipment/tools used in the two experiments are listed in Used equipment viscometer test rig, [Appendix C](#), except for this modification:

- Food dye (black)

Experiment specifications

The first experiment used syrup 1 as heavy fluid and black dyed water as light fluid. The two water based liquids would create a contrast which simplifies the observation of the light fluids travel. The second experiment used OBM 1 as heavy fluid and olive oil as light fluid. These two fluids had the same fluid purpose as for viscometer ex. 1, just with regard to the heavy liquid.

More parameter information is displayed in the table below:

Experiment	Viscometer ex. 1	Viscometer ex. 2
Light fluid	water + strong dye	Olive oil
Heavy fluid	syrup 1	OBM 1
Inclination	90	90
Heavy light ratio	2:1	2:1
RPM	3, 6, 100, 200	3, 6, 100, 200
Duration	5.42 min	14.33 min
Direction of rotation	Clockwise	Clockwise

Table 35: Displays the technical data for viscometer ex. 1 and 2. [02]

Execution

[Viscometer experiments 1 and 2 followed the same procedure and execution]

The execution procedure listed in Experiment execution test rig 3 in [Appendix C](#).

Specific uncertainties

No specific uncertainties were detected.

4.6.2 Fluid system description

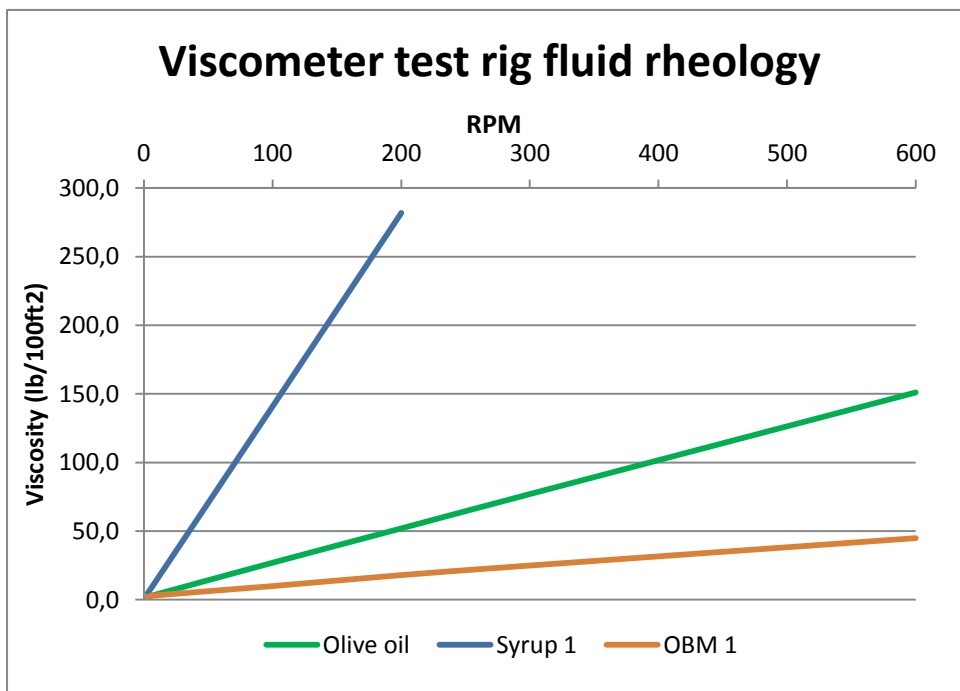
The rheology of the heavy fluids was measured using a (Fann) Viscometer. The liquids density was determined by using a mud scale.

Rpm	Syrup 1	OBM 1	Olive oil
ø600	>300	45,0	151,0
ø300	>300	25,0	77,0
ø200	282,0	18,0	52,0
ø100	141,0	10,0	27,0
ø6	9,0	3,0	3,0
ø3	5,0	2,0	2,0

PV (cp)		20,0	74,0
YP (lb/100 ft ²)		5,0	3,0

ρ (s.g)	1,380	1,210	0,910
n		0,848	0,971

Table 36: Showing the fluid properties for the heavy and light fluids used in test rig 3#. [02]
 = Not able to measure/beyond the scale.



Graph 29: Displays the fluid rheology to the liquids used in test rig 3#. [02]







4.6.3 Results and analysis







This subsection presents the results obtained from the two experiments conducted with viscometer test rig and discusses their significance. The discussion part of the subsection will discuss the results from “Experiment sheet”, pictures, as well as edited and unedited footage.

All measurable movement of the mixing zone in test rig 3# experiments were documented. Results of that documentation are shown below.

Viscometer experiments 1 and 2

Results from the two experiments are displayed using screenshots from the experimental footage ^[03].

Viscometer experiment 1					
Ex. Start Time 00.00	RPM				Ex. Stop Time 05.42
	3	6	100	200	
					

Viscometer experiment 2					
Ex. Start Time 00.00	RPM				Ex. Stop Time 14.33
	3	6	100	200	
					

Screenshot tables 13: Screenshots from ex. footage taken under the execution of viscometer experiments 1 and 2. [03]

As seen in screenshot tables 14 both experiments show that the most intensive mixing happens at 200 RPM. At this rotational speed waves form in the heavy light interface. After a while these waves break out and form new interfaces. This process continues until the fluids in the plastic cup are completely mixed. This indicated that high RPM enhances mixing, and suggest that it is recommended to stay under 200 RPM to avoid extensive mixing (in this wellbore/drill pipe ratio scenario).

At lower RPM the interface seems unaffected and stable. 100 RPM showed some minor indications of disturbances in the heavy light interface, but they are incomparable to mixing propagation shown at 200 RPM. It can therefore be assumed that low RPM alone does not enhance the mixing interface movement.

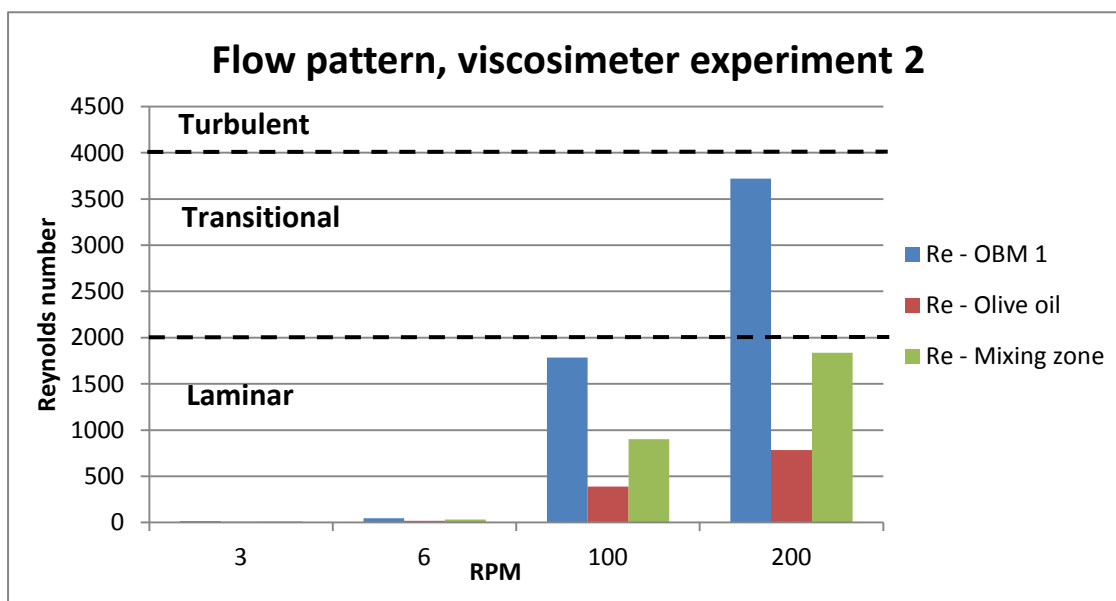


Chart 7: Viscosimeter experiment 2s flow pattern. [02]

As seen in chart 7, the assumptions drawn from the screenshots seem to be supported by the calculated Reynolds numbers from viscosimeter experiment 2. Viscosimeter experiment 1s Reynolds numbers couldn't be calculated because of syrup 1s rheology.

No significant mixing was observed under 3, 6 and 100 RPM, which suggest that a laminar flow characteristic may not have an impact on the heavy light interface movement.

At 100 RPM, some activity was seen in the test system, but this may be due to the OBM 1s Reynolds number approaching transitional flow.

As mentioned, no accelerated mixing started before rotation speed was up to 200 RPM. The graph above shows that interfaces movement may have been caused by the OBM 1s flow nearly entering a turbulent pattern. As shown in the screenshot tables, the OBM mixes into the olive oil, which complies with the data given by the chart for 200 RPM. It illustrates that it is only the OBM 1s Re-number which enters transitional flow.

High transitional/turbulent flow seems to have a profound effect on the distribution of the mixing zone.

5 Discussion

In this section, results from all three test rigs will be summarized and scaled up to realistic sizes. This will be done to clarify each parameters potential effect on heavy light interface movement in a realistic scale. The importance and impact of these parameters will also be discussed.

Two Reelwell WB and pipe scenarios are used to give a clear representation of the different parameters effect on the mixing zone in real size. This will simplify the process of predicting the interface movement.

The scenarios are the same that were scaled down for construction of test rig 3 (see section § [4.5.2](#) Experimental setup, test rig 3).

Reelwell scenarios	Scenario 1#		Scenario 2#	
	Meters	Inch	Meters	Inch
Wellbore diameter	0,31	12,25	0,22	8,5
Drill pipe diameter	0,19	7,5	0,19	7,5

Table 37: Displays the two Reelwell scenarios wellbore and drill pipe diameter. [R05]

The two scenarios depend on parameter information given by Reelwell:

	Range
Inclination	1°
RPM	20 - 200
ROP (m/h)	5 - 10

Table 38: Parameter information. [R05]

And the fluid configuration:

Mud type	SG [kg/l]	PPG	PV [cP]	YP [lbs/100ft ²]
Heavy OBM	1.40	11.7	30	20
Light OBM	1.10	9.2	20	20

Table 39: Reelwell fluid configuration. [R05]

These data will be used as a reference for the discussion.

Density difference

Density difference is an essential parameter in Reelwells heavy light concept. The difference in density between the two fluids keeps them separated and creates the heavy light interface.

Throughout the experiments conducted with the 3 main test rigs and the viscometer rig, the density difference between the heavy and light liquid has been varied, but only to a small degree. Because variations in the fluid rheology occur when heavy particles are added or removed, it was difficult to interpret the interface movement results as a product of the change in rheology or the density.

Since density is a single parameter and rheology has a more complex composition, the fluid densities were held in the proximity of Reelwells fluid setup. The effect of varying density differences on interface was therefore not extensively investigated. According to the theory of gravity, it can be assumed that an increase in density difference will slow down mixing zone propagation. To test this assumption, fluids with similar rheological properties but different densities should be tested in the heavy light scenario. This would illustrate the true effect of density difference. Because of the mentioned difficulties, these investigations were not performed in this thesis.

Information from Reelwell suggests that the concept is still under development, and that no fixed heavy light density configuration has yet been decided.

Inclination

The parameter inclination is a leading factor in the heavy light concept, since it governs the length of the mixing interface (in stagnant position) and the magnitude of gravity's effect on the system. Using the parameter information given by Reelwell together with data from scenario 1 and 2, two potential mixing lengths can be calculated. Equation 24 is used:

$$L_{MZ} = D_w \cot \theta$$

Scenario	θ	D_w (m)	Calculation, equation 24	L_{MZ} (m)
1	1°	0,31	$L_{MZ,1} = 0,31 \cot 1$	17,75
2		0,22	$L_{MZ,2} = 0,22 \cot 1$	12,60

Table 40: Showing the calculation of scenario 1 and 2s mixing zone lengths.

Since no axial force is affecting the test system other than gravity, no axial movement of the two fluids should occur. If that is the case, the mixing zone length for the two scenarios will not be longer than indicated in table 40.

Test rig	θ	D_w (m)	Calculation	$L_{MZ, test\ rig\ 3}$ (m)
3	2°	0,032	$L_{MZ, test\ rig\ 3} = 0,032 \cot 2$	0,912

Table 41: Showing the calculation of scenario 1 and 2s mixing zone length.

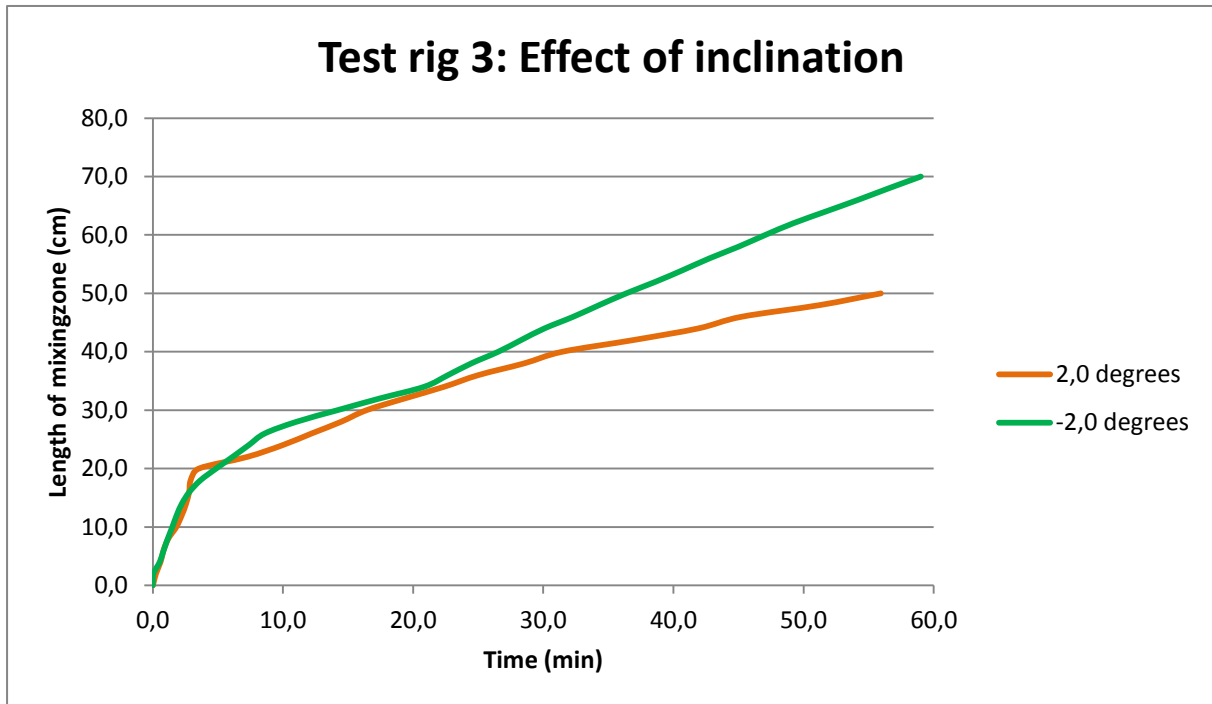
When performing the same calculations on test rig 3s wellbore (displayed in table above), in a 2 degree inclination, expected maximum mixing zone length is **0,912 m**. When comparing this length with the mixing distances derived from experiments conducted with test rig 3, it is we observe that none of the experiments have a longer mixing zone spread. As shown in the table below, experiment 25 has the mixing distance that approaches the $L_{MZ, test\ rig\ 3}$ to the highest degree.

Experiment nr.	Mixing distance (m)
Ex.21	0,36
Ex.22	0,06
Ex.24	0,04
Ex.25	0,86
Ex.26	0,50
Ex.27	0,28
Ex.28	0,10
Ex.29	0,16

Table 42: Displaying various experiments mixing distances.

This experiment is a worst case scenario (see [Experiment 25, Effect of low viscous light fluid](#)) and will therefore represent the longest mixing distance recorded with the given inclination. Since the worst case scenario has not reached the expected mixing zone length and all experiments conducted with positive inclination have a declining mixing slope, it can be assumed that mixing zone length will not be significantly longer than the expected L_{MZ} . Because of the limited duration of the experiments (longest: 60 min) it is likely that some of the tests would experience longer interface distances if they were run for an extended time. However the decreasing mixing rate of the interface movement would render the extra distance gained meaningless. This event seems to be applicable for all experiments conducted with positive inclination. For negative inclination, interface movement has a different characteristic.

As seen in the graph 30, the two lines begin quite similarly, but after a while the +inclination line decreases mixing rate and seems to evolve in a horizontal direction. After the stabilization of the two fluids and the interface, the -inclination line continues in a positive linear slope.



Graph 30: Displays the mixing slopes of experiments conducted with positive and negative inclination. [02]
All other parameters than the inclination is held constant.

The linear slope indicates that the force of gravity and the rotational force lie in equilibrium, with gravity trying to pull the heavy fluid downwards while the force of rotation maintains a stable interface. This is clearly shown in attached experimental CD, Experiment 30, where the heavy light interface moves at a steady speed down the acrylic pipe. This linear slope is also seen in [Experiment 31](#), where an extreme inclination of -90 degrees is held.

Summarizing the discussion and the experimental data above; wellbores with a positive inclination will not experience significantly longer mixing zone lengths than the calculated L_{MZ} .

Wellbores with negative inclination will, after the fluid stabilization process, see a linear mixing slope which directly correlates with the negative WB inclination i.e. higher negative inclination will have an increased stable mixing rate, while a lower negative inclination will have a decreased stable mixing rate.

Pipe size

Varying pipe size is an important parameter in the heavy light concept. It affects the amount of liquid inside and outside of the drill pipe, which again affects the buoyancy factor of the pipe. Fluid rotational velocity is also dependent on the pipe size, together with RPM. Large and small pipe sizes seem to have distinct differences in how they influence the two fluids:

A larger pipe size exposes the external fluid for more surface friction and will thereby have a large effect on the overall fluid velocity. An increased pipe diameter will strengthen the rotational force on the liquids (as seen in [Experiment 31](#)).

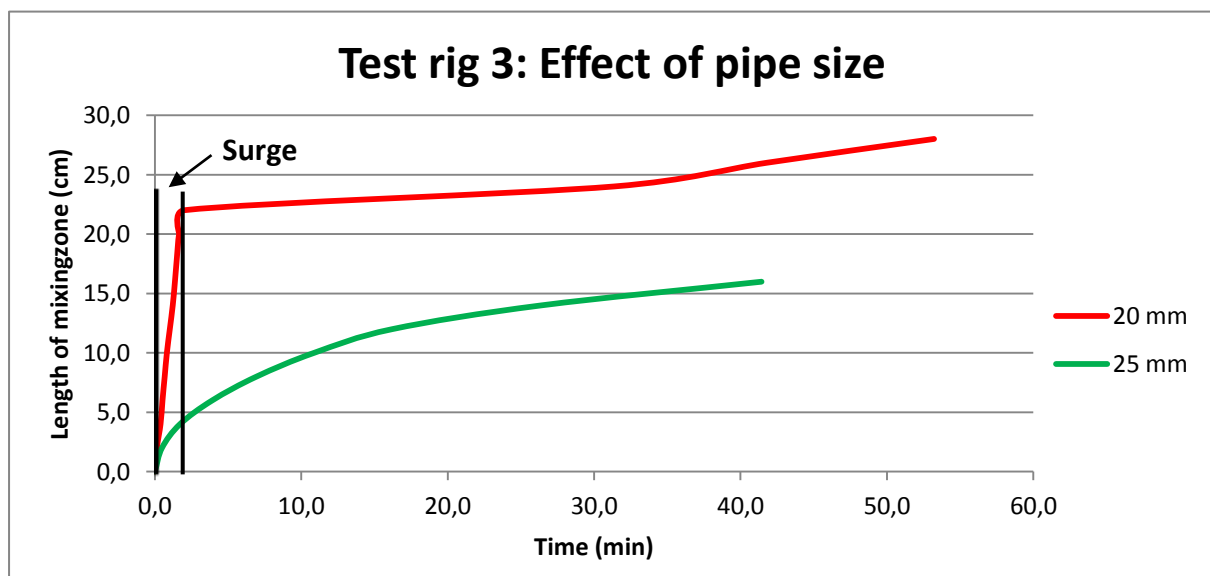
The reduced ratio between wellbore and pipe also has a decreasing effect on the flow's Reynolds number. This means that drilling scenarios performed with large pipe sizes are more likely to operate in a laminar rotational flow.

A small pipe size has a limited surface area and therefore a limited pull on the system fluids. The pipes surface friction is not able to affect the entire fluid volume and therefore has difficulties in creating stable rotational fluid velocity.

Small pipe sizes have the tendency to struggle with stabilizing the heavy and light fluid at low inclinations. The interface manages to “sneak” (especially at low RPM) under the rotating pipe and travel at a high rate before being picked up by the pipes force of rotation. This is characterized by a mixing *surge* (see graph 31).

In contradiction to large pipe sizes, pipes with limited diameters increases the Reynolds number of the flow. This may throw the rotational flow into a transitional or turbulent flow pattern.

As seen in graph 31 and chart 8 (next page), these characteristics seem to be supported by the experimental data.



Graph 31: Displays the difference in heavy light interface movement between two pipe sizes. [02]
A mixing surge area is indicated for the 20 mm pipes mixing zone movement. All other parameters than the pipe size held constant.
20 mm = ex. 27
25 mm = ex. 29

As shown in graph 31, the illustrated *surge* creates a significant increase in mixing propagation for the small pipe size (20 mm). This is due to the mentioned “sneaking” effect of the interface which is easily seen in the attached experimental CD for Experiment 27.

For the larger pipe (25 mm), no substantial mixing *surge* is observed. Heavy light interface movement is predictable and slowly decreasing (see attached experimental CD for Experiment 29).

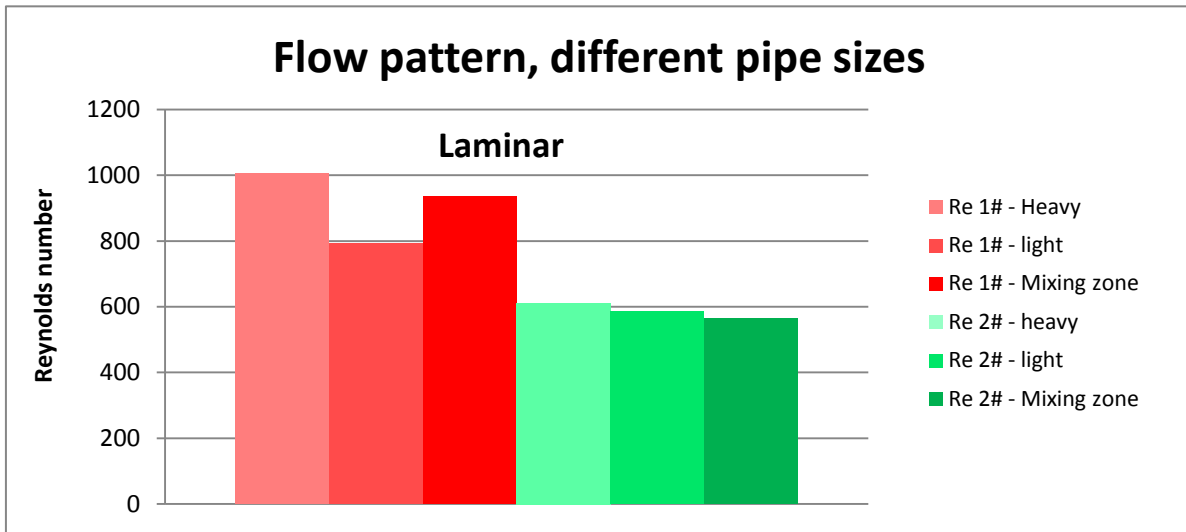


Chart 8: Displaying the flow pattern differences between two pipe sizes. [02]

1# = Small pipe size (20 mm)

2# = Large pipe size (25 mm)

The flow pattern for the two pipe sizes show that the 20 mm pipe size has higher Reynolds numbers than for the 25 mm. As mentioned, this may indicate a more troubled rotational flow in the small pipe system, which may again explain the higher interface movement.

Scaled flow patterns for scenario 1 and 2 in chart 9 indicates the same phenomenon.

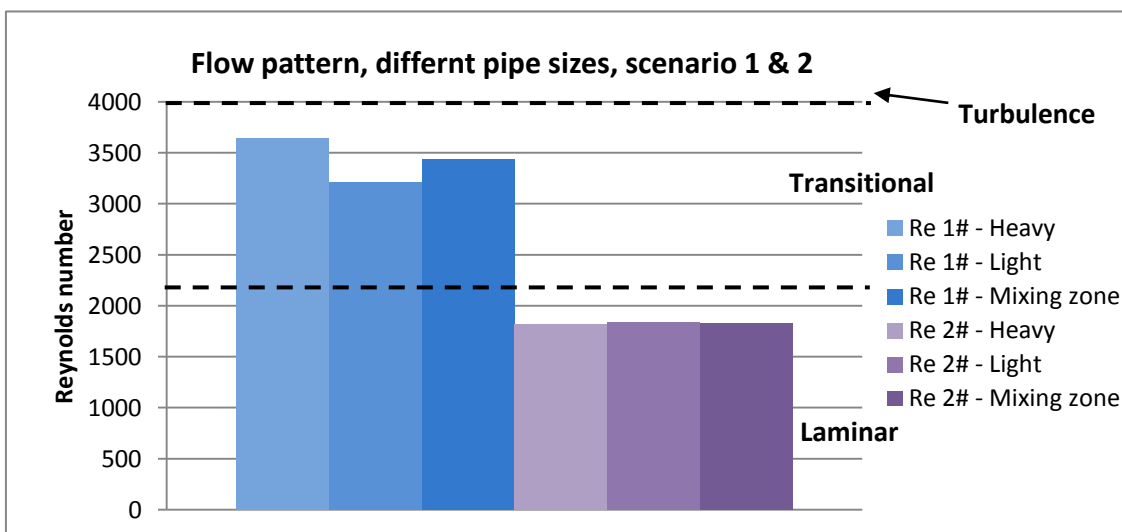


Chart 9: Displaying the flow pattern differences between two pipe sizes. [02]

1# = Scenario 1

2# = Scenario 2

To summarize the experimental data and discussion above; a large pipe size, or at least a small wellbore/pipe diameter ratio, will stabilize the fluids and hinder mixing. Smaller pipe sizes will create a more unpredictable mixing situation and may accelerate the heavy light interface movement.

[Unpredictable pipe movement in the wellbore is not taken into account in the derivation of different pipe sizes effect on mixing zone. It is assumed that the effect of pipe size on mixing zone spread shown above is independent of drill pipe position in wellbore.]

Note:

Large pipe size/diameter = Small WB pipe ratio
Small size/diameter = Large WB pipe ratio

RPM

Together with pipe size, RPM is the parameter that governs the surface velocity of the rotating pipe. RPM is therefore a huge factor when it comes to determining the rotational flows pattern.

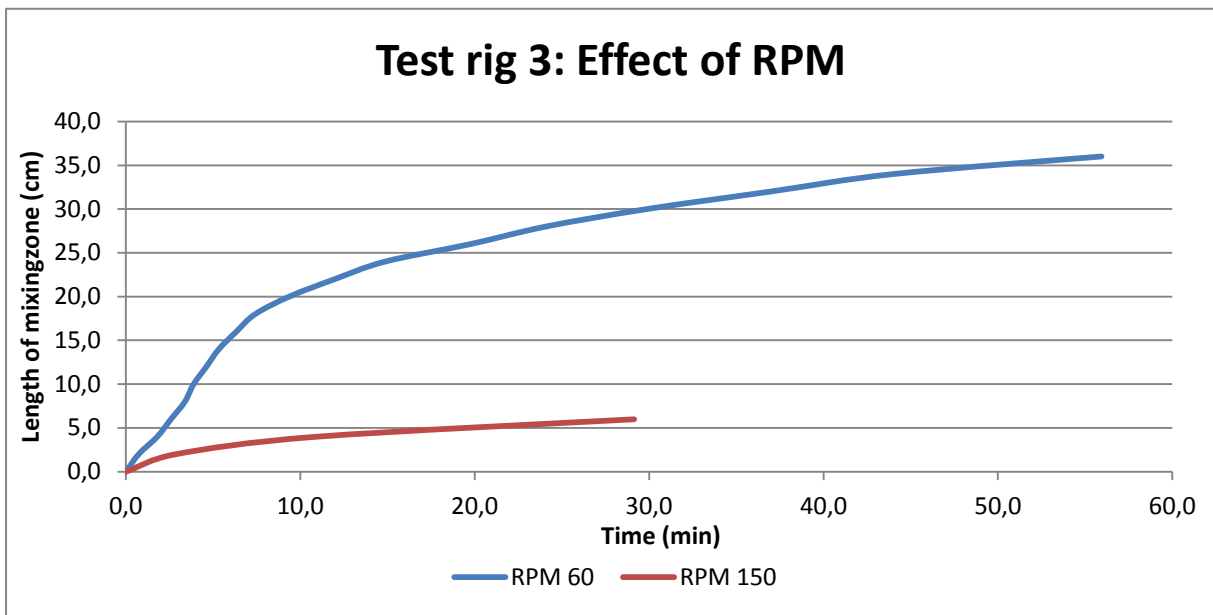
As seen in the viscometer tests, an increase in RPM alone has a substantial effect in the heavy light interface. Since these experiments were conducted with a 90 degree system setup, inclination did not affect the results and confirmed that any interface movement was due to the rotational speed. [Viscometer experiment 2s flow pattern](#) showed a clear RPM induced Reynolds number elevation (see chart 7) which led to following chain of assumptions:

High RPM → elevated Re number → turbulent rotational flow → increased mixing

These assumptions seem to be applicable to all inclination neutral (90°) wellbore setups. For low inclination scenarios in the 9 first test rig 3 experiments, the RPM interface effect seemed a bit different.

As shown in the graph 32 and chart 10, the Reynolds numbers don't cohere with the observed mixing seen in [matrix 1 and 2](#). If the experiments would had followed the assumptions given by the viscometer tests, highest mixing should be observed in experiments conducted with highest RPM. This is not the case.

As mentioned in [Results and analysis, test rig 3](#) this may be due to the RPM induced Re numbers is inside the laminar area. The increased mixing movement may therefore be governed by other parameters or mixing phenomenon's (example mixing *surge*).



Graph 32: Displays the mixing effect of two different RPM. [02]
All other parameters than the RPM of the pipes is held constant.
60 RPM = ex. 21
150 RPM = ex. 23

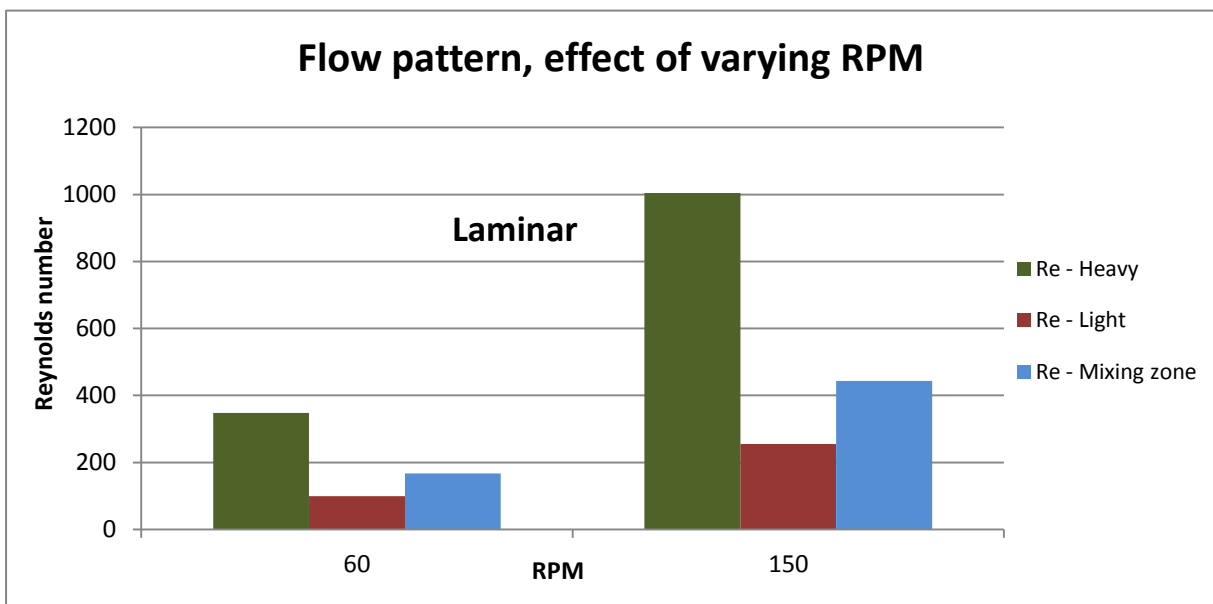


Chart 10: Displaying the flow pattern differences between two RPM. [02]

When comparing the flow pattern drawn from test rig 3 to the Reelwell scenarios flow characteristics, we observe that there is a substantial difference in Re number quantity.

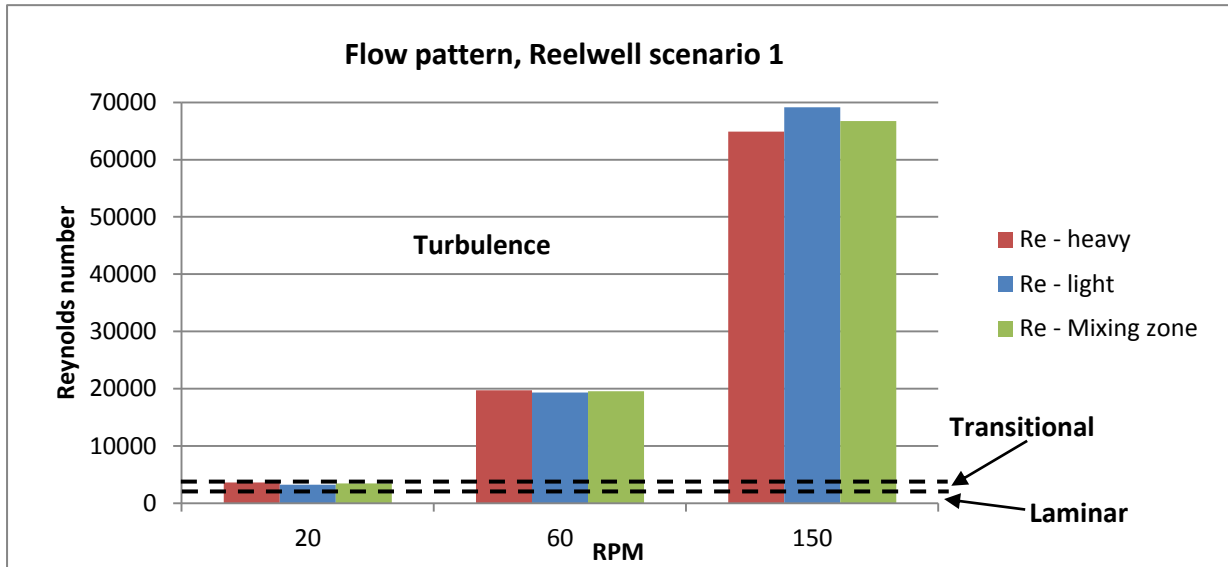


Chart 11: Displaying the flow pattern differences between three RPM for Reelwell scenario 1. [02]

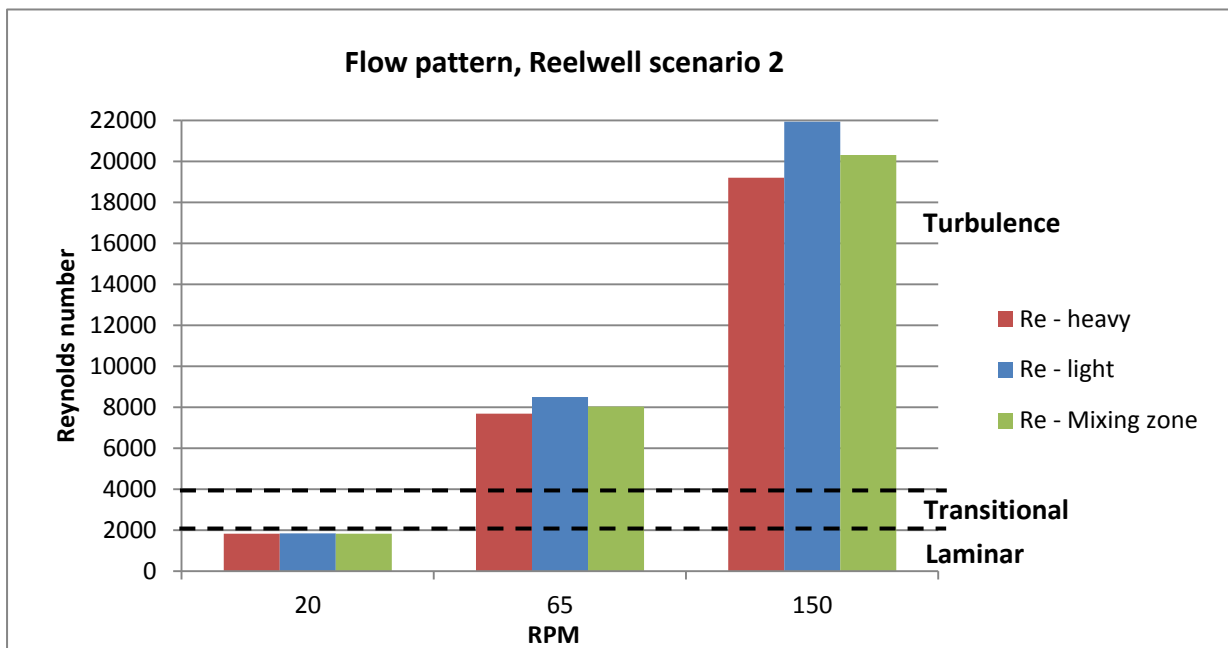


Chart 12: Displaying the flow pattern differences between three RPM for Reelwell scenario 2. [02]

When looking at the flow patterns of the two scenarios we clearly see that the high RPM held in the test rig 3 experiments (RPM 65 and 150) will lead to turbulent rotational flow. To stay within the laminar area, pipe rotation must be held under 20 RPM and Reelwells WB and pipe scenario number 2 should be used (see parameter pipe size for details). This may ensure that rotational flow alone will not expedite mixing zone movement.

If the chain of assumptions is repeated for the two Reelwell scenarios, it would look like

High RPM → elevated Re number → turbulent rotational flow → not known

Since none of the experiments have been conducted in a realistic scale, the effect of the turbulent rotational flow on the systems fluids is **not known**. It can be assumed, with regard to the test rig 3 results, that the turbulent flow pattern may enhance mixing zone propagation.

Summarizing the discussion and the experimental data above; High RPM may induce turbulent rotational flow, which will affect the heavy light interface.

Low RPM may keep the rotational flow inside the laminar range and enable predictable mixing patterns.

Too low RPM will enable the fluids to slip out of suspension, and a semi horizontal interface may form. These unbeneficial interfaces may be seen as *surges*.

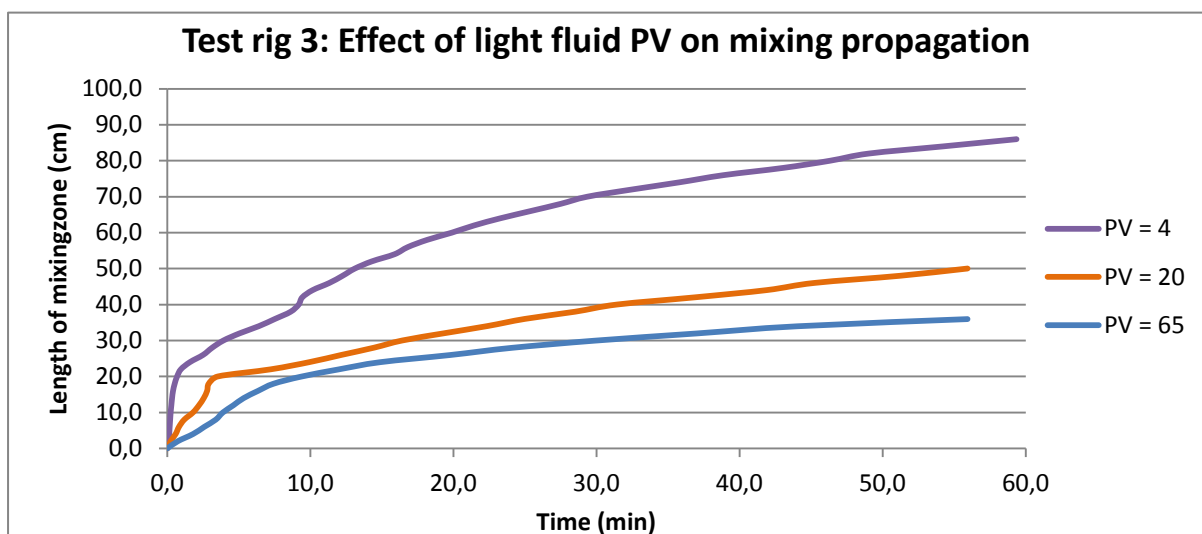
Note:

The definition of high and low RPM influence on the Reynolds number is totally dependent on the pipes diameter.

Viscosity effect

The viscosity of the fluids seems to have a significant effect on the spread of the mixing zone. Both heavy and light fluid viscosity may retard or accelerate the interfaces movement in the system. The retardation and acceleration effect of heavy fluid viscosity has not been investigated in detail, but it is assumed that the heavy fluid will follow similar characteristics as for the light liquid.

As seen in the graph below, the light fluid plastic viscosity correlates with the mixing distance and rate. Low PV in the light fluid seem to encourage more vigorous mixing, while a minor increase in PV drastically reduces mixing zone movement.



Graph 33: Displays the effect of low viscous light fluid have on mixing propagation in test rig 3. [02]
All other parameters than the light fluids properties and rheology is held constant.
Data is collected from ex. 21 (PV 65), ex. 25 (PV 4) and ex. 26 (PV 20).

The table 43 calculated mixing distance and mixing rate show a similar indication:

PV	Mixing distance (cm)	Mixing rate (cm/min)
4	86	1,4274
20	50	0,8187
65	36	0,6248

Table 43: Mixing distance and rate for PV 4, 20 and 65.

The effect of increasing light fluid PV in the purpose of hindering heavy light interface movement, seems to be less and less effective. The reduction in mixing zone movement looks to be most effective when increasing PV from a low value.

When scaling up the mixing distances and rates we clearly see that mixing zone distribution is more than doubled from a high light fluid PV to a low light fluid PV.

	Scenario 1		Scenario 2	
PV	Mixing distance (m)	Mixing rate (m/h)	Mixing distance (m)	Mixing rate (m/h)
4	8,33	8,29	5,91	5,89
20	4,84	4,76	3,44	3,38
65	3,49	3,63	2,48	2,58

Table 44: Mixing distance and rate for PV 4, 20 and 65 scaled up to scenario 1 and 2. The three experiments had test duration of 1 hour, the mixing distance and mixing rate has thereby roughly the same value.

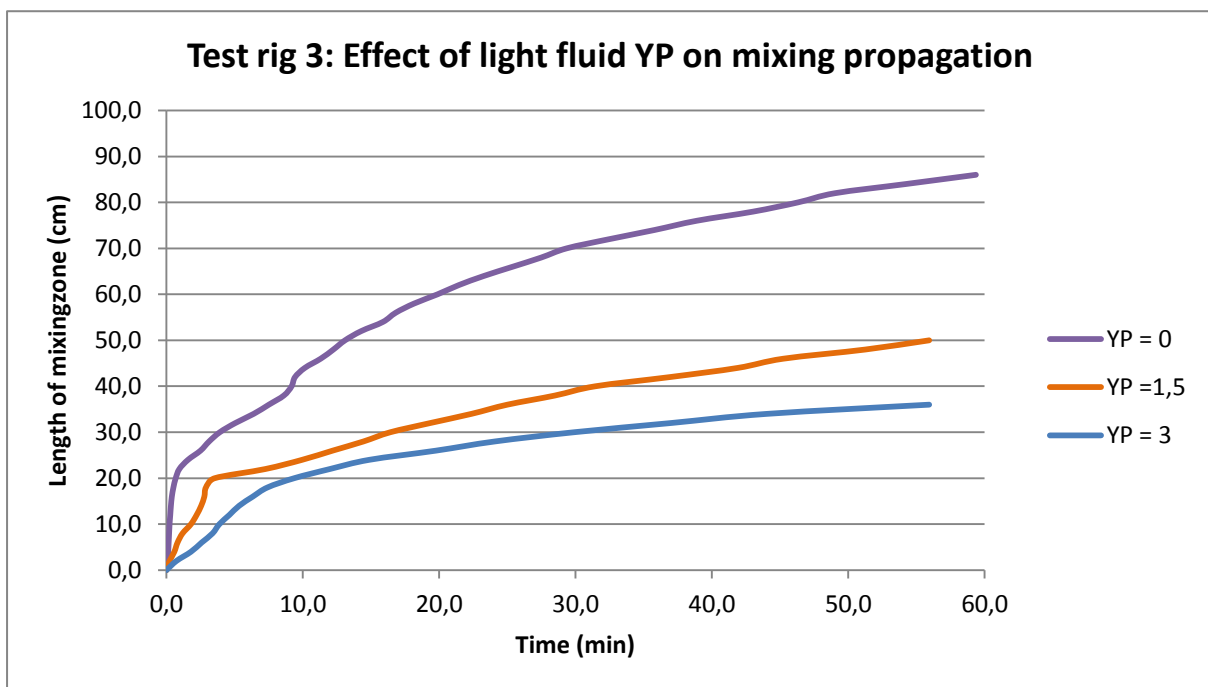
When looking at Reelwells fluid configuration it is shown that they use fluids with PV of 20 and above. As mentioned, higher plastic viscosity values will have a positive effect on reducing mixing zone movement. Reelwells PV configuration will therefore be well suited with regard to reducing heavy light interface spread.

To sum up the discussed effect of viscosity; High PV in a fluid will try to hinder mixing zone movement.

Fluids with low PV has a higher likelihood of being mixed together, because of the low internal resistance in the fluids.

Yield point (YP)

Together with plastic viscosity, the heavy light fluids yield point seem to be the leading rheological parameters when it comes to effect on interface propagation. As for viscosity, the heavy and the light fluids YP has a significant impact on the mixing zone distribution. As shown in [Experiments](#), both the heavy and light liquids mixing effect from YP were investigated.



Graph 34: Displays the effect of Yield point differences have on mixing propagation in test rig 3. [02]
All other parameters than the light fluids properties and rheology is held constant.

As seen on the modified graph above, the YP also correlates with the mixing distance and rate. The minor increases in YP works together with the plastic viscosity and slows down the mixing procedure. Since the variation between the yield points are so small (ranging from 0 to 3) it can be assumed that YP is not the leading parameter in this scenario. Still, small yield point elevations in the light fluid seem to impede the mixing zone movement.

Yield point induced mixing zone deceleration is also seen in test rig 1 experiments 4 and 6, where a heavy fluid with high yield point is used. As mentioned in [Results and analysis, Test rig 1](#), the experiments resulted in none to minimal interface movement. As seen in fluid table 1 these liquids yield points were 25 (Bentonite 1) and 22 (sheared Bentonite 1). These are the only two tests with fluids that approached the Reelwell fluids yield point values. Even with the crude test rig, they showed that fluids with high yield properties can withstand extensive mixing forces.

Since the experiments were not performed with a simulated drill pipe creating the disturbances, it is hard to conclude that the high YP has a dominant effect on the mixing zone propagation. It can be assumed that it has a potential positive effect, and high YP may be implemented in the heavy light fluid configuration.

Summary of major investigations

Table 45 shows the major investigation obtained out of the thesis research work. Each parameter mixing effect is summarized in the following table:

	Mixing effect	
	Low/small	High/large
Density difference	Low density difference is assumed negative. With less gravitational forces working on the fluids, increased mixing may occur.	High density difference is assumed positive. Reduced mixing may be an effect of the increased gravitational difference between the fluids.
Inclination	Low inclination or low negative inclination will allow for an accelerated interface spread.	High inclination will reduce interface length and therefore mixing zone length.
Pipe size*	Small pipe sizes will at low inclinations struggle with establishing consistent and clear mixing interfaces	Large pipe sizes will tend to stabilize the fluid system faster and create a predictable interface progression.
RPM**	Low RPM will allow the rotational flow to stabilize and will keep it inside the laminar area.	High RPM will create turbulent rotational flow, which will affect the interface movement in a negative way.
Viscosity	Low viscous fluids allow for more turbulence under rotation and lower resistance against mixing forces.	Fluids with high viscosity are resistant against changes in their structure and will therefore counteract mixing forces.
Yield point	Low YP in a fluid will increase its mixing potential and thereby enhance heavy light interface movement.	A fluid with high YP will stagger the mixing propagation and keep the fluids separated.

Table 45: Displays the parameters effect on mixing zone movement.

- = Increased mixing effect
- = Decreased mixing effect
- = Assumed mixing effect

Red = Assumed increased mixing effect
Green = Assumed decreased mixing effect

* = Large pipe size is considered the same as small wellbore pipe ratio, and small pipe size is regarded as large wellbore pipe ratio.

** = RPM effect on the interface is relative to the diameter of the rotating pipe.

6 Conclusion

The experimental result on the mixing between two stationary fluids in a near horizontal well section indicates the following:

- The mixing zone seems to be limited to approximately the predicted stationary mixing zone length L_{MZ} .
- The well inclination has the most governing effect of the parameters. It decides the interface length and thereby the extent of the mixing zone.
- The interface movement is normally slow, but depends on parameters: density difference, inclination, pipe size, RPM, viscosity and Yield point.

Even with an unbeneficial combination of the parameters, the mixing zone appears not to move in a rapid rate. This is because the positive inclination will prevent the heavy light interface from progressing, and will limit its reach.

To avoid high mixing speed at the heavy light interface, it is preferred to use:

- Clear density difference between the fluids*
- Large pipe size relatively to the wellbore
- Low RPM
- High plastic viscosity and Yield point of the fluids

* = Needs further detailed investigation.

Further research based on advanced numerical and analytical models may reveal the dynamics in the mixing zone.

Abbreviations

Abbreviation	Full version
ACW	Anticlockwise
CD	Compact disk
cP	centipoise
CW	Clockwise
Ex.	Experiment
ft	Feet
FPS	Frames Per Second
HSE	Health, Safety, Environment
OBM	Oil based mud
OWR	Oil water ratio
Pas	Pascal seconds
PV	Plastic viscosity
RDM	Reelwell Drilling Method
RPM	Rotation per minute
sg/s.g	Specific gravity
sqft	Square feet
YP	Yield point
WBM	Water based mud

Table 46: Abbreviation table.

Difficult words and phrases

i.e. – “That is”

Surge – To increase suddenly.

Sweet spot – a situation where a combination of parameters results in a maximum response for a given amount of effort

U-tubing – An event where a low density fluid is positioned below a high density fluid in a confined space (example a tube). Because of gravitational forces, these fluids will try to switch places, and will do so in a varying rate, depending on the difference in density, inclination and rheological factors.

References

General:

- 01 Eirik Aasberg Vandvik, UIS, Personal notes and pictures (taken with iPhone 4), February – May 2014.
- 02 Eirik Aasberg Vandvik, UIS, "Experiments sheet", June 2014.
- 03 Eirik Aasberg Vandvik, UIS, "Experimental CD", June 2014.
- 04 Eirik Aasberg Vandvik, UIS, Drawn figures/illustrations, June 2014.
- 05 Belayneh M, UIS, given information, February 2014
- 06 Sakhalin project, <http://www.ordons.com/asia/far-east/9976-sakhalin-1-project-drills-worlds-longest-extended-reach-well.html>. [Downloaded 16.03.14] 2011.
- 07 Sonowal, K., Bennetzen, B., Maersk Oil Qatar AS, K&M Technology group, Schlumberger D&M, "How Continuous Improvement Lead to the Longest Horizontal Well in the World", SPE/IADC 119506, 2009.

Reelwell:

- R01 Reelwell, Reelwell homepage, Available from: <http://www.reelwell.no/>. [Downloaded 09.04.14] 2011.
- R02 Ola Michael Vestavik, Reelwell Drilling Method, [SPE-119491], 2009, presented at SPE/IADC Drilling Conference and Exhibition, 17-19 March, Amsterdam, The Netherlands.
- R03 O. Vestavik, Reelwell, M. Egorenkov, Merlin ERD, B. Schmalhorst, RWE Dea AG, J. Falcao, Petrobras, M. Roedbro, Shell Technology Norway, "Extended Reach Drilling - new solution with a unique potential", 2013.
- R04 Reelwell, Challenge and solutions, Available from: <http://www.reelwell.no/Extended-Reach-Drilling/Challenges-Solutions>, [Downloaded 07.05.14] 2011.
- R05 Reelwell, Internal information and figures/illustrations, February 2014.

Theory

- T01 Bernt, Aadnøy, Iain Cooper, Stefan Miska, Robert Mitchell, and Mitchael Payne, 2009// Advanced Drilling and Well Technology, Society of Petroleum Engineers ISBN978-1-55563-145-1
- T02 Olaf Skjeggstad, "Boreslamteknologi", 1989 ISBN 978-82-419-0010-5
- T03 Belayneh M: Advanced drilling Engineering lecture note, UIS, 2014
- T04 T. Bourgoyne Jr., Keith K. Millheim, Martin E. Chenevert and F.S. Young Jr., Applied Drilling Engineering, Vol. 2. 1991. Richardson, Texas: SPE Textbook Series, Society of Petroleum Engineers.
- T05 Ramadan Mohammed Ahmed and Stefan Z. Miska 2008, Experimental Study and Modeling of Yield Power-Law Fluid Flow in Annuli with Drillpipe Rotation, SPE 112604, 2008. IADC/SPE Drilling Conference.
- T06 Steinar Evje and Kjell Kåre Fjelde: "Hybrid Flux-Splitting Schemes for a Two-Phase Flow Model", Journal of Computational Physics 175, 2002, p. 674-701.

Appendix A – Equations

Number	Equation	Number	Equation
(1)	$F_{g,heavy} > F_{g,light}$	(17)	$v = \frac{Q}{A}$
(2)	$\dot{\gamma} = \frac{\omega r_{DP}}{r_w - r_{DP}}$	(18)	$V_r = \omega r_i$
(3)	$\tau = \mu \gamma$	(19)	$Re, slot = \frac{785 D_{eff} \rho v_r}{\eta}$
(4)	$\tau = \mu_p \gamma + \tau_y$	(20)	$D_{eff} = D_w - D_p$
(5)	$\mu_p(cP) = \theta_{600} - \theta_{300}$	(21)	$\eta = \mu_p + \frac{5YP(D_w - D_p)}{V_r}$
(6)	$YP = \theta_{300} - PV$	(22)	$L_I = \frac{D_w}{\sin \theta}$
(7)	$YP = 2\theta_{300} - \theta_{600}$	(23)	$L_{MZ} = \sqrt{L_I^2 - D_w^2}$
(8)	$\tau = k\gamma^n$	(24)	$L_{MZ} = D_w \cot \theta$
(9)	$n = 3.321 \log \left(\frac{R_{600}}{R_{300}} \right)$	(25)	$\rho_{mix} = \rho_g \alpha_g + (1 - \alpha_g) \rho_m$
(10)	$k = \frac{R_{300}}{511^n} = \frac{R_{600}}{1022^n}$	(26)	$\alpha_l = 1 - \alpha_g$
(11)	$\tau_w = \tau_y + k\gamma^m$	(27)	$\rho_{effective-mud} = \rho_{mix}(1 - C_v) + \rho_{cutting} C_v$
(12)	$\gamma = \sqrt{\gamma_{\theta z}^2 + \gamma_{rz}^2}$	(28)	$\mu_{mix} = \mu_l \alpha_l + \mu_g \alpha_g$
(13)	$\gamma_z^* = \frac{1 + 2N}{3N} \frac{12U}{D_o - D_i}$	(29)	$\alpha_l = 1 - \alpha_h$
(14)	$\gamma_\theta^* = \frac{\omega D_i}{D_o - D_i}$	(30)	$m_p = \frac{\rho_p}{\rho_f} * \frac{\rho_{ff} - \rho_f}{\rho_p - \rho_{ff}} * m_f$
(15)	$\frac{3N}{2N+1} = \frac{3m}{2m+1} \left[1 - \left(\frac{1}{m+1} \right)^x - \left(\frac{m}{m+1} \right)^x \right]$	(31)	$Size\ ratio = \frac{wellbore\ diameter}{pipe\ OD}$
(16)	$\omega = \frac{2\pi}{60} RPM$	(32)	$Rod\ diameter = \frac{acrylic\ pipe\ ID}{size\ ratio}$

Table 47: Table of equations.

Appendix B – Reelwell technology

Reelwell Drilling Method vs. Conventional drilling method

[Information about RDM vs. conventional drilling method is given by Reelwell and may be bias, and is therefore open for discussion]

Figure 7 displays conventional drilling vs. RDM Drilling technology. As seen in the figure below, in conventional drilling, mud gets pumped down through the drill pipe and up the annulus carrying cuttings. In the RDM, drilling mud gets pumped down through the outer drill pipe in the dual drill string (DDS) and pumped up again through the inner pipe.

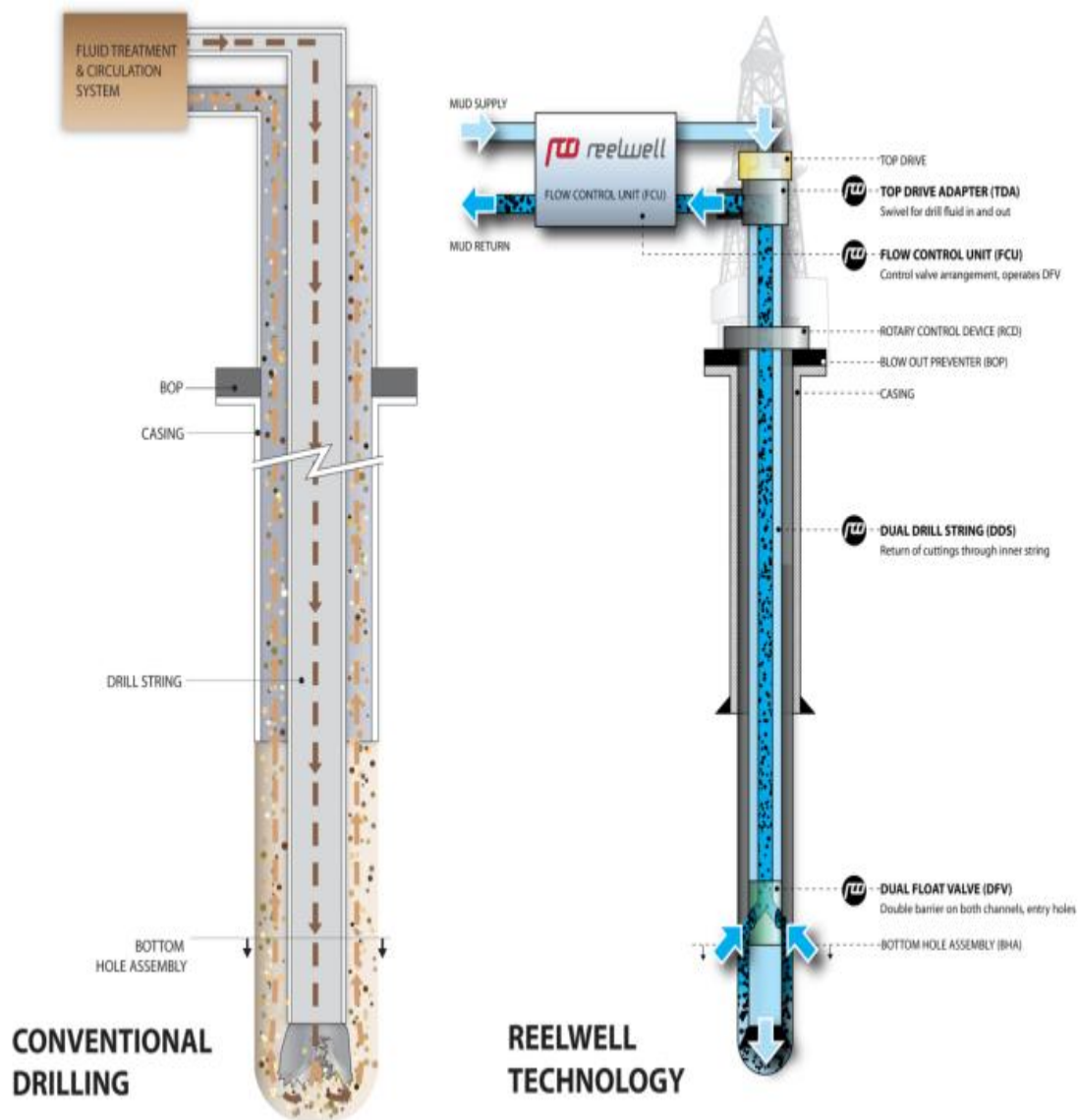


Figure R1: Conventional vs. RDM technology [R02]

As shown in the illustration above, the two drilling methods differ in several areas. The simplicity of the conventional method is replaced with more complex and advanced solutions in the RDM. Several of the features of the RDM have advantages and disadvantages when compared to the conventional drilling method:

- ✓ The double drill string of the RDM creates a more narrow space for the cuttings. This may limit the transportation capacity, but may also increase the transportation rate because of enhanced flow rate.
- ✓ The double drill strings two channels demand a thicker drill string to allow for required flow (even thicker if aluminum is used). The bigger pipe diameter will create a larger friction area between the drill pipe and the wellbore wall. The enlarged diameter will also reduce the risk of buckling, and will not hinder cuttings from flowing to the surface because of the Double Drill String (DDS) system.

Reelwell claims that their method surpasses traditional EDR solutions. Listed below is their own description of the ERD challenges and the benefits of the RDM [R04]:

Challenges for comparable ERD solutions	RDM benefits
The accumulation of cuttings in deviated and horizontal wells can lead to stuck pipe.	Wellbore cuttings are removed from the hole near the bit. Virtually no cuttings in the well at any time
Pipe twists-off due to stick slip problems.	Large diameter drill pipe reduces downhole vibrations.
Buckling of drill pipe.	Large diameter drill pipe reduces buckling of drill pipe.
Length of open hole horizontal section can be limited by Equivalent Circulation Density (ECD) issues. Pressure differential between toe and heel can result in loss at toe and influx at the heel.	By taking advantage of well geometrics, wellbore fluids below the piston could be static i.e. toe and heel pressure are virtually the same. Pressure is kept constant along the horizontal hole section, allowing for drilling longer open hole sections where narrow pressure windows exists.
ECD spikes in open hole when starting circulation can fracture formations.	The Dual Float Valve (DFV) opens when pressure above it balances the pressure in the well, minimizing formation damage.
High drilling fluid volume required to circulate cutting out via the annulus.	The pipe-in-pipe system requires a lower drilling fluid circulation volume to remove cuttings – RDM uses approximately 50% of the volume used by conventional drilling. Less active drilling fluid volume and flow rate reduces the consumption of chemicals and load on treatment facilities, leading to a more cost efficient and environmentally friendly system.
Bottoms-up circulation takes 20-100 min per 1000 m depending on well design.	RDM bottoms-up circulation takes 6-7 min per 1000 m.

Table R1: Displays the challenges for conventional ERD solutions vs. RDM benefits. [R04]

Reelwell method equipment

[Information about Reelwell equipment is taken from [R01, R03].]

The RDM is comprised of several vital components. Shown below is a figure that presents a schematic of the basic arrangement for RDM and the following arrangements and special tools used in RDM.

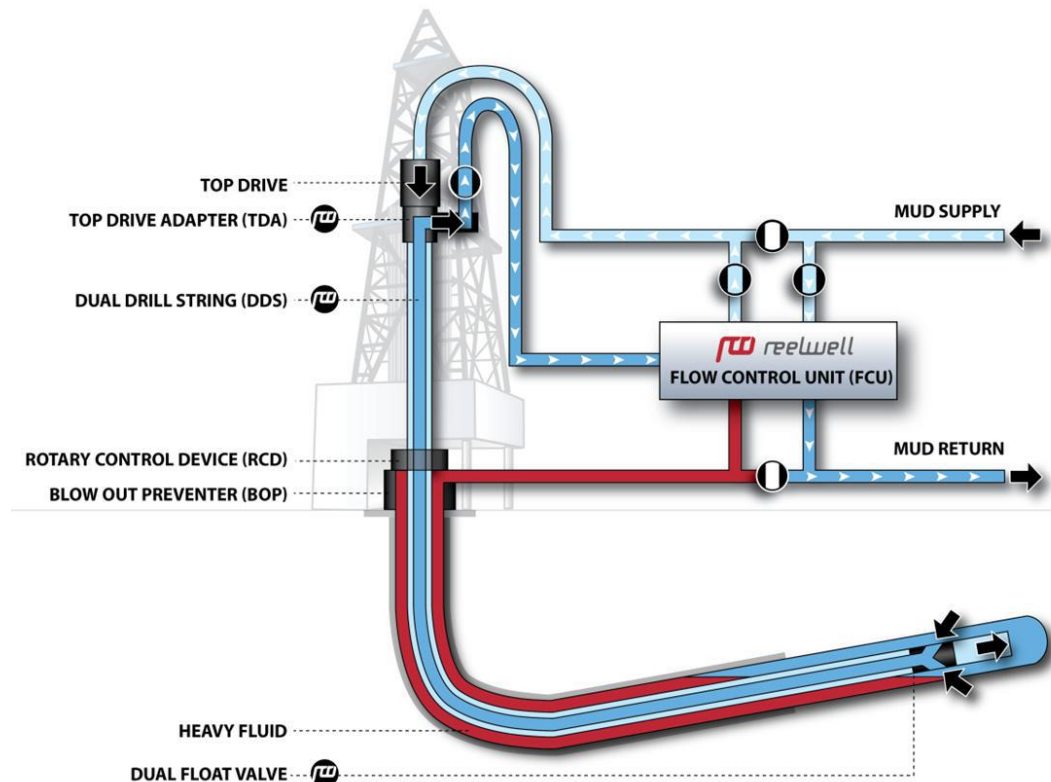


Figure 6: Displays the heavy light setup with all RDM components. [R03]

- **Top Drive Adapter (TDA):** The TDA is a unique swivel made to adapt and allow rotation of the DDS with the top drive. The TDA is connected to the Reelwell Control Unit through a mud hose and a mounted stand pipe.
- **Flow Control Unit (FCU):** The FCU is a control valve arrangement fitted with flow and pressure sensors for flow and pressure control of the system. All the flow paths of the system are connected to the control unit.
- **Dual Drill String (DDS):** The DDS is a dual wall drill string where the outer channel is used for pumping liquid down to the drill bit and the inner channel is used to transport the drill cuttings back to the surface.

- **Dual Float Valve (DFV):** The DFV cuts of the DDS into a conventional BHA. The DFV is made up of a flow x-over from the well annulus into the inner channel of the DDS and is fitted with valves to isolate the drill pipe during connections. Figure ... and ... displays the opening and closing sequence of the DFV

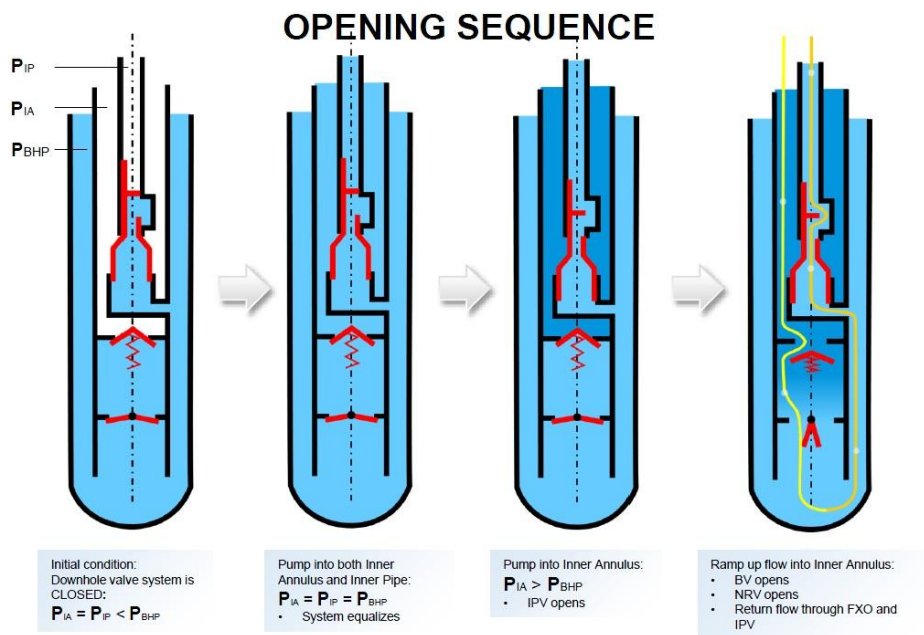


Figure R2: The opening sequence of Reelwells DFV. [R05]

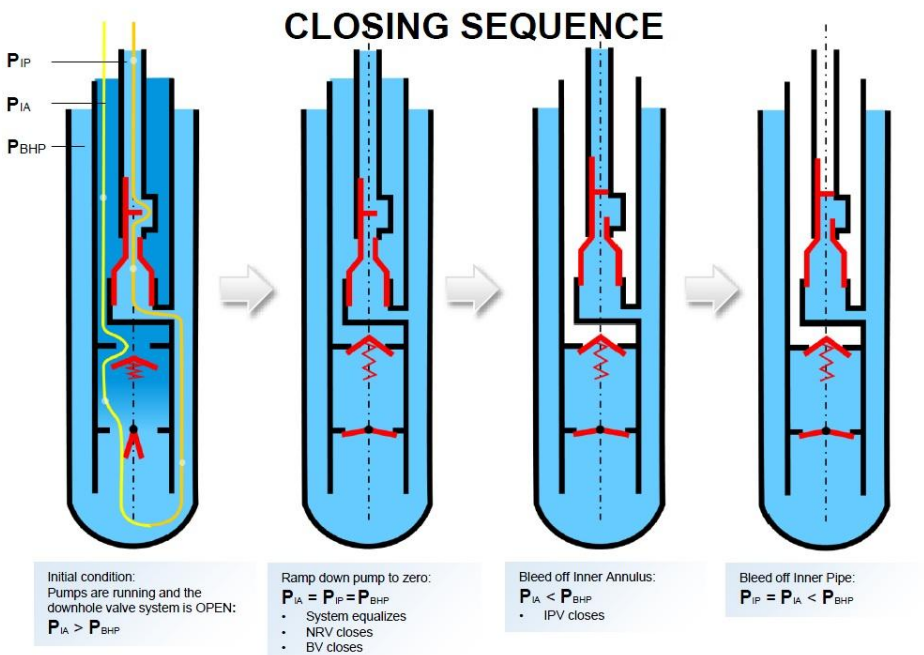


Figure R3: The closing sequence of Reelwells DFV. [R05]

- The active circulating fluid, in blue colour, is used to power downhole tools and to clean the well.
The stagnant well fluid, in red colour, trapped by the well design, uses high density to stabilize the hole and to create the buoyancy of the string.

- **Hydraulic WOB***
(optional): A sliding piston which is inserted as a part of the drill string. It isolates the well bore fluids and uses the hydraulic pressure behind the piston to push the bit forward.
* = Hydraulic WOB is not part of the heavy over light setup.

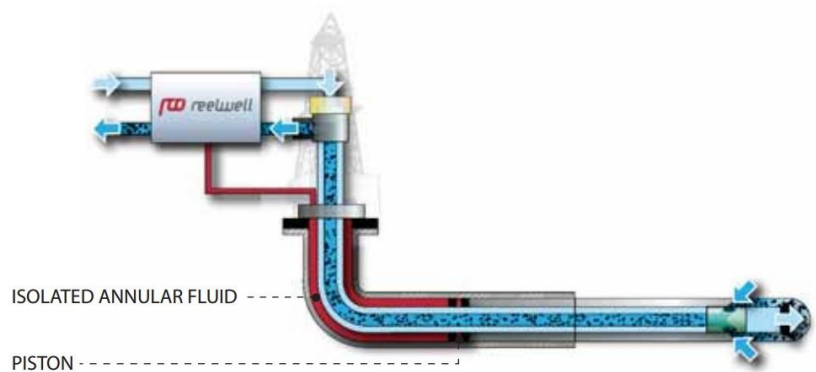


Figure R4: Reelwell hydraulic WOB. [R01]

Appendix C – Test rig construction and general specifications

Test rig 1

Test rig construction and setup

[See [Appendix D](#) for detailed information about used equipment and tools.]

To construct test rig 1, the following equipment and tools were used:

- Duct tape
- Ruler
- Thread seal tape
- Utility knife
- Vernier Caliper

The first test rig was comprised of a 515,0 mm long acrylic cylinder with an OD of 39,7 mm and a ID of 29,5 mm. It would serve as an ideal representation of a wellbore, without any migration routes or cavities for the fluid to get caught or flow through.

To contain the fluid within the systems parameters (the acrylic tube) 2 plugs were made:

Top plug: A foam-based, conical plug which was formed out of a whiteboard sponge. The plug was cut out of the sponge with a utility knife and ground down to a conical shape with sand paper. The sponge plug was designed to be oversized to ensure a tight fit.

Bottom plug: A red, "hat" shaped plastic plug wrapped in thread seal tape. The plastic plug blocked the lower opening, while the sealing tape prevented the fluid from leaking out.

Allowing for disturbances in the system, a drill fitted with a 14 mm wood drill bit was attached through the top plug. The drill bit would simulate a simplified wellhead and the related turbulence in bottom of the wellbore.

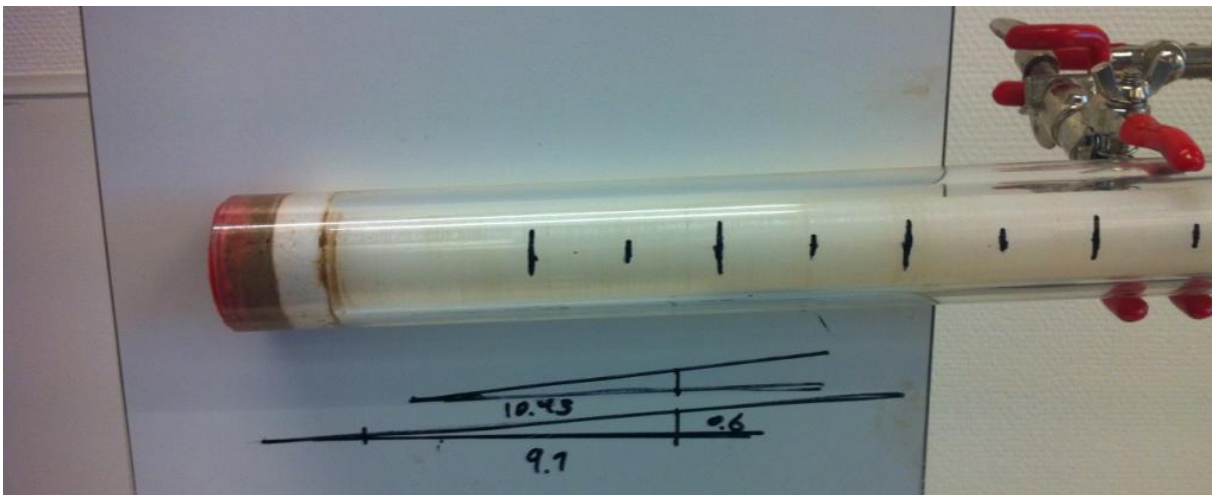
Picture 1 shows that the cylinder and drill was held in place by weighted down stands that reduced vibrations and allowed for different angles/inclinations of the acrylic tube.

2,5 cm measuring lines were marked on the acrylic tube with a marker. This was done to track the progression of the fluid interface when it shifted downwards the tube. The lines were drawn in 2,5 cm intervals to create a crude but illustrative representation of the mixing propagation. See picture 5 for a visual presentation of the lines.



Picture C1: Displaying the acrylic tube with drawn measuring lines. Portrayed to the right is the polystyrene “donut” and the bottom plug. [01]

To determine the inclination of the tube, a plank was used. The plank was placed on the horizontal plane and marked with a parallel line as a reference point. Another line was drawn by following the acrylic tube’s tilt. Where both lines overlapped, a ruler was used to measure from the point of overlap to the end of each line. Theorem of Pythagoras was then used to determine the inclination. Picture C2 shows the process.



Picture C2: Displays the process of determining the angle of the acrylic tube using the plank (the plastic rod from test rig 2 is positioned inside the acrylic tube). The same procedure was used in test rig 1 without the rod inside). [01]

To record the experiments two different cameras were used. An iPhone filmed the first two experiments, but was replaced with a GoPro Hero 2 for the rest of the test rig 1# experiments. GoPro Hero 2 was preferred because of its durability and extended battery life. The cameras were mounted to a camera stand and placed in front of the rig.

Test rig 1 was completed and ready for testing.

General specifications

Experiments conducted with test rig 1 contain diversities in regard to used equipment, execution etc. but have some constant factors. In the subsections below these constant factors and parameters for experiments performed with test rig 1 are listed.

Used equipment test rig 1

[See [Appendix D](#) for detailed information about used equipment and tools]

Equipment and tools utilized when performing experiments with test rig 1:

- Beaker glass
- Disposable syringe
- Drill (1st)
- Duct tape
- Food dye
- iPhone 4
- Grease/lubricator
- GoPro Hero 2
- Laboratory stand
- Plank
- Small plastic pipe
- Utility knife

Safety equipment

- Safety glasses
- Laboratory coat



Picture C3: Shows a sponge plug after it has been cut in to shape by the utility knife to the right. [01]

Experimental procedure

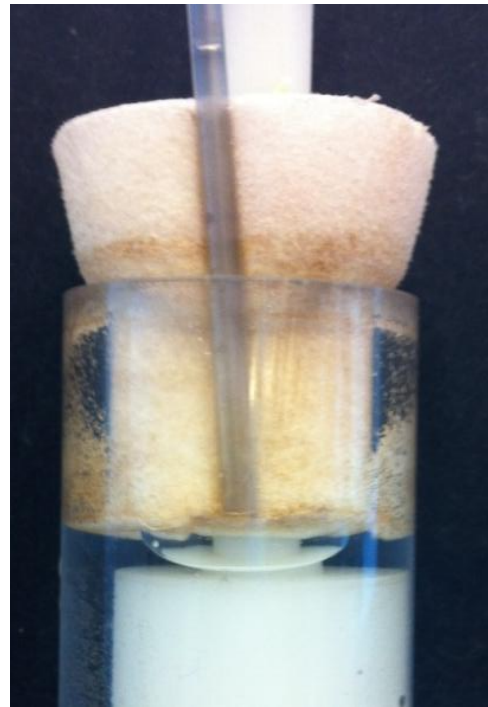
[All experiments conducted with test rig 1 followed the same procedure and execution]

1. The Acrylic tube was first filled with ... (see experiment specification) using a beaker glass.
2. A disposable syringe filled with ... (see experiment specification) dyed water topped off the acrylic tube.
3. To seal off the tube, the sponge plugs pierced hole was lubricated and mounted with the wood drill bit. The drill bit and sponge was then squeezed onto the top of the acrylic tube with the help of a small plastic pipe, which drained the redundant air out of the test system.
4. The filled and sealed acrylic was then positioned into a stand, which then was adjusted to desired inclination (see experiment specification) using the plank (see picture 6).
5. The drill was then attached to a stand, and connected onto the drill bit.
6. A camera was positioned onto the camera stand and in front of the test rig to record the experiment.
7. The experiment could now commence.
8. To start the experiment, a piece of duct tape was wrapped around the drills trigger.
9. Rotation began.
10. During the experiment, the extension of the mixing zone was recorded by following the measurement lines on the acrylic tube. The time it took to reach the different lines were documented at a later point using Adobe Premiere Pro C6.
11. After 20 min. of rotation, the experiment was ended by the duct tape being cut over with a utility knife.
12. Rotation stopped.
13. The rig was dismantled and washed to make ready for the next experiment.

General uncertainties test rig 1

All experiments conducted with test rig 1 are exposed to certain general uncertainties. Listed uncertainties apply for all tests performed with rig 1:

- The interpretation of the spread of the mixing zone done in Adobe Premiere Pro C6 is exposed to the human factor, and may contain inaccuracies.
- Stopping the experiment by cutting the duct tape may cause the experiment to run longer or shorter than intended. Estimated uncertainty is ± 10 sec.
- The inclination determined by the plank may not be correct because of the uncertainties this crude method is subjected to.
- The stand that holds the acrylic tube is exposed to unplanned disturbances, which may disrupt the held inclination.
- When sealing the acrylic tube with a sponge plug, air may leak into the system. This can affect the mixing of the fluids.
- Because of the surface tension of the heavy and light liquids the volume level read when filling the acrylic tube may be inaccurate. This can disrupt the planned ratio heavy light liquid ratio.
- Because of the limitations of the first drill an important factor as RPM couldn't be varied in a constant and accurate rate. RPM for the experiments done with the first test rig was therefore set as the maximum rotation rate of the drill (could vary depending on the battery level of the drill). Using a GoPro Hero 2 and the video editing program Adobe Premier Pro (see [Appendix D](#)) the speed of rotation was observed to be over 1000 RPM.



Picture C4: Displays the process of draining the acrylic tube of excess air before execution of a experiment. [01]

Test rig 2

Test rig construction and setup

[See [Appendix D](#) for detailed information about used equipment and tools]

To construct test rig 2, following equipment and tools were used:

- Industrial saw
- Lathe
- Sandpaper
- Utility knife
- Vernier Caliper
- Water resistant marker pen

The second test rig was featured with the same components as the first, but had an additional trait that made the system more similar to an actual drilling situation. Instead of having a wood bit to simulate the wellhead, a plastic rod served as a replacement for the drill string. This would expose the entire tube to the rotation, and not only a small percentage of the pipe.

The acrylic pipe would act as the wellbore while the plastic rod would represent the pipe. As previously mentioned the ID of the acrylic pipe used in test rig 1# was 29,5 mm. With these 3 measurements it was possible to calculate the diameter of the plastic rod (see [Appendix A](#) for equations):

With the correct diameter calculated, the fabrication of the plastic rod could begin.

A long plastic rod was cut to a length of 560 mm and lathed down from a diameter of 25,5 mm to the calculated 25,43 mm. As shown in the pictures C5 and C6 both ends were lathed down to a diameter of 10 mm. The tip where the drill would be attached was lathed to a length of 90 mm. These tips were also sanded down to minimize friction when rotating the rod. The end caps would ensure stability and reduce vibrations in the system. When rotated this rod would create a more realistic representation of Reelwells heavy over light method.



Picture C5: Showing the small tip being lathed and sanded down to correct size. [01]



Picture C6: The rod positioned into the lathe after completing lathing the long tip. [01]



Picture C7: The finished plastic rod. [01]

To stabilize and center the rod, a "donut" of polystyrene was positioned on top of the bottom plug. The "donut" was designed to match the small tip of plastic rod and to prevent it from creating uncontrolled disturbances.

Test rig 2 general specifications

Experiments conducted with test rig 2 contains diversities in regard to used equipment, execution etc. but has some constant factors. In the subsections below these constant factors and parameters for experiments performed with test rig 2 are listed.

Used equipment test rig 2

[See [Appendix D](#) for detailed information about used equipment and tools]

Equipment and tools used when performing experiments with test rig 2

- Beaker glass
- Disposable syringe
- Drill (1st)
- Duct tape
- Food dye
- Grease/lubricator
- GoPro Hero 2
- Plank
- Small plastic pipe
- Utility knife

Safety equipment

- Safety glasses
- Laboratory coat

Experimental procedure

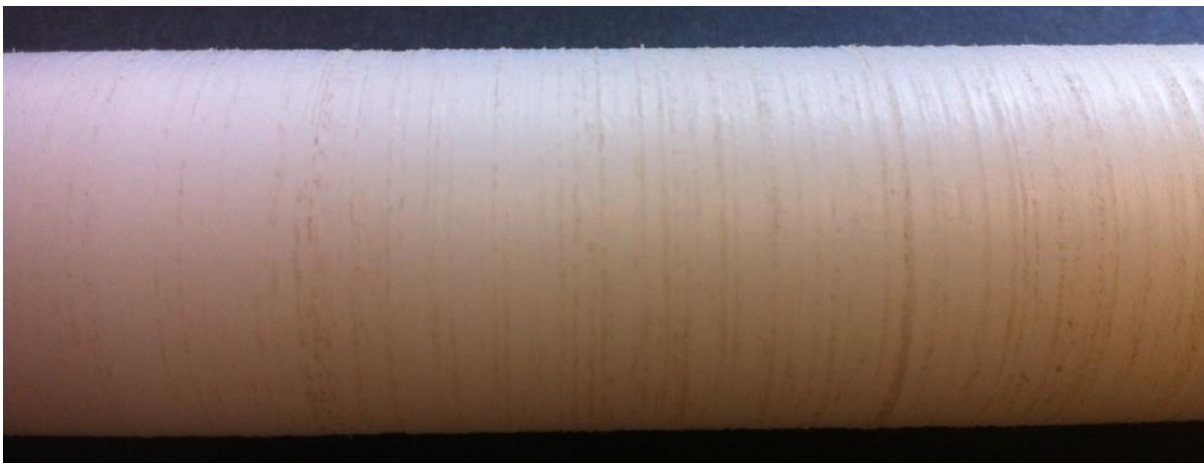
[All experiments conducted with test rig 2 followed the same procedure and execution]

1. The plastic rod was first placed into the acrylic tube, and centred by the polystyrene "donut".
2. The acrylic tube was then filled with ... (see experiment specification) using a beaker glass.
3. A disposable syringe filled with ... (see experiment specification) dyed water topped off the acrylic tube.
4. To seal off the tube, the sponge plugs pierced hole was lubricated and mounted on the long tip of the plastic rod. The sponge was then squeezed down the tip and onto the top of the acrylic tube with the help of a small plastic pipe. The pipe drained the redundant air out of the test system.
5. The filled and sealed acrylic was then positioned into a stand, which then was adjusted to desired inclination (see experiment specification) using the plank.
6. The drill was then attached to a stand, and connected onto the drill bit.
7. A camera was positioned onto the camera stand and in front of the test rig to record the experiment.
8. The experiment could now commence.
9. To start the experiment, a piece of duct tape was wrapped around the drills trigger.
10. Rotation began.
11. During the experiment, the extension of the mixing zone was recorded by following the measurement lines on the acrylic tube. The time it took to reach the different lines were documented at a later point using Adobe Premiere Pro C6.
12. After 20 min. of rotation, the experiment was ended by the duct tape being cut over with a utility knife.
13. Rotation stopped.
14. The rig was dismantled and washed to make ready for the next experiment.

General uncertainties test rig 2

All experiments conducted with test rig 2 are exposed to certain general uncertainties. Listed uncertainties apply for all tests performed with rig 1:

- The sponge plug used in test rig 1 and 2 had an off-center hole which in experiments conducted with rig 2 caused uneven rotation (effect assumed negligible on test rig 1). This may have accelerated the development of the mixing zone. On the other hand this mishap caused the test system to behave more realistically.
- As for test rig 1, the cutting of the duct tape may cause the experiment to run longer or shorter than intended. Estimated uncertainty is ± 10 sec.
- As for test rig 1, the inclination determined by the plank may not be correct because of the uncertainties this crude method are subjected to. An inaccurate inclination may accelerate or reduce the expansion of the mixing zone.
- The plastic rod has cyclical grooves after the lathing process (see picture 12). This can affect the mixing zones propagation through the acrylic tube. The mixing impact of these grooves will be investigated in experiments 14 and 15.



Picture C8: Close-up of the plastic rod, showing the lathe induced grooves. [01]

Test rig 3

Test rig construction and setup

[See [Appendix D](#) for detailed information about used equipment and tools]

During the construction of test rig 3 following equipment and tools were used:

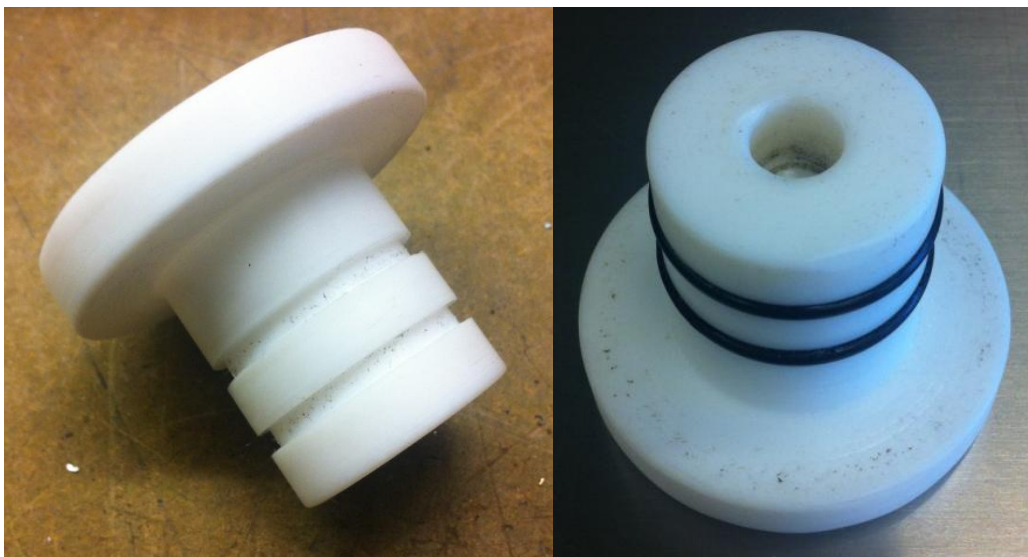
- Belt sander
- Carpenter rule
- Industrial saw
- Lathe
- Oxyacetylene torch
- Sand paper
- Silicon sealant
- Soft hammer
- Vernier caliper
- Water resistant marker
- White spray paint

The third and last test rig abandoned the main components from the two previous rigs. The small tube was replaced with a 2000 mm long acrylic pipe with an OD of 38 mm and an ID of 32,0 mm. The pipe would make it possible to observe mixing distribution for a significantly increased time and distance.

As in the construction of test rig 1, two plugs were made to contain the systems parameter:

Top plug: A foam based, conical plug made with the same material and design as used for the sponge plug in test rig 1 and 2.

Bottom plug: A plastic, hat shaped plug lathed from a solid cylinder of hard plastic. As shown in picture C9 it has two different sized ODs. The smaller OD is designed to fit inside the acrylic tube, and seal it of using seal rings. The larger diameter was cut to simplify the fitting and the dismantling of the plug. A hole was also drilled into the thinner part.



Picture C9: Displaying the plastic bottom plug; freshly fabricated to the right, and used to the left.
[01]

To create disturbances in the system, two different sized aluminum pipes were used. The pipes were scaled after pipe and wellbore size data from Reelwell. The pipe sizes 20 mm and 25 mm were used.

The aluminum pipes would be rotated inside the acrylic tube simulating a drill pipe inside a wellbore (same principle as used in test rig 2).

To adapt the pipes to the system, they were cut down to 1900 mm using a carpenter rule and an industrial saw. The edges were sanded down using a belt sander to remove excess metal after the cut.

To prevent fluid from leaking into the aluminum pipes during experiments they were sealed using 4 metal plugs (two for each pipe) which were lathed into shape. As shown in the picture C10 there were two types of plugs; one long, which was placed on the top of the pipe and one short for the lower end of the pipe. The two plugs were designed after the tips of the plastic rod in the second test rig. The long tip would connect the pipe to the drill while the short would be placed into the hole in the bottom plug and help stabilize the pipes rotation.



Picture C10: Showing the 4 metal plugs. [01]

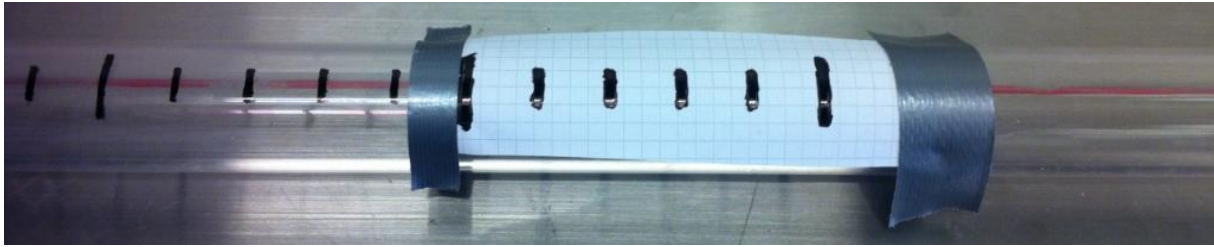
To connect the plugs to the aluminum pipes, a oxyacetylene torch heated the pipe ends and a soft hammer hammered the metal plugs in. The four plugs were designed to be oversized to ensure a tight fit. The belt sander and sandpaper were then used to sand down the deformations of the pipes.

To secure that no fluid could enter the aluminum rods, silicon sealant was smeared into the crack between the plug and the pipe.

To simplify the observation of the mixing zone the aluminum pipes were then painted white. The pipes could now be mounted into the acrylic tube.

As for test rig 1 and 2 measurement lines were drawn on the acrylic tube. A red, removable marker was used to draw a uniform line along the pipe. A paper stencil was then positioned along the line and a water resistant marker marked the measurement lines through it (see picture C11). The measurement lines configuration was 20 mm between the short lines and 100 mm between the long lines.

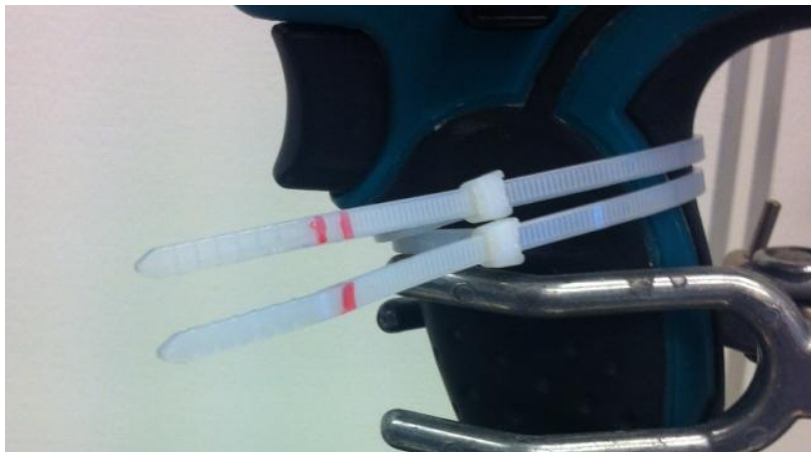
After the lines had dried, the removable marker was washed away and the acrylic tube was finished.



Picture C11: Displaying the paper stencil positioned on the acrylic tube. [01]

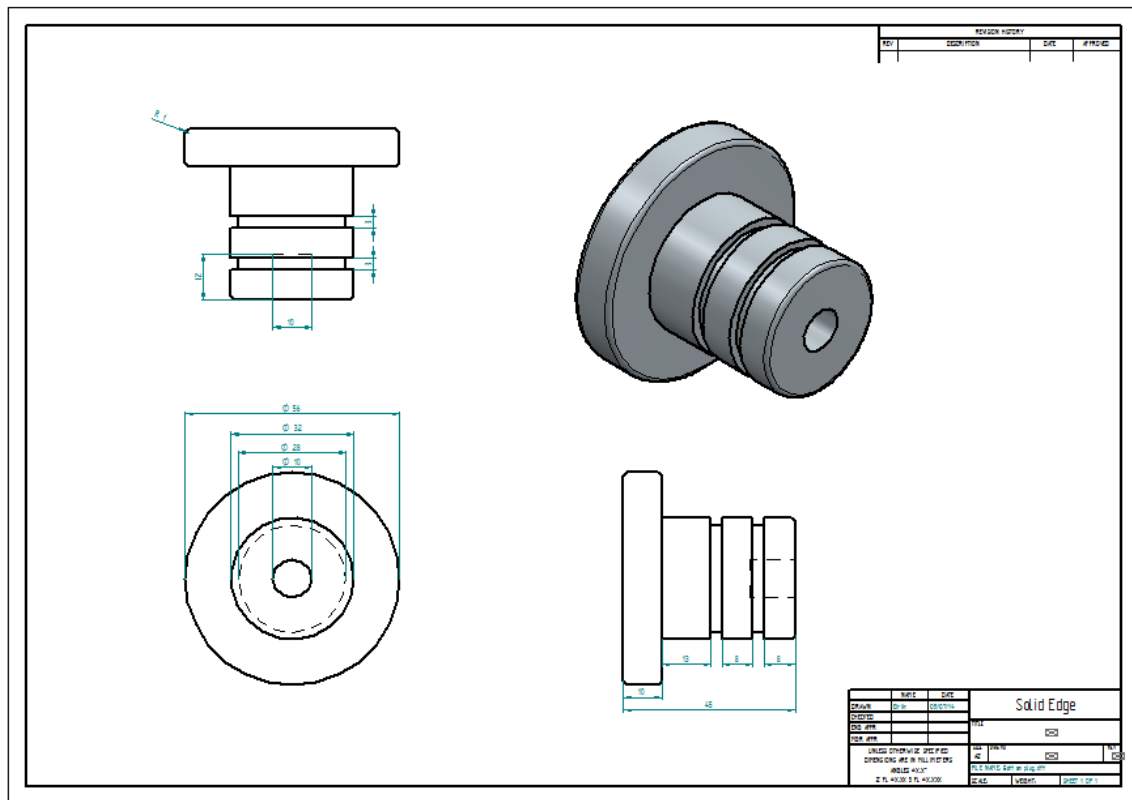
The main components of the third test rig were now complete and ready for assembly.

To run test rig 3 a new drill and trigger restraining method was needed. The new drill had prolonged battery life and more power, which would contribute to the rigs stability and reliability. To restrain the trigger two pre-tightened plastic strips were used (see picture ...). They were marked with red lines to differ them: 1 line = 150 RPM, 2 lines = 60 RPM. All components of the rig were now ready.



Picture C12: Showing the plastic strips around the drills handle. [01]

The third test rig was now finished and experiment operative.



Technical drawing 1: The technical drawing of the bottom plug. [04]

Test rig 3 general specifications

Experiments conducted with test rig 3 contained diversities in regard to equipment used, execution etc. however some factors are kept constant throughout the tests. In the subsections below these constant factors and parameters for experiments performed with test rig 3 are listed.

Used equipment test rig 3

[See [Appendix D](#) for detailed information about used equipment and tools]

Equipment and tools used when performing experiments with test rig 3

- Beaker glass
- Digital protractor
- Disposable syringe
- Drill (2nd)
- Grease/lubricator
- GoPro Hero 2 and 3
- Plastic strips (60 and 150 RPM)
- Small plastic pipe
- Workshop stand

Safety equipment

- Safety glasses
- Laboratory coat

Experimental procedure

[All experiments conducted with test rig 3 followed the same procedure and execution]

1. The plastic plug was first placed onto the lower part of the acrylic tube and sealed off.
2. Then a plastic hose was stuffed down the tube and the test rig was positioned vertical onto a wall.
3. A beaker glass containing ... (see experimental procedure) poured a previously calculated volume through the hose and into the tube. The test rig was left standing for 5 minutes to drain the remaining fluid from the hose.
4. The plastic hose was then removed and the ... (see experiment specification) aluminum pipe was positioned into the acrylic tube. The test rig was then replaced vertically onto a wall.
5. The remaining volume of the acrylic tube was then filled with ... (see experiment specification) using a beaker glass.
6. To seal off the tube, the sponge plugs pierced hole was lubricated and mounted on the long tip of the aluminum pipe. The sponge was then squeezed down the tip and onto the top of the acrylic tube with the help of a small plastic pipe. The pipe drained the redundant air out of the test system.
7. The filled and sealed acrylic was then positioned into a stand, which then was adjusted to desired inclination (see experiment specification) using a digital protractor.
8. The drill was then attached to a stand, and connected onto the drill bit.
9. A camera (GoPro 2 and 3) was positioned onto the camera stand and in front of the test rig to record the experiment.
10. The experiment could now commence.
11. To start the experiment, one of two pre tightened plastic strips were placed around the drills trigger.
12. Rotation began.
13. During the experiment, the extension of the mixing zone was recorded by following the measurement lines on the acrylic tube. The time it took to reach the different lines were documented at a later point using Adobe Premiere Pro C6.
14. After 60 min. of rotation, the experiment was ended by removing the plastic strip from the drills trigger.
15. Rotation stopped.
16. The rig was dismantled and washed to make ready for the next experiment.

General uncertainties test rig 3

All experiments conducted with test rig 3 were exposed to certain general uncertainties. Listed uncertainties apply for all tests performed with rig 1:

- Both aluminum pipes have slightly off-center long tips, which caused unplanned movement of the pipes when they were exposed to rotation. This may have accelerated the propagation of the mixing zone. On the other hand, this design flaw caused the pipe to move more realistically around in the acrylic tube rather than an unlikely centered rotation.
- The plastic strips used to hold the drills trigger in place were subjected to uncertainties which may have caused higher or lower rotational speeds in certain experiments. The increase or decrease in pipe RPM may have caused an accelerated or decelerated movement of the mixing zone.



Picture C13: Displays the process of cleaning the long acrylic tube using paper towels as an improvised “Pig”. [01]

Viscometer test rig

Test rig construction and setup

[See [Appendix D](#) for detailed information about used equipment and tools]

To construct viscometer test rig, the following equipment and tools were used:

- Ruler
- Vernier Caliper
- Utility knife

The viscometer test rig was comprised of two components: A viscometer and a plastic cup. The viscometer was kept in original shape as described in [Appendix D](#). The plastic cup was made out of a water bottle. The bottle was measured using a ruler to the desired height and cut in two using an utility knife. Depth and diameter was later measured (using a Vernier caliper) to 150 mm and 56,3 mm. A scale was then positioned on the side of the cup, and the test rig was complete

Viscometer test rig general specifications

Experiments conducted with viscometer test rig contained diversities in regard to equipment used, execution etc. however some factors are kept constant throughout the tests. In the subsections below these constant factors and parameters for experiments performed with viscometer test rig are listed.

Used equipment viscometer test rig

[See [Appendix D](#) for detailed information about used equipment and tools]

Equipment and tools used when performing experiments with viscometer test rig

- Beaker glass
- GoPro Hero 2
- Disposable syringe
- Viscometer

Safety equipment

- Safety glasses
- Laboratory coat

Experimental procedure

[The two experiments conducted with Viscometer test rig followed the same procedure and execution]

1. The plastic cup was first filled $\frac{2}{3}$ of the total fluid volume with ... (see experiment specification) using a beaker glass.
2. A disposable syringe filled $\frac{1}{3}$ of the total fluid volume with ... (see experiment specification) into the plastic cup.
3. The cup was then positioned onto the Viscometer.
4. The experiment could begin.
5. RPM was gradually increased in the viscometers RPM intervals (3, 6, 100, 200) until heavy light mixing was complete.
6. The rig was dismantled and washed to make ready for the next experiment.

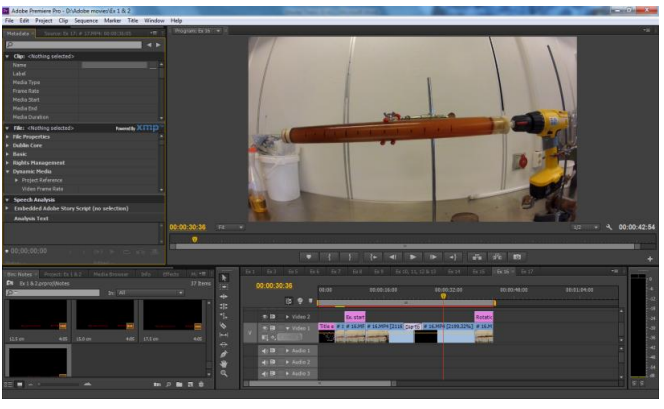

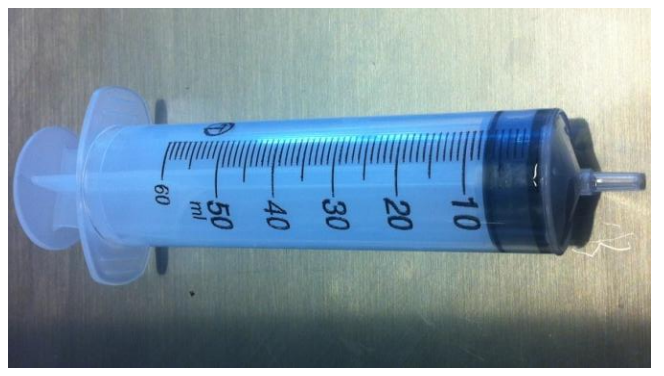
General uncertainties viscometer test rig



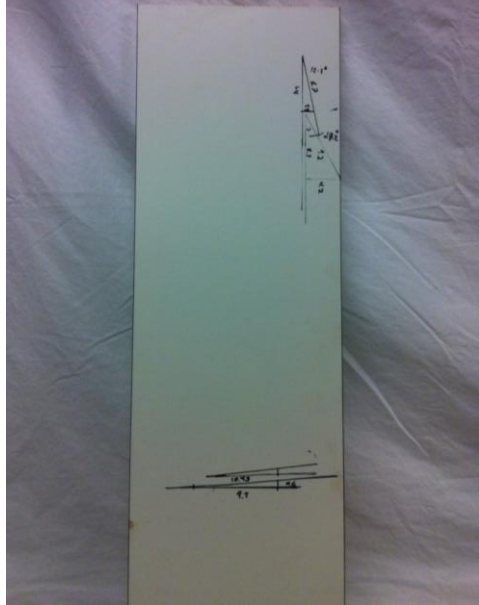
The two experiments conducted with Viscometer test rig were exposed to certain general uncertainties. Listed uncertainties apply for the two tests performed with the viscometer test rig:



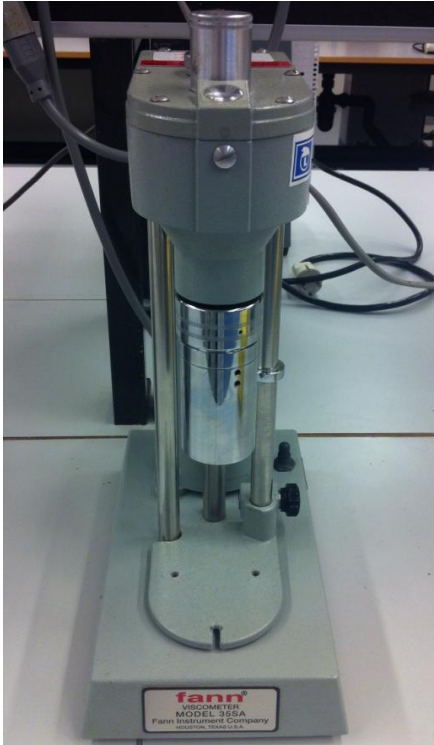
- The general uncertainty of the Viscometer in question applies for the two experiments. The RPM settings may be inaccurate, which would affect the perceived mixing at the specific RPM.
- The plastic cup may not have been positioned in the middle of the Viscometer. This may have affected the mixing effect.

Appendix D – Equipment/tools



Measuring equipment



Nr	Name	Description	Picture [01]
M1	<u>Adobe Premier Pro C6</u>	A high grade editing program used to shape and alter any type of video. Used as a measurement equipment together with GoPro Hero2 when determining RPM.	
M2	<u>Digital protractor</u>	Digital tool used to measure the angle of flat surfaces and other tilted objects. It is fitted with a tubular spirit level that ensures that the measurement is taken with a perfectly horizontal plane as a reference point. Has a angular resolution of 0,1° and a measurement accuracy of ±0,5°.	
M3	<u>Disposable syringe</u>	A device used to precisely measure a small quantity of liquid. Has a max capacity of 60 ml.	




Nr	Name	Description	Picture [01]
M4	<u>Laboratory scale</u>	An accurate measuring tool used to precisely weigh small quantities of different experimental components or ingredients. The scale is able to measure down to 1/10 of a gram.	
M5	<u>Mud balance/scale</u>	A device used to measure the density of any type of liquid such as drilling fluids and other viscous liquids.	
M6	<u>Plank</u>	A tool used together with a marker pen to determine angles.	




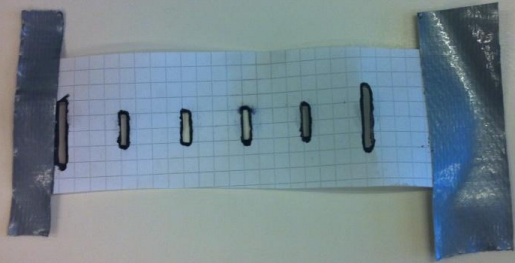
Nr	Name	Description	Picture [01]
M7	<u>Ruler/carpenters rule</u>	Measuring device used to measure small distances.	
M8	<u>Vernier Caliper</u>	Measuring tool specialized for measuring OD, ID and depth of tubes and pipes. The Vernier Calipers provide a precision to 0.01 mm or a 1/1000 of an inch. Can measure accurately up to 182,9 mm or 7,2 inch.	
M9	<u>Viscometer</u>	An instrument used to measure the viscosity of a fluid. It rotates a tube at different RPM's that is dipped into the tested fluid. Inside the tube there is a spring mounted cylinder which reacts to the different rotation speeds and the viscosity of the fluid. The movement of this cylinder is displayed on a scale on the top of the device.	







Experiment tools

Nr	Name	Description	Picture [01]
E1	<u>Beaker glass</u>	A container of glass which purpose is to retain a measured amount of liquid and be able to pour this liquid in a controlled manner.	
E2	<u>Camera stand</u>	A stand used to support the cameras, and position them in the right place and height.	




Nr	Name	Description	Picture [01]
E3	<u>Drill</u>	<p>[Pictures on the right from the top; Drill nr. 1 and nr. 2]</p> <p>A tool designed to rotate devices/objects at different speeds and torque.</p>	
E4	<u>Duct tape</u>	<p>A strong tape used to restrain and secure objects for a period of time.</p>	







Nr	Name	Description	Picture [01]
E5	<u>Food dye</u>	<p>[The picture shows only one of many food dyes used]</p> <p>An additive used to color fluid and liquids. This helps with distinguishing them from each other.</p>	
E6	<u>GoPro Hero (2/3)</u>	<p>A action camera used to film high quality footage. The camera is able to film with high frame rates (FPS), allowing for slow motion. Combined with the editing program Adobe Premier Pro C6 and the marker tape, the GoPro is used to determine RPM.</p>	
E7	<u>Grease/lubricator</u>	<p>A lubricating element used to decrease friction and heat generation in the interface between a stagnant and a moving object.</p>	

Nr	Name	Description	Picture [01]
E8	<u>iPhone 4</u>	[Picture taken with another iPhone 4] A smart mobile telephone fitted with among other things, video recording capabilities. Used to document experiments before the GoPro Hero2 was put to use.	
E9	<u>Laboratory stand</u>	A stand is designed to place and secure laboratory equipment in desired positions.	
E10	<u>Marker tape</u>	[Pictures on the right from the top; Marker tape nr. 1 and nr. 2] A piece of tape placed on a rotating object to be able to determine its RPM. This is done together with Adobe Premiere Pro C6 and GoPro Hero 2 and 3.	
E11	<u>Paper stencil</u>	A tool used to produce constant shapes on an underlying surface by applying pigment.	




Nr	Name	Description	Picture [01]
E12	<u>Plastic hose</u>	An elastic plastic tube used to transport liquid from one point to another in a clean manner.	
E13	<u>Plastic strips</u>	A tool designed to restrain small objects	
E14	<u>Small plastic pipe</u>	A device used to remove excess air.	
E15	<u>Thread seal tape</u>	A low friction tape which molds itself when put under pressure. Is most commonly used to seal threads and other tight fits.	
E16	<u>Utility knife</u>	A tool used to cut and shape soft objects.	
E17	<u>Workshop stand</u>	Stand used to stabilize cylindrical objects.	

Fabrication Equipment

Nr	Name	Description	Picture [01]
F1	<u>Belt sander</u>	A grinding tool fitted with a seamless loop of abrasive sandpaper which is rotated at high speed. The belt sander is mainly used to grind down metal parts into a desired shape.	
F2	<u>Industrial saw</u>	A heavy duty saw designed to cut metal and hard plastics in a fast and safe manner. The saw has a nozzle which sprays coolant on the saw blade to ensure minimum heat development in the material.	
F3	<u>Lathe</u>	An equipment/tool used to reduce the diameter and size of circular metal and hard plastic objects. It is fitted with carbide cutting tools which shave off pieces of the rotated material.	

Nr	Name	Description	Picture [01]
F4	<u>Oxyacetylene torch</u>	An oxyacetylene powered torch used to cut and heat metal objects. The torch can also be used for soldering.	
F5	<u>Sand paper</u>	An abrasive paper designed to file different objects down to the desired shape.	
F6	<u>Silicon sealant</u>	A tool used to seal gaps and cracks from intruding liquids.	
F7	<u>Soft hammer</u>	A hammer designed with soft tips. This is done to protect the object that is being hammered from unnecessary deformations and damages.	
F8	<u>Water resistant marker pen</u>	Pen used to mark and draw on objects that are exposed to water and other liquids.	
F9	<u>White spray paint</u>	Spray paint used to cover various surfaces.	

Safety equipment

Nr	Name	Description	Picture [01]
S1	<u>Gloves - workshop and welding</u>	Gloves used to protect the hands from warm and sharp objects.	
S2	<u>Laboratory coat</u>	Protective gear used to shield the body from exposure to dangerous elements, mainly liquids.	
S3	<u>Protective glasses</u>	Glasses built to withstand small high-speed projectiles and protect the eyes from other hazardous objects or liquids.	

Appendix E – List of charts

	Page
Chart 1: The flow pattern of test rig 2 experiments conducted with Syrup 2 and water. [02]	59
Chart 2: Shown the flow pattern of experiments conducted with OBM 1 and olive oil. [02]	67
Chart 3: The flow pattern for experiments conducted according to Matrix 1. [02]	80
Chart 4: Displays the flow pattern of experiment 25. [02]	82
Chart 5: The flow pattern of the experiments conducted in matrix 2. [02]	86
Chart 6: The flow pattern of experiments 30 and 31. [02]	90
Chart 7: Viscometer experiment 2s flow pattern. [02]	96
Chart 8: Displaying the flow pattern differences between two pipe sizes. [02]	102
Chart 9: Displaying the flow pattern differences between two pipe sizes. [02]	102
Chart 10: Displaying the flow pattern differences between two RPM. [02]	104
Chart 11: Displaying the flow pattern differences between three RPM for Reelwell scenario 1. [02]	105
Chart 12: Displaying the flow pattern differences between three RPM for Reelwell scenario 2. [02]	105

Appendix F – List of figures

Figures

	Page
Figure 1: Extended reach drilling envelope. [07]	6
Figure 2: Comparison of Conventional drainage area vs. Reelwell drainage area. [R02]	7
Figure 3: Displays Reelwells heavy over light concept. [R02]	7
Figure 4: Illustrates Reelwells heavy over light method. [R02]	8
Figure 5: Figures illustrating how inclination is perceived in the thesis. [04]	9
Figure 6: Displays the heavy light setup with all RDM components. [R03]	11
Figure 7: Bottom view of a rotation drill pipe in a wellbore. [04]	15
Figure 8: Helical flow of YPL fluid in concentric annulus. [T05]	20
Figure 9: Displays the three flow regimes. [T02]	23
Figure 10: The heavy light fluid scenario displayed with the applicable component names and setup. [04]	24
Figure 11: Showing the assumed heavy light interface when only the force of gravity affects the fluids. The dashed lines running throughout the figure represent the drill pipe. [04]	25
Figure 12: Showing the assumed heavy light interface when the forces of gravity and rotation affect the fluids. The dashed lines running throughout the figure represent the drill pipe. [04]	25
Figure R1: Conventional vs. RDM technology [R02]	115
Figure R2: The opening sequence of Reelwells DFV. [R05]	118
Figure R3: The closing sequence of Reelwells DFV. [R05]	118
Figure R4: Reelwell hydraulic WOB. [R01]	119
Technical drawing 1: The technical drawing of the bottom plug. [04]	133

Pictures

	Page
Picture 1: Test rig 1 # layout with used equipment positioned for a test of feasibility of future experiments. The acrylic pipe displayed has an inclination of 3,3° relative to the horizontal plane. The wood bit is as showed mounded trough the sponge plug into the drill. Weights are placed on both stands to ensure stability. [01]	33
Picture 2: Test rig 2 # setup with used equipment positioned for a test of feasibility of future experiments. The acrylic pipe displayed has an inclination of 3,3° relative to the horizontal plane. The plastic rod is mounded trough the sponge plug into the drill. Weights are placed on both stands to ensure stability. [01]	48

Picture 3: Test rig 3 # setup with used equipment positioned for a test of feasibility of future experiments. The acrylic pipe displayed has an inclination of 2,0° relative to the horizontal plane. The 20 mm diameter aluminum pipe is mounded through the sponge plug into the drill. The drill are fitted with different tensioned plastic strips. Weights are placed on both stands to ensure stability, while the workshop stand holds the heavy end in angle. [01]	70
Picture 4: Viscometer test rig setup. The plastic cup is displayed positioned onto the Viscometers steel cylinder, filled with fluids from the first experiment. The scale to the left is placed to simplify the observation of the mixing zone movement. [01]	92
Picture C1: Displaying the acrylic tube with drawn measuring lines. Portrayed to the right is the polystyrene “donut” and the bottom plug. [01]	121
Picture C2: Displays the process of determining the angle of the acrylic tube using the <u>plank</u> (the plastic rod from test rig 2 is positioned inside the acrylic tube. The same procedure was used in test rig 1 without the rod inside). [01]	121
Picture C3: Shows a sponge plug after it has been cut in to shape by the utility knife to the right. [01]	122
Picture C4: Displays the process of draining the acrylic tube of excess air before execution of a experiment. [01]	124
Picture C5: Showing the small tip being lathed and sanded down to correct size. [01]	125
Picture C6: The rod positioned into the lathe after completing lathing the long tip. [01]	125
Picture C7: The finished plastic rod. [01]	126
Picture C8: Close-up of the plastic rod, showing the lathe induced grooves. [01]	129
Picture C9: Displaying the plastic bottom plug; freshly fabricated to the right, and used to the left. [01]	130
Picture C10: Showing the 4 metal plugs. [01]	131
Picture C11: Displaying the paper stencil positioned on the acrylic tube. [01]	132
Picture C12: Showing the plastic strips around the drills handle. [01]	132
Picture C13: Displays the process of cleaning the long acrylic tube using paper towels as an improvised “Pig”. [01]	135

Appendix G – List of graphs

	Page
Graph 1: Displays buoyancy effects on drag in a RDM drilling scenario. [R03]	13
Graph 2: Shows the effect of buoyancy and drill pipe material has on torque. [R03]	15
Graph 3: Displays the models shear stress-shear rate behavior. [T03]	17
Graph 4: Displaying the distribution of density in the mixing zone. [02]	26
Graph 5: Displays the fluid rheology to the liquids used in test rig 1#. [02]	40
Graph 6: Illustrates the propagation of the mixing interface for all applicable experiments conducted with test rig 1#. [02]	41
Graph 7: Displays the effect of inclination gained from experiment 1, 2 and 3. [02]	42
Graph 8: Trend lines of the curves displayed in graph 6. [02]	43
Graph 9: Visual presentation of inclinations effect on mixing distance and mixing rate. [02]	43
Graph 10: Displays the data gained from experiment 4. [02]	44
Graph 11: Displays the data gained from experiment 7. [02]	45
Graph 12: Displays the fluid rheology to the liquids used in test rig 2#. [02]	58
Graph 13: Illustrates the propagation of the mixing interface for all applicable experiments conducted with test rig 2#. [02]	59
Graph 14: Displays the effect of CW and ACW gained from experiment 14 and 15. [02]	63
Graph 15: Trend lines of the curves displayed in graph 14. [02]	63
Graph 16: Displays the mixing effect of heavy OBM and negative inclination gained from experiments 17, 19 and 20. [02]	66
Graph 17: Trend lines of the curves displayed in graph 16. [02]	66
Graph 18: Displays the fluid rheology to the liquids used in test rig 3#. [02]	76
Graph 19: Displays the fluid rheology to OBM 1, 2 and 3. [02]	77
Graph 20: Displays the fluid rheology to the liquids used in test rig 3#. [02]	77
Graph 21: Displays the mixing effect of RPM and pipe size gained from experiments 21, 22, 23 and 24. [02]	79
Graph 22: Trend lines of the curves displayed in graph 21. [02]	79
Graph 23: Displays the mixing effect of RPM and pipe size gained from experiments 21, 22, 23 and 24. [02]	81
Graph 24: Displays the mixing effect of RPM and pipe size gained from experiments 26, 27, 28 and 29. [02]	84
Graph 25: Trend lines of the curves displayed in graph 24. [02]	84

Graph 26: Displays the mixing effect of negative inclination gained from experiments 30 and 31. [02]	88
Graph 27: Trend lines of the curves displayed in graph 26. [02]	88
Graph 28: Displays the areas of surge and reduced mixing in experiment 31. [02]	89
Graph 29: Displays the fluid rheology to the liquids used in test rig 3#. [02]	94
Graph 30: Displays the mixing slopes of experiments conducted with positive and negative inclination. [02]	100
Graph 31: Displays the difference in heavy light interface movement between two pipe sizes. [02]	101
Graph 32: Displays the mixing effect of two different RPM. All other parameters than the RPM of the pipes is held constant. [02]	104
Graph 33: Displays the effect of low viscous light fluid have on mixing propagation in test rig 3. [02]	106
Graph 34: Displays the effect of Yield point differences have on mixing propagation in test rig 3. [02]	108

Appendix H – List of tables

Tables

	Page
Table 1: Effect of density difference on buoyancy. [R03, 02]	12
Table 2: Reelwell heavy light fluid properties. [R05]	28
Table 3: Mud formulation and ingredients. [05]	30
Table 4: Trial and error diesel rapeseed ratio.	31
Table 5: Test rig 1# setup specifics.	33
Table 6: Shows the technical data for experiments 1, 2 and 3. [02]	34
Table 7: Shows the technical data for ex. 4 and 6. [02]	36
Table 8: Displays the technical data for ex. 5 and 7. [02]	38
Table 9: Showing the fluid properties for the heavy liquids used in test rig 1#. [02]	40
Table 10: Displaying the numerical data for the three experiments.	43
Table 11: Summary of viable results from test rig 1#.	46
Table 12: Test rig 2# setup specifics.	48
Table 13: Displays the technical data for ex. 8 and 9. [02]	49
Table 14: Displays the technical data for ex. 10, 11, 12 and 13. [02]	51
Table 15: Displays the technical data for ex. 14 and 15. [02]	53
Table 16: Displays the technical data for ex. 16 and 18. [02]	54
Table 17: Displays the technical data for ex. 17, 19 and 20. [02]	56
Table 18: Showing the fluid properties for the heavy and light fluids used in test rig 2#. [02]	58
Table 19: Summary of viable results from test rig 2#.	67
Table 20: Aluminum pipe OD calculation. [02]	69
Table 21: Test rig 3# specifics.	69
Table 22: Displays the technical data for ex. 21, 22, 23 and 24. [02]	71
Table 23: Displays the technical data for ex. 25. [02]	73
Table 24: Displays the technical data for ex. 26, 27, 28 and 29. [02]	74
Table 25: Displays the technical data for ex. 30 and 31. [02]	75
Table 26: Showing the fluid properties for the heavy and light fluids used in test rig 3#. [02]	76
Table 27: Displays matrix nr. 1.	79
Table 28: Displays the mixing zone movement results from ex. 21, 22, 23 and 24. [02]	80

Table 29: Displays the mixing zone movement result from ex. 25. [02]	82
Table 30: Displays matrix nr. 2.	84
Table 31: Displays the mixing zone movement results from ex. 26, 27, 28 and 29. [02]	85
Table 32: Displays the mixing zone movement results from ex. 30 and 31. [02]	89
Table 33: Summary of viable results from test rig 3#.	91
Table 34: Viscometer test rig specifics.	92
Table 35: Displays the technical data for viscometer ex. 1 and 2. [02]	93
Table 36: Showing the fluid properties for the heavy and light fluids used in test rig 3#. [02]	94
Table 37: Displays the two Reelwell scenarios wellbore and drill pipe diameter. [R05]	97
Table 38: Parameter information. [R05]	97
Table 39: Reelwell fluid configuration. [R05]	97
Table 40: Showing the calculation of scenario 1 and 2s mixing zone lengths.	98
Table 41: Showing the calculation of scenario 1 and 2s mixing zone length.	99
Table 42: Displaying various experiments	99
Table 43: Mixing distance and rate for PV	107
Table 44: Mixing distance and rate for PV 4, 20 and 65 scaled up to scenario 1 and 2.	107
Table 45: Displays the parameters effect on mixing zone movement.	109
Table 46: Abbreviation table.	111
Table 47: Table of equations.	114

Screenshot tables

	Page
Screenshot table 1: Screenshots from the experimental footage taken under the execution of experiments 1, 2 and 3. [03]	42
Screenshot table 2: Screenshots of the experimental footage from the execution of experiments 4 and 6. [03]	44
Screenshot table 3: Screenshots of the experimental footage from execution of experiments 5 and 7. [03]	45
Screenshot tables 4: Screenshots from the experimental footage taken under the execution of experiments 8 and 9. [03]	60
Screenshot tables 5: Screenshots from the footage taken under the execution of experiments 10, 11, 12 and 13. [03]	61
Screenshot tables 6: Screenshots from the experimental footage taken under the execution of experiments 14 and 15. [03]	62

Screenshot tables 7: Screenshots from experimental the footage taken under the execution of experiments 16 and 18. [03]	64
Screenshot tables 8: Screenshots from the experimental footage taken under the execution of experiments 17, 19 and 20. [03]	65
Screenshot tables 9: Screenshots from ex. footage taken under the execution of experiments 21, 22, 23 and 24. The bended illustration of some of the experiments is due to a fish eyed lens, not experiment setup. [03]	78
Screenshot tables 10: Screenshots from ex. footage taken under the execution of experiment 25. The bended illustration of some of the experiments screenshots are due to a fish eyed lens, not experiment setup. [03]	81
Screenshot tables 11: Screenshots from ex. footage taken under the execution of experiments 26, 27, 28 and 29. The bended illustrations of some of the experiments are due to a fish eyed lens, not experiment setup. [03]	83
Screenshot tables 12: Screenshots from ex. footage taken under the execution of experiments 30 and 31. Screenshots from experiment 31 is taken two different cameras. The second camera took over when the mixing zone had moved passed the range of the lens. As seen in the top of the third screenshot from the left, the mixing zone is moving downwards. The bended illustration of some of the experiments is due to a fish eyed lens, not experiment setup. [03]	87
Screenshot tables 13: Screenshots from ex. footage taken under the execution of viscometer experiments 1 and 2. [03]	95

Attachment – Experimental CD

Experimental data are available in the attached CD at the back cover of the thesis.